Ife Journal of Technology

Vol. 23, No. 2, 2015

Editorial Board

General Information

The Ife Journal of technology is an international journal published by the Faculty of Technology, Obafemi Awolowo University, Ile-Ife, Nigeria.

The journal accepts original manuscripts from anywhere in the world in all engineering and related disciplines as listed below:

i. Agricultural Engineering
ii. Chemical Engineering
iii. Civil Engineering
iv. Computer Science and Technology
v. Electronic and Electrical Engineering
vi. Food Science and Technology
vii. Materials Science and Engineering
viii. Mechanical Engineering
ix. Technology Planning, Development and Management
x. Other engineering and related topics

The journal provides a vehicle for the fast and wide dissemination of results and findings of well-conducted researches in engineering and related fields mainly as research papers (theoretical and experimental), research notes and review articles. The journal also publishes book reviews, news and announcements.

Frequency of Publication

The journal is published twice a year in May and November

Annual Subscription (including postage)

Within Nigeria:	Outside Nigeria
Individuals: N3000.00	Individuals: $50
Institutions: N5000.00	Institutions: $100

Advertisement Rates

Full page (inside): N10,000
Half page (Inside): N5000
Additional for color: N5,000

Correspondence

All correspondence should be addressed to:

The Editor,
Ife Journal of Technology,
Dean's Office
Faculty of Technology,
Obafemi Awolowo University,
Ile-Ife,Nig

Visit our website at http://www.ijtonline.org

IFE JOURNAL OF TECHNOLOGY

Vol. 23, No. 2, 2015

Published by Faculty of Technology, Obafemi Awolowo University,
Ile-Ife, Nigeria

ISSN: 1115-9782

Full Paper

DEVELOPMENT OF A MACHINE FOR EXPRESSING *VERNONIA AMYGDALINA* LEAF JUICE

A.O. Oke
Department of Mechanical Engineering,
Faculty of Technology, Obafemi Awolowo University,
Ile-Ife, Nigeria.
toyinaoke@gmail.com

O.A. Koya
Department of Mechanical Engineering,
Faculty of Technology, Obafemi Awolowo University,
Ile-Ife, Nigeria.

C.T. Akanbi
Department of Food Science and Technology,
Faculty of Technology, Obafemi Awolowo University,
Ile-Ife, Nigeria.

ABSTRACT

Vernonia amygdalina leaf juice is known for its nutritive value and as food supplement. There is therefore, a need for a simple processing device for the leaf juice expression. This study developed a machine for producing contamination-free *V. amygdalina* leaf juice. The design of the machine was based on the principle of a pressure deferential applied to the incoming leaf mash compared with that applied to the discharged material. Macerated leaves were compressed through a tapered screw conveyor; whose shaft terminates as a rising but short conical kink. The maximum juice yield of 41.39% was expressed from the leaf mash at pressing pressure and residence time of 6.09 MPa and 11 min, respectively. The throughput of the machine was 9.60 kg/h and the juice extraction rate was 1.86 /h at leaf to water ratio of 1: 0.8. The maximum juice expression efficiency was 15.54% at 1:1.2 leaf to water ratio, 60 rpm constant rotational motor speed and 11.99 kg/h feeding rate. Approximately 26.38% of the inherent moisture content of the leaf was expressed by the machine. It is expected that the machine may be used to express juice from other plant leaves having comparative physical properties. The machine therefore provides a viable technique for mechanical expression of good quality *V. amygdalina* leaf juice.

Keywords: *Vernonia amygdalina* leaf juice, machine throughput, bioactive substances.

1. INTRODUCTION

Vernonia amygdalina (bitter leaf) has been noted for its high nutritional qualities being a good source of its crude protein and different kinds of minerals like phosphorus, calcium, sulfur, magnesium. The juice is, therefore used as a supplement in health food products; in particular, its concentrate which is high in protein (Tangka, 2003). It is also prescribed in the treatment of malaria fever, ameobic dysentery, several other intestinal parasites and stomach-aches (Huffman, 2003). The proximate analysis of the leaf as reported by Tangka and Penda (2007) consist of (dry weight basis): moisture content (13.12%); fat (12.29%); protein (16.34%); crude fibre (3.40%); ash (0.63%) and total resins (18.75).

Traditionally, the bitter leaves are macerated with mortar and pestle. After this step, the macerated leaves are kept inside a cloth and squeezed with hand. The practice is tedious, time- consuming and sometimes unhygienic. Juice from vegetable leaves has been expressed by different methods. Such are planetary mill and grinding machine, which significantly accelerate the process of mass transfer. In some other devices, pulsation, vibration, electric pulses, and other factors were also used to intensify the production of the juice (Ivanov *et al.*, 2004). However, these techniques were used without considering the structure and the strength of the plant parts such as the root, the bark, the stem, the leaf and the flower. Consequently, the juice expressed was turbid most importantly while processing plant leaf and flowers. Furthermore, it had been noted that when the mechanical strength of the individual types of raw material is not taken into consideration, the machine parts wear rapidly and break down (Kreshchenyuk *et al.*, 1971). It is therefore necessary to select the optimal process conditions of the specific plant material and, consequently, the most appropriate method of juice expression; hence, the main objective of the research was to develop a machine for the expression of *V. amygdalina* leaf juice.

2. MATERIALS AND METHODS

2.1. Sample Collection and Preparation

Fully expanded and freshly harvested *Vernonia amygdalina* leaves were collected for the experiment from the Teaching and Research Farm of Obafemi Awolowo University, Ile–Ife, during the dry season, in the month of February. Approximately 500 g of fresh *V. amygdalina* leaves were obtained. The leaves were sorted, cleaned, and comminuted manually to obtain a homogenous mash. The mash was kept in a sealed polythene bag to prevent evaporation prior to use. The initial moisture content (%,wb), of the leaf mash was determined according to standard S358.2 (ASAE, 2001) as:

$$MC = \frac{M_L}{M_S} \times 100\ \% \quad (1)$$

Where: MC (%) is moisture content, M_L is mass of moisture loss (g) and M_S is mass of leaf sample (g).

2.2. Determination of Optimal Processing Conditions for Juice Expression

A measure of 50 g leaf mash sample was weighed. The weighed sample was transferred to the pressing rig shown in Fig.1, where the juice was expressed. The mash sample was wrapped inside a cheese cloth which was placed inside the pressing cylinder, and the compression load was increased gradually with the use of a hydraulic jack. The quantities of juice expressed were weighed at intervals of 2 min until there was noticeable flow of the expressed juice. Pressing

pressures at different values of 4, 5, and 6 MPa; pressing time of 10 min at 2 min interval, and the pressed leaf mash initial and final moisture content were determined against the juice yield and the compression ratio. The juice yield J_Y, in percentage of leaf mash, was calculated using equation 2:

$$J_Y = {}^{100M_J}/_{M_S}\,\% \qquad (2)$$

Where: M_J is the mass of juice expressed in g, M_S is the mass of leaf mash sample in g.

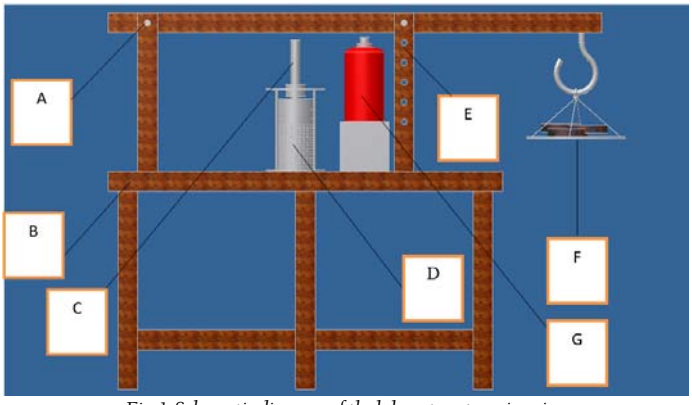

Fig. 1: Schematic diagram of the laboratory pressing rig.
A – Fulcrum, B – Table, C – Piston, D – Perforated cylinder enclosed, E – Support, F – Loading point, and G – Hydraulic press

The compression ratio (C. R) is defined by Equation. 3. It was used as an indication for the rate of pressing.

$$C.R = {}^{h_1}/_{h_2} \qquad (3)$$

Where, h_1 and h_2 are respectively the initial and the final height of pressed mash sample in mm.

2.3. The Experimental Juice Machine

The principle of a pressure deferential applied to the incoming leaf mash versus that applied to the discharge material is the working mechanism for the machine. The compression ratio is one of the most important criteria influencing the performance of a screw press. It was defined as the ratio of volume of material displaced per revolution of the shaft at the feed section to the volume displaced at the discharge section.

2.3.1. Design Considerations

The development of the experimental machine was based on information available and data from the compression experiment through the laboratory pressing rig. The machine was designed to:

i. effectively compress the juice through the tapered shaft at the discharge end; and
ii. have minimal damage on the expressed juice chemical content without contamination of the juice expressed.

The experimental machine was considered to be simple in design and easy to fabricate, and its operation does not require any previous technical training.

2.3.2. Forces Acting on the Screw Thread

The two main forces acting on the screw thread are the compression force required to convey and press the leaves, and the frictional force resulting from the screw motion. The worm shaft is subjected to pressure due to the compression of leaves. This pressure increases from a minimum value at the feed end to a maximum value at the discharge end. Fig. 2 shows the elemental load, L acting on the unit length of the thread. The load, L acts normal to the threaded surface along line XO. The axial and radial forces are resolved, such that:

$$F_t = (P_{max} \times A_{cs})\,\mu + F_c \qquad (4)$$

where, F_t is the resultant tangential force in N; μ is coefficient of static friction; P_{max} is the maximum pressure required for expression of leaf mash in MPa; A_{cs} is the curved surface area of the pressing zone in m^2; F_c is the compression force due to the maximum pressure for expression of juice from leaf mash in N.

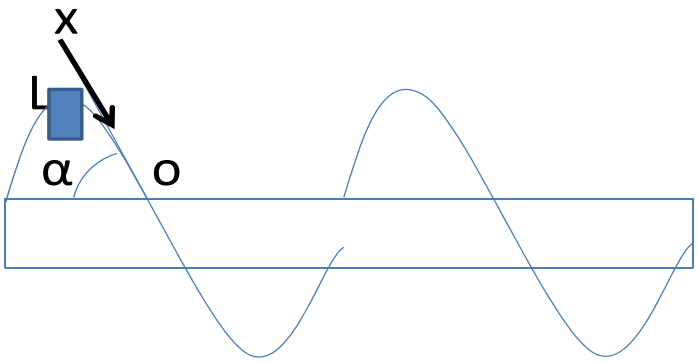

Fig. 2: Schematic diagram of tangential force acting on the conveyor flight screw.

2.3.3. Machine Components Design

The machine was designed according to engineering design standards. The details of the machine components are shown in Appendix A. The Specification of major components of the experimental juice machine is shown in Table 1.

Table 1 Specification of major components of the experimental juice machine

S/N	Component	Specification	Material
01	Screw shaft diameter	25.00 mm	Stainless steel
02	Kink diameter	52.00 mm	Stainless steel
03	Barrel diameters: Feed point discharge point	 140.00 mm 60.00 mm	Stainless steel
04	Screw pitch	40.00 mm	Stainless steel
05	Screw length per turn	80.00 mm	Stainless steel
06	Power rating of electric motor	1.5 kW	composite

2.4. Assembly of the Experimental Juice Machine

The experimental machine (Fig. 3) consists of the following parts: a tapered barrel having a screw conveyor; a shaft on which is welded the screw (or helix), a hopper surmounted on the barrel. The tapered barrel, made of stainless steel, had 140 mm inside diameter at feed point and 60 mm at discharge point. It had a length of 400 mm and a screen of full length. It was through this screen that the juice was pressed into a basin by the juice outlet. The shaft was made of stainless steel. It had a diameter of 25.0 mm, while the adjustable cone was bolted to the end part. The two ends of the shaft were in thrust bearings and one end carried the pulley through which power was transmitted by a V–belt from an electric motor. The screw flight was made of stainless steel sheet of 25 mm inner diameter, 60 mm outer diameter and 1.5 mm thickness, wound and welded to the shaft in the

clockwise direction. The constant pitch of the screw was 40 mm. The hopper was made of stainless steel sheet of 1.5 mm thickness. The macerated leaf mash was introduced into the compression barrel through the hopper. The frame was constructed from 50 x 50 mm angle iron. The overall dimensions of the machine were 1500 mm high, 200 mm wide and 700 mm long. A 1.5 kW gear reduction motor rotating at 90 rpm was used to supply the required power to rotate the screw shaft. A pulley of diameter 45 mm was used to further reduce the speed to 60 rpm. The parts' list is shown on Table 2. The orthographic views of the machine are shown on Fig. 4.

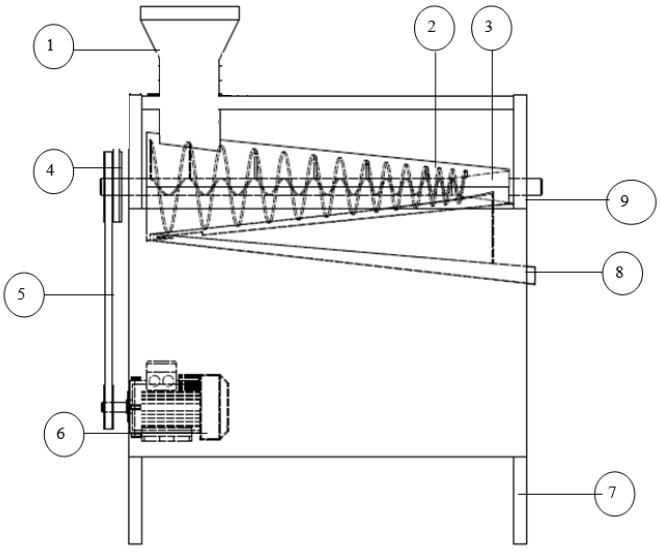

Fig. 3: The experimental machine components. (1) Hopper, (2) compression barrel, (3) kink, (4) pulley, (5) belt, (6) electric motor, (7) frame, (8) juice chute, (9) leaf mash chute.

2.5. Performance Evaluation of the Machine

Fresh *Vernonia amygdalina* leaves were obtained, sorted and macerated to 5 mm broad-bands leaf mash. The machine was set into operation and 200 g of the leaf mash was mixed with measured quantity of water and then introduced into the machine through the hopper. In the pressing barrel, the screw shaft conveyed, pressed the leaf mash to express the juice. Both the juice extracted and the pressed leaf mash were collected and weighed separately. From the values obtained, juice yield, expression efficiency and machine throughput were computed. Mathematically, juice yield, J_Y, expression efficiency, J_E and machine throughput, M_T were expressed (Oyeleke and Olaniyan, 2007; Arlabosse *et al.*, 2011) as:

$$J_Y = \frac{100W_J}{W_S} \% \quad (5)$$

$$J_E = \frac{100W_J C_J}{W_S C_S} \% \quad (6)$$

Table 2: parts List of the Machine

ITEM	QTY	PART	MATERIAL
1	1	Hopper	Stainless Steel
2	1	Tapered Barrel	Stainless steel
3	1	V-Belt	Rubber
4	1	Frame	Mild Steel
5	2	Pulley	Mild Steel
6	1	Juice Chute	Stainless Steel
7	1	Electric Motor	Composite
8	2	Side Cover	Mild Steel

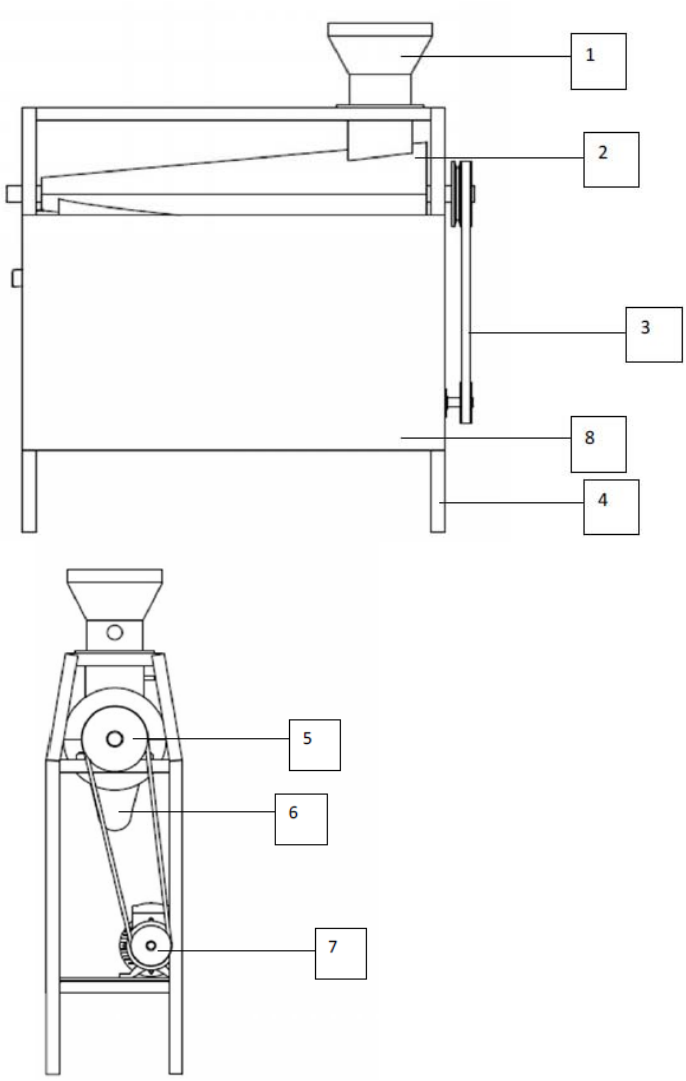

Fig. 4: Orthographic views of the experimental machine

$$M_T = \frac{W_S}{T_P} \text{ kg/h} \quad (7)$$

where, W_J is the mass of the juice expressed in g, W_S is the mass of leaf mash sample in g, W_J is the mass of leaf juice expressed in g, C_J is the flavonoid content of the juice yield in %, C_S is the flavonoid content of the leaf sample in %, and T_P is processing time in h.

2.6. Proximate Analysis of the Expressed Juice

The physical and chemical properties tests were carried out on the expressed juice, to determine of the chemical constituents of the expressed juice. The properties consist of the dry solid content, protein content, ash content, ether extract and the pH level of the juice using standard methods. The contents were determined from juice and pressed mash according to standards (ASAE, 2001; AOAC, 2004).

3. RESULTS AND DISCUSSION

3.1. Results of preliminary tests

The experiments on the *V. amygdalina* leaf mash revealed the effects of pressing pressure; residence time and their relationship on the juice yield. The summary of the data is shown in Table 3 and the results are discussed below.

3.2. Effect of pressing pressure on the juice yield

The effect of pressing pressure on the juice yield at different residence times is shown on Fig. 5. Increase of the pressing pressure progressively increases the juice yield exponentially at each residence time. Similar trends had been reported by previous researchers on juice expression (Sharif *et al*., 1993; Sinha *et al*., 2000). The relationship between the juice yield and the pressing pressure at 10 min residence time was determined using regression analysis as presented in Equation 7.

$$J_y = -2.475P^2 + 30.135P - 50.34 \quad (R^2 = 0.999) \qquad (7)$$

Where, J_y is the juice yield in % and P is pressing pressure in MPa. The maximum pressing pressure and the juice yield were obtained as 6.09 MPa and 41.39% respectively. The maximum pressing pressure is significant in determining the power required for an appropriate plant leaf juice expressing machine.

Fig. 6 shows the relationship between the pressing pressure and the moisture content of the plant leaf mash. From the graph, a power transformed regression analysis equation was developed, as presented in Equation 8.

$$MC = 82.629P^{-0.076} \quad (R^2 = 0.852) \qquad (8)$$

where, P is applied pressure (MPa), and MC is final moisture content (%w.b).

Sinha *et al.* (2000) developed a similar expression relating the final moisture content of pressed alfalfa mash to the applied pressure in the form $MC = 68.4P^{-0.0442}$. The predicted moisture content was lower than the pressed pulp in the present study, implying that the correlation is material specific. This might due to the difference in the textural resistance and the initial moisture contents of alfalfa leaf and *Vernonia amygdalina* leaf. Pressure at 6.09 MPa reduced the moisture content of the plant leaf mash from 80.48 to 72.03%. This indicates the minimum moisture content at which addtional pressing pressure will not increase yield significantly. Approximately 52% of the total moisture content was removed. In order to further reduce the moisture content or improve on the juice yield, tissue softening additional methods may be employed, such as, pulse electric field-assisted press (Lebovka *et al*., 2003).; thermally assisted mechanical dewatering (TAMD) (Praporscic *et al*., 2006; Kerfai *et al*., 2011).

Table 3: Design related properties of Vernonia amygdalina leaf mash

Properties	Sample size N	Mean Value
Angle of repose (degree)	3	48.33(±2.89)
Coefficient of friction (stainless steel)	3	1.12(±0.3)
Bulk density of leaf mash (kg/m^3)	3	111.22 (±0.0011)
Moisture content (%, w.b)	3	80.48 (±0.53)
Compression ratio at maximum Pressure, 6.09 MPa	3	6.73 (±0.44)
Leaf juice density (kg/m^3)	3	1090 (5.03)

** Data in parenthesis are the standard deviations*

3.3. Effect of residence time on the juice yield

The juice yield at the different pressing pressures with respect to pressing time is shown in Fig. 7. At each pressing pressure, there is a progressive increase in the juice yield. The juice yield gradually reduces with time as the pressure increases above 5 MPa. This is explained by the fact that the plant leaf mash is initially compressed rapidly; as its thickness increases, the juice released also reduces. The juice flows out almost immediately; about 85% of the juice is recovered after 8 min. Pirie (1987) reported a similar result during his research on an economical unit for pressing juice from fibrous pulps.

From Equation 9, the residence time at the maximum juice yield corresponding to 6.09 MPa was approximately determined as 11 min.

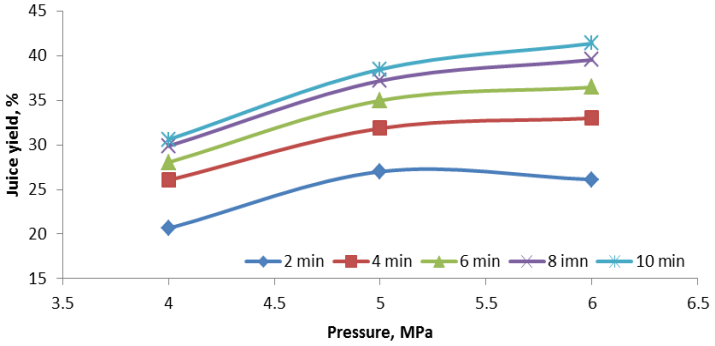

Fig. 5: Effect of pressing pressure on juice yield at different residence times.

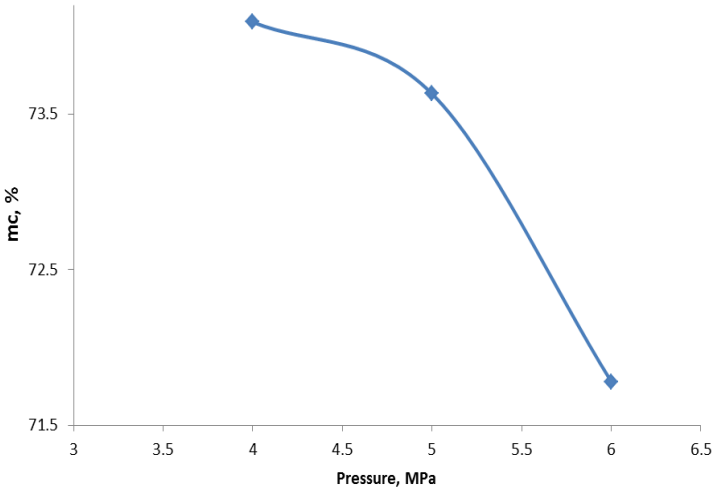

Fig. 6: Effect of pressure on moisture content for 10 mins residence time.

$$J_Y = -0.1868X^2 + 4.0944X + 18.942 \quad (R^2 = 0.995) \qquad (9)$$

where, J_Y is the juice yield in percentage and X is the residence time in minutes

The data provided are primary data for the design of the leaf juice expressing machine.

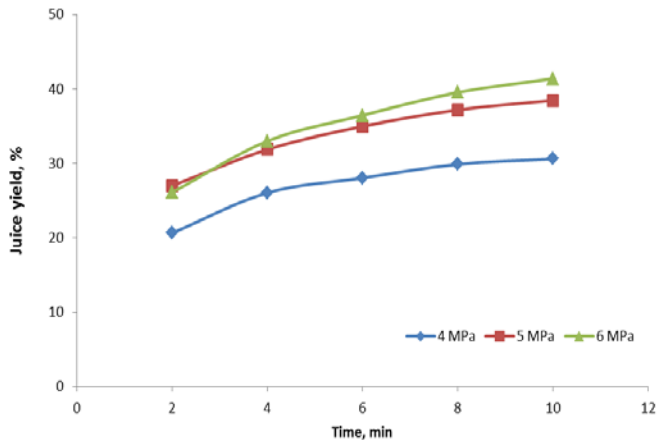

Fig. 7: Effect of residence time on juice yield at different pressing pressures.

3.4. Effect of Water Addition on the Expression Efficiency of the Machine

The pictures of the experimental juice machine, the leaf juice expressed; the leaf mash before and after expression are shown on Plates 1, 2, 3 and 4 respectively. Fig. 8 shows the juice yield and expression efficiency of the machine at the different leaf to water ratios. As the quantity of water increases, the efficiency also increases. At the ratio of 1:1.2, the highest efficiency of 15.54% was attained; while, the least efficiency of 3.67% was recorded at 1:0.8. Generally, the results give a low performance of the machine at all ratios. This may due to the low compression ratio of the machine. The need to attain the optimum contrition at the discharge has been a major limitation of screw presses (Singh and Bargale 2000). However, it is shown that the preliminary wetting of the mash enhances the process of expression in the experimental machine. Ivanov *et al.* (2004) had reported similar trend in the study of medicinal plant material extraction using a planetary mill.

The machine throughput has the maximum values of 9.6 kg/h at leaf to water ratio of 1: 1.1.2 (Table 3); so that the juice extraction rate was 1.83 kg/h or 1.68 l/h.

Plate 1. The experimental juice extracting machine

Plate 3. The leaf mash before expression

Plate 2. The expressed leaf juice

Plate 4. The leaf mash after expression

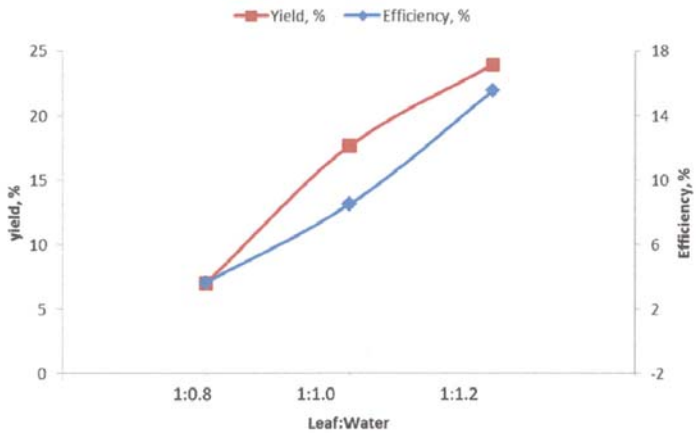

Fig. 8: Effect of water addition on Juice expression efficiency and juice yield.

3.5. Some Physico-Chemical Properties of Fresh Leaf and the Expressed Juice

Some physico-chemical properties (dry solid matter, ash content, ether extract and protein content) of the fresh leaf and the juice yield are shown in Table 4. At leaf to water ratio 1:0.8, the chemical constituents were at maximum: dry solid was 2.83%, protein was 23.63% and ash was 0.79%. Also, at 1:1.2, the minimum values were recorded: dry solid was 1.33%, protein was 19.03%, and ash was 0.26%. The ether extract was highest, 0.047% at leaf to water ratio 1: 1.0 and lowest, 0.01% at 1: 0.8. The difference in the values shows the effect of water addition on the juice yield. At leaf to water ratio of 1:1.2, the chemical constituents (dry solid, protein and ash content) decreased with an increase in the water addition. Ogblechi (2006) had reported a similar result in the expression of date palm fruit juice. Furthermore, the quality of the juice was unaffected by the expression process since the chemical constituents of the expressed juice varied moderately when compared with the fresh leaf. Also, the proximate analysis of the juice using the compression test rig (i.e no water addition) gave higher values than the juice from the machine except the protein content (15.97%) which was the lowest. This may be due to chemical reaction that increased the quantity of protein in the juice from the machine (i.e. with water addition). Aregbesola *et al.* (2009) also identified a similar occurrence in their study of production of herbal tea from *Hibiscus sabdariffa* calyxes.

*Table 4: Effect of Water addition on the Machine Throughput**

S/n	Quantity of leaf, g	Quantity of water, g	Time taken, s	Juice yield, g	Extraction rate, kg/h	Machine Throughput, kg/h
1	160	128	71	19.32(1.17)**	0.98	8.11
2	200	160	80	31.99(5.08)	1.44	9.00
3	240	192	90	45.65(12.54)	1.83	9.60

**Values determined at 1:0.8 (Leaf to water ratio). **Number in parentheses are standard deviations.*

Table 5: Proximate Analysis of fresh leaf and the juice expressed.

Sample Leaf :Water	Juice yield (%)	Solid Matter (%)	Moisture (%) (w. b.)	Ash, %	Crude protein (%)	Ether extract (%)	P_H
Fresh leaf	-	20.16	79.84	1.6**	25.66**	0.25**	-
No water*	41.37	7.51	92.49	1.88	15.97	0.150	4.9
1:0.8	7.02	2.83	97.17	0.79	23.63	0.010	6.7
1:1.0	17.63	1.61	98.39	0.34	22.53	0.047	5.4
1:1.2	23.95	1.33	98.67	0.26	19.03	0.033	4.7

**Data in the row was carried out using the laboratory press. **Source: Tangka and Penda (2007)*

4. CONCLUSIONS

A simple machine for the expression of leaf juice has been developed for *Vernonia amygdalina* leaf. The results from the compression experiment showed that the maximum pressing pressure and the juice yield were 6.09 MPa and 41.39% at 10 min residence time. The machine gave maximum juice yield of 1.86 l/h and throughput of 9.6 kg/h at leaf to water ratio of 1:1.2. The maximum juice expression efficiency was 15.54% at 200 g sample leaf mash, 60 rpm motor speed and 11.99 kg/h feeding rate. The juice expression efficiency increased (3.67–15.54%) with leaf to water ratio (1:0.8 – 1:1.2). Approximately 26.38% of the inherent moisture content of the leaf was expressed by the machine. The proximate analysis results show that preliminary wetting of the mash intensifies the process of juice expression using the experimental machine. It is expected that the machine may be used to express juice from other plant leaves having comparative physical properties.

ACKNOWLEDGMENT

The authors are grateful to Mr. Kayode Ogunyemi of Department of Animal Science, the technical staff of Mechanical and Agricultural Engineering, Obafemi Awolwo University, Ile-Ife, for their technical supports in the course of this work.

Notations

A_{cs}	Curved surface area of the pressing zone, m^2
C_J	Flavonoid content of the juice yield, %
C. R.	Compression Ratio
C_S	Initial flavonoid content of the leaf sample, %
F_c	Compression force due to the maximum pressure for expression of leaf mash, N
F_t	Tangential force, N
h_1	Initial height of pressed mash sample, mm
h_2	Final height of pressed mash sample, mm
J_E	Juice expression efficiency, %
J_Y	Juice yield, g
M_C	Machine throughput, kg/h
MC	Moisture content of sample, % (w.b)
P_{max}	Maximum pressure required for expression of leaf mash, MPa
T_P	Time of processing, h
W_L	Mass of moisture loss, g
W_J	Mass of leaf juice expressed, g
W_S	Mass of leaf mash sample, g;
μ	Coefficient of static friction

REFERENCES

AOAC. Official methods of analysis. Association of Official Analytical Chemists, Washington, D. C. 54 –57, 2004.

Aregbesola, O. A., Faborode, M. O. and Hounkanrin, B.A. Studies on the production of herbal tea from *Hibiscus sabdariffa* (Roselle) calyxes. 3rd Proceedings of Nigerian Institute of Agricultural Engineering, 210–213, 2009.

Arlabosse, P., Blanca, M., Kerfaïc, S. and Fernandezc, A. Production of green juice with an intensive thermo-mechanical fraction process. Part I: effect of processing conditions on the dewatering kinetics. *Chemical Engineering Journal* 168: 586–592, 2011.

ASAE Standards. Moisture measurement–forages, 47th edition. American Society of Agricultural Engineers, ASAE S358.2, St. Joseph, Michigan. 57–59, 2001.

Huffman, M. A. Animal self–medication and ethno–medicine: exploitation and exploration of medicinal properties of plants. Proceedings of the Nutrition Society, 62: 371–381, 2003.

Ivanov, E. V., Shvyrev M. V., Minina S. A., and Kochnev V. G. Method of medicinal plant material extraction in a planetary mill. *Pharmaceutical Chemistry Journal*. 38 (11): 29–32, 2004.

Kerfai S., Fernandez A., Mathe S., Alfenore S., Arlabosse P. Production of green juice with an intensive thermo-mechanical fraction process. Part II: effect of processing conditions on the liquid fraction properties. *Chemical Engineering Journal* 167: 132-139, 2011.

Kreshchenyuk, S. I., Litvinenko V. I. and Prokopenko A. P. Machines for grinding medicinal plant raw material. *Khar,kov Scientific–Research Institute of Pharmaceutical Chemistry*, 5 (6): 46–48, 1971.

Lebovka, N. I., Bazhal, M. I., and Vorobiev, E. Enhanced expression of juice from soft vegetable tissues by pulsed electric fields: consolidation stages analysis. *Journal of Food Engineering* 59: 309–317, 2003.

Ogblechi, S.R. Development of a Mechanical Extractor for Date Fruit Juice Processing. Unpublished M.Sc. thesis, Department of Agricultural Engineering, Obafemi Awolowo University, Ile-Ife. 72–75, 2006.

Oke, A. O. Development of a Machine for Expressing *Vernonia amygdalina* Leaf Juice. M. Sc. Thesis, Department of Mechanical Engineering, Obafemi Awolowo University, Ile-Ife, Nigeria, 2012.

Okoye, C. N., Jiang, J., Hui, L. Y. Design and development of secondary controlled industrial palm kernel nut vegetable oil expeller plant for energy saving and recuperation. *Journal of Food Engineering*, 87: 578–590, 2008.
Oyeleke, F.I. and Olaniyan, A. M. Extraction of juice from tropical fruits using a small scale multi–fruit juice extractor. African Crop Science Conference Proceedings. 8: 1803–1808, 2007.
Pirie N. W. An economical unit for pressing juice from fibrous pulps. Journal of Agricultural Engineering Research. 38: 217–222, 1987.
Sharif, H. I., Al–Mashat, and Carlos, A. Z. Stress relaxation behavior of apple pomace and effect of temperature, pressing aid and compaction rate on juice yield. *Journal of Food Engineering*. 20:247–266, 1993.
Singh, J. and Bargale P. C. Development of a small capacity double stage compression screw press for oil expression. *Journal of Food Engineering*. 43: 75–82, 2000.
Sinha, S., Sokhansanj, S., Crerar, W. J., Yang, W., Tabil, L. G., Khoshtaghaza, M. H. and Patil, R.T. Mechanical dewatering of chopped alfalfa using an experimental piston–cylinder assembly. *Canadian Agricultural Engineering* 42 (3): 153–156, 2000.
Tangka, J. K. Analysis of the thermal energy requirements for the extraction of leaf protein concentrate from some green plants. *Biosystems Engineering*, 86 (4): 473–479, 2003.
Tangka, J. K. and Penda, P.M. Development and performance evaluation of a medium–scale system for processing bitter leaf. *Biosystems Engineering*, 96 (2): 223–229, 2007.

APPENDIX A: DESIGN OF THE MACHINE COMPONENTS

Determination of compression ratio

Compression experiment was carried out to determine the theoretical compression ratio (C. R) of the leaf mash at maximum pressing pressure. The design compression ratio is thus calculated:

$$C.R = \frac{D_1^2 - d^2}{D_2^2 - D^2} \quad \text{(A1)}$$

where D_1 is barrel diameter at feed point, D_2 is Barrel diameter at discharge point, D is the kink diameter, and d is the shaft diameter. Given: d is 25 mm, D is 52 mm, D_1 is 82 mm and then D_2 is 60 mm. The shaft at the discharge end was made conical to increase the compression of the juice from the leaf mash.

Determination of theoretical screw volume

The theoretical screw volume is given by

V_s = screw area x pitch

$$V_s = \frac{\pi(D_1^2 - d^2)P}{4} \quad \text{(A2)}$$

where, D_1 is the barrel diameter at feed, d is the shaft diameter, P is the pitch

Substituting into the formula

$$V_s = \frac{\pi(0.082^2 - 0.025^2)0.004}{4}$$

$$= 1.92 \times 10^{-5}\ m^3$$

Determination of mass flow rate

Mass flowrate is dependent on bulk density, theoretical screw volume, speed of screw and filling factor.

$$\dot{m} = V_s N \rho \varphi \quad \text{(A3)}$$

where, V_s is Screw volume, N is speed of rotation, ρ is leaf mash bulk density, kg/m³, φ is filling factor, 45 % (Altamuro, 1996).

= 1.92 x 10^{-5} x 6.284 x 111.22 x 0.45

= 0.00604 kg/s

= 21.74 kg/h

The power requirement

The input power during expression of plant materials depends on the rate of energy consumption within the limits of the transport and pressing zones. The highest power consumption is required in the pressing zone, where the highest pressures arise in the material to be expressed. From the experimental results, a maximum pressure 16 MPa is required at the pressing zone. Varying the shaft speed with the expressing pressure, the optimal power required was generated (Oke, 2012). A power source of 1.0 kW at a speed of not more than 60 rpm was determined. For this work, a 1.5 kW reduction gear motor was used.

The Barrel

The barrel was a tapered pipe, made of stainless steel. The barrel was designed on the basis of the required internal pressure for the juice expression. Using the standard stress analysis techniques applied to thin wall pressure vessels (Khurmi and Gupta, 2010), the tangential stress, σ, perpendicular to the axis of the barrel was as stated below:

$$\sigma = \frac{P_{max} R_I}{2t} \quad \text{(A4)}$$

where, P is the internal pressure in the cylinder, R_I is the inner radius of cylinder; and t is the thickness of the cylinder. Given that P_{max} is 16.0 MPa, r is 30 mm, σ is 56 x 10^6 N/m², so that the thickness, t is 4.29 mm. Therefore, the barrel thickness of 4.5 mm was used.

Determination of forces acting on the auger shaft

From the experimental result, the maximum pressure required to express the leaf juice from the leaf mash is 6.09 MPa. Using a method described by Bernard *et al.* (1999) for determining the factor of safety, such as the quality of materials used, control over load applied to parts, accuracy of experimental data, danger to end users and economic impart. A factor of safety of 2.63 was used. Hence, the pressure used as the maximum pressure for this design was 16.0 MPa.

The curved surface area of the pressing zone, A_{CS}

$$A_{CS} = \frac{\pi D_2 L_k}{2} \quad \text{(A5)}$$

where, D_2 is the barrel diameter at discharge, 60 mm and L_k is the length of the kink, 40 mm.

Therefore A_{CS} = 0.00377 m²

The cross–sectional area of the pressing zone (the discharge end), A_C

$$A_C = \frac{\pi(D_2^2 - D^2)}{4} \quad \text{(A6)}$$

where, D_2 is the barrel diameter at discharge, 60 mm and D is the kink diameter, 52 mm.

Therefore A_C = 0.000704 m²

$$F_c = P_{max} \times A_c$$

(A7)

$$= 11.26 \text{ kN}$$

The static coefficient of friction, μ is calculated as thus:

$$\mu = \tan \theta$$

where θ, is the angle of inclination at which the leaf mash just begins to move on the inclined plane.

Then, μ was calculated as 1.12 using stainless steel as the surface in contact.

Now, for a conservative design based on the maximum pressure P_{max} of 16.0 MPa, the coefficient of friction μ of 1.12, the cross–sectional area of the pressing zone A_c of 0.000704 m^2, the curved surface area A_{cs} of 0.377 m^2, the compression force F_c of 11.26 kN. Therefore, the tangential force F_t was 78.83 k N.

Determination of auger shaft diameter

The shaft on which the screw material was wound was designed based on the following assumptions:

(i) The solid shaft was made from austenitic stainless steel (0.3% C, 18% Cr, and 8% Ni) with a yield strength of 280 MN/m^2. The density, ρ_s was 8030 kg/m^3; the modulus of elasticity, *G* was 206 GN/m^2; the modulus of rigidity, *R was* 73 GN/m^2; the maximum permissible angle of twist, β is 1^0 per 300 mm length, (Hall *et al.*, 1961) i.e. 2.0^0 for the 0.6 m length, thus, the length, L was 0.5 m from bearing to bearing. The design of the shaft was based on the maximum shear theory (Spotts, 1971).

$$\tau_{max} = \frac{0.5\tau_{yp}}{FS}$$

(A8)

where, τ_{max} is the maximum shear stress in N/m^2, τ_{yp} is the yield strenght in N/m^2 and FS is the factor of safety.

The factor of safety was calculated using a method described by Bernard *et al.* (1999). The factors considered include: the quality of materials used, control over load applied to parts, accuracy of experimental data, danger to end users and economic impart. A factor of safety of 2.5 was used.

Then,

$$\tau_{max} = 56 \times 10^6 \text{ N/m}^2$$

But

$$\tau_{max} = \frac{16T}{\pi d^3} \quad \text{(A9)}$$

Where, d is the required shaft diameter in mm, T is the Torque in Nm.

$$T = \frac{9550 \times P_R(\text{kW})}{N} \quad \text{(A10)}$$

P_R is power required, kW

Given that speed, N = 60 rpm, P = 1.0 kW

= 159.17 Nm

Then d = 25 mm;

Therefore, r is 12.5 mm.

As a design check, the torsion of shafts equation for a solid circular shaft is:

$$\frac{T}{J} = \frac{\tau}{r} = \frac{G\beta}{L} \quad \text{(A11)}$$

from which

$$\tau = \frac{rG\beta}{L} \quad \text{(A12)}$$

Given that r is 12.5 mm, then τ is 61.782 x 10^8 MN/m^2.

As 56 x 10^6 MN/m^2 is less than 61.782 x 10^8 MN/m^2, the shaft radius of 12.5 mm is safe for a twist angle of 2^0 on a length of 0.5 m, that is, the shaft of diameter 25 mm can withstand a stress of 61.782 x 10^8 MN/m^2 which is more than the calculated stress of 56 x 10^6 MN/m^2.

For the applied torque

$$T = \frac{G\beta J}{L} = 189.54 \text{ Nm}$$

i.e. a shaft of radius 12.5 mm will also withstand a torque of 189.54 Nm which is higher than the torque of 159.16 Nm calculated, hence it is safe to use the 25.0 mm diameter shaft. The shaft will not fail due to shear stress, torque or torsion.

Shaft Component Diagrams

⊟ Material

Material		Stainless steel
Modulus of Elasticity	E	206000 MPa
Modulus of Rigidity	G	80000 MPa
Density	ρ	7860 kg/m^3
Length	L	681.000 mm
Mass	Mass	2.984 kg
Results		
Ideal diameter	d	10.19mm
Maximum bending moment	BM_{max}	5.19 Nm

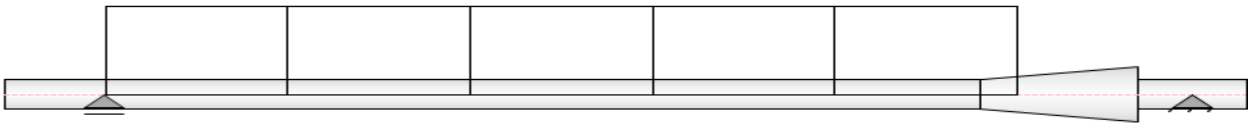

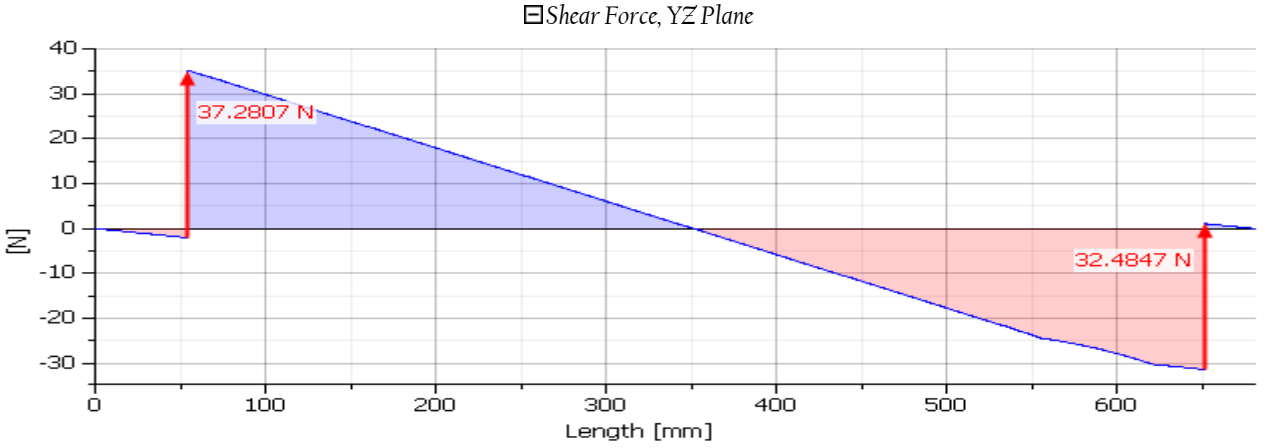

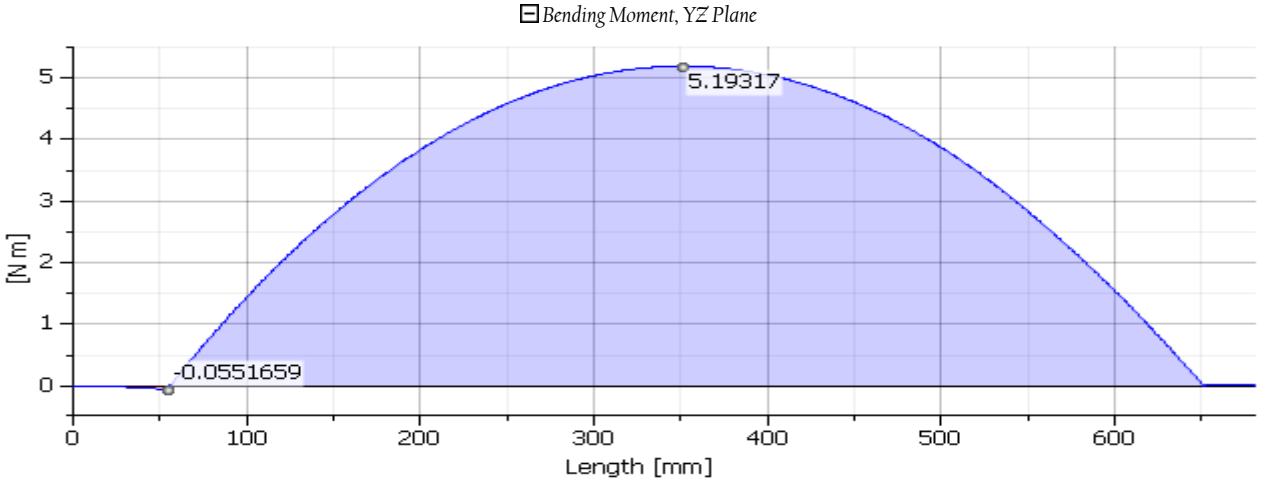

Ideal Diameter

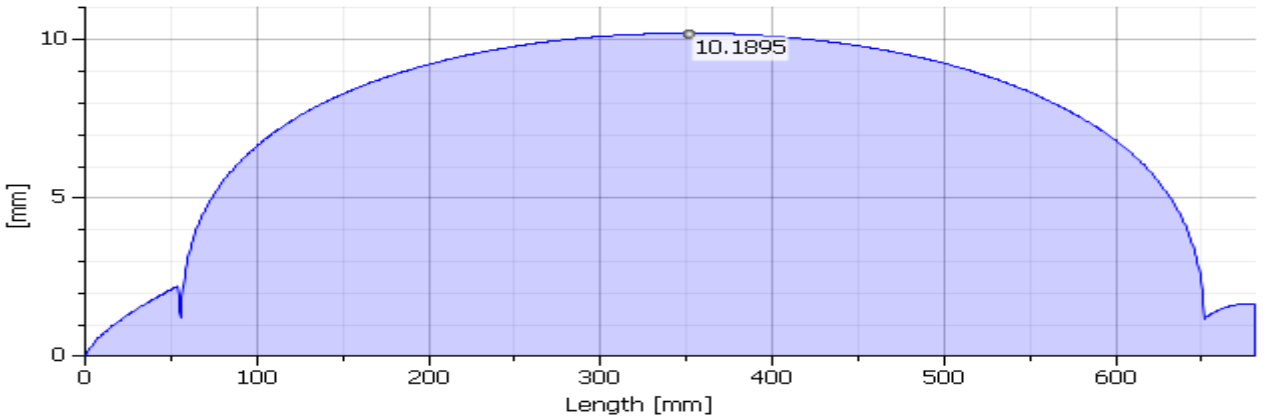

Full Paper

FINE PARTICULATE CONCENTRATIONS IN THE AMBIENT ENVIRONMENT OF A MAJOR HAULAGE VEHICLE PARK

B. S. Fakinle
Department of Chemical Engineering
Landmark University, Omu-Aran, Nigeria.

J. A. Adeniran
Department of Chemical Engineering,
University of Ilorin, Ilorin, Nigeria

O.B. Okedere
College of Science, Engineering and Technology
Osun State University, Osogbo, Nigeria

L. A. Jimoda
Department of Chemical Engineering,
Ladoke Akintola University of Technology, Ogbomoso Nigeria

J.A. Sonibare
Department of Chemical Engineering
Obafemi Awolowo University, Ile-Ife, Nigeria
asonibar@yahoo.com

ABSTRACT

The study was carried out to determine the levels of particulates in the airshed of major vehicular park and suggest appropriate ways of controlling the ambient particulate concentrations. The ambient fine mode particulate number concentrations were measured at five different designated points in the park using the Met-One mode GT-321 particulate air monitor. Measurements were conducted both in the wet and dry seasons. The Results showed that the averaged 8 hr daytime particulate concentrations for 0.3, 0.5 and 1.0µm PM within the park were of the range 1.19 x 10^8 - 2.52 x 10^8 particles/m^3 with an average of 2.25 x 10^8 particles/m3, 2.66 x 10^7 - 7.59 x 10^7 particles/m^3 with an average of 5.08 x 10^7 particle/m^3 and 3.17 x 10^6 - 9.82 x 10^6 particles/m^3 with average of 6.97 x 10^6 particles/m^3 respectively during the wet season and 1.22 x 10^8 - 1.73 x 10^8 particles/m^3 with an average of 1.41 x 10^8 particles/m^3, 1.58 x 10^7 - 3.99 x 10^7 particles/m^3 with an average of 2.94 x 10^7 particles/m^3 and 3.74 x 10^6 - 9.67 x 10^6 particles/m^3 with an average of 6.48 x 10^6 particles/m^3 respectively during the dry season. The Particulate Concentrations measured during the two seasons were within the maximum permitted limit of ISO Class 9 for PM1 required for a clean zone by International Standard Organization-ISO 146441. The study showed that vehicular activity could be one of the major contributors to ambient particulate concentration. Hence effective control measures such as cleaner technology, the use of catalytic converters, the use of alternative fuel and clean fuel and the implementation of emission standard should be employed in order to have an improved air quality based on ambient particulate concentration.

Keywords: *Ambient environment, fine particles, transport system, haulage vehicle park, meteorological parameters*

1. INTRODUCTION

Particulate matter (PM), a complex mixture of extremely small particles and liquid droplets found in the air (Libby, 2007) could pose serious challenge to both the environment and human health. Some particles are large or dark enough to be seen as soot, while some (including fine particles) are tiny and generally not visible to the naked eye. The fine mode particulate matter is of health concern because they can reach the deepest regions of the lungs. Pathogenesis by fine particles depends on the physical characteristics (size, shape, concentration, composition and aggregation effects) of the particles and host body defense systems (DEH, 2004; Maynard and Kuempel, 2005; Baveye, 2008). The Health effects include asthma, difficult or painful breathing, and chronic bronchitis, especially in children and the elderly (Donaldson *et al*., 1988; Bate, 1995; Atkinson *et al*., 1999; Pope III, 2000; Cacciola *et al*., 2002).

Transportation sector makes a vital contribution to the economy and plays a crucial role on daily activities in Nigeria like many other developing countries. However, it is becoming a significant source of air pollution and is currently one of the major emission sources in megacities with subsequent adverse effects on human health (Colvile *et al*., 2001). Although, road transport has the advantage of providing door-to-door transportation and convenience for man's daily life, its fuel requirement in combustion and emissions are much higher than other transport modes (Masjuki et al., 2004; Soylu, 2007). These emissions from road transport are serious threats to urban air quality and global warming (Saija and Romano, 2002).

Vehicular activities are one of the major primary fine particulate matter sources. They account for approximately 15 – 50 % of total fine aerosol mass in urban areas (Sheesley *et al*., 2007). Diesel-powered vehicles and engines contribute more than half of the mobile source particulate emissions (Ramachandran *et al*., 2005; Morawska *et al*., 2008).

The measurement of fine particle exposure can be determined in terms of size distribution, particle number concentration, surface area concentration and mass concentration (Cheng *et al*., 2008). Fine particulate matter contributes significantly to particle number concentration (PNC), but little to particle mass concentration (ECJRC, 2002) hence particle number concentration and surface area are more likely to be related in potential health effects than particle mass concentration. The mass concentration from fine particle is low and size-dependent particles can possibly impact on respiratory system areas through translocation and biological response (Oberdörster, 2000).

To examine the impacts of vehicular activities on ambient air quality in a haulage vehicle park, this study measured the particulate number concentrations from a major haulage vehicle park located at Ogere, Ogun State, Nigeria. This park is strategically located in transport corridor leading to Lagos and Ibadan which are emerging megacities in Nigeria. Its features have earlier been discussed (Fakinle et al., 2013). The information derived from this will assist in developing appropriate control measures for the abatement of particulate emission in haulage parks. It will also assist in legislating

on ambient air quality standards around haulage vehicle parks, and also add to the data bank on aerial pollution in Nigeria.

2. METHODOLOGY

The study area (Fig. 1) has been earlier described in Fakinle *et al*, (2013). Fine mode particulate number concentrations were measured at five different locations designated within the park using the Met one Isokinetic particle air monitor (Met One model GT-321). Measurement with the isokinetic monitor was set to operate between 10.00 am - 18.00 pm at each of the sampling points throughout the months of July and December 2010 which are the months in rainy and dry season, respectively. The isokinetic monitor is a small and portable unit with self-contained power supply. The LCD display of the unit allows viewing of two discrete particle-counting channels in real time simultaneously. The sampling time is typically 5 minutes for all cases with logging interval of about 15 min. its battery can last about 24 hours between periods of recharge.

2.1. Meteorological Condition

The meteorological conditions of the site were measured using the Kestrel 4000 pocket weather tracker which is an easy weather monitoring device that instantly measures environmental condition accurately. It is set up to display the following meteorological parameters: relative humidity, temperature, wind speed, pressure and altitude. These measured parameters have also been reported earlier by Fakinle *et al*., 2012.

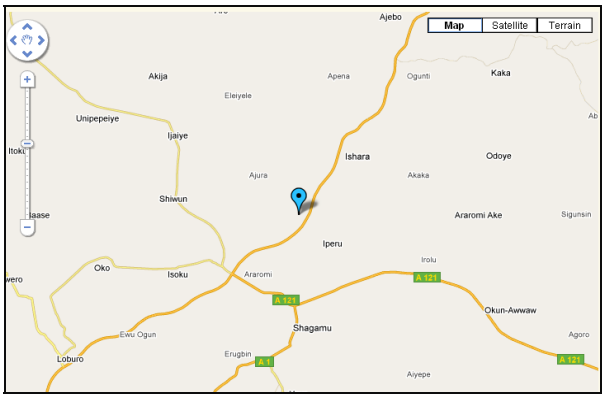

Fig. 1. Sampling Points at Ogere, Ogun State
Source: Google map (2010)

3. RESULTS AND DISCUSSION

Summarized in Table 1 and Table 2 are the 8-hr averaging period measured fine particulate number concentrations (particles/m^3) at the various sampling points. The concentrations ranged between 1.91 x 10^8 - 2.52 x 10^8 particles/m^{3}with an average of 2.25 x 10^8 particles/m^3, 2.66 x 10^7 - 7.59 x 10^7 particles/m^3 with an average of 5.08 x 10^7 particles/m^3, 3.17 x 10^6 - 9.82 x 10^6 particles/m^3 with an average of 6.97 x 10^6 particles/m^3 for particles with size fraction 0.3 µm, 0.5 µm, 1.0 µm respectively during the rainy season, while the ranges were 1.22 x 10^8 - 1.73 x 10^8 particles/m^3 with an average of 1.41 x 10^8 particles/m^3, 1.58 x 10^7 - 3.99 x 10^7 particles/m^3 with an average of 2.94 x 10^7 particles/m^3, 3.74 x 10^6 - 9.67 x 10^6 particles/m^3 with an average of 6.48 x 10^6 particles/m^3 respectively in the dry season. During the rainy season the minimum and maximum $PM_{0.3}$ concentrations were at S1 and S3 respectively, but for $PM_{0.5}$ the minimum and maximum concentration they were at S5 and S4 respectively while sampling points S5 and S4 had the minimum and maximum respectively for PM_1 respectively. In the dry season the minimum $PM_{0.3}$, was at sampling point S5 while $PM_{0.5}$ and PM_1 both had their minimum at S4. The maximum concentrations for all the size fractions were at sampling point S1.

In sampling locations S4 and S5 the minimum $PM_{0.5}$ and PM_1 for both seasons which could be attributed to lesser haulage vehicle activities compared to the other locations. However, in the dry season S1 which is located at the median of the dual carriageway experiencing higher traffic volumes as compared to other sampling locations had the maximum particle concentrations for all the size fractions. The maximum concentrations of all the size fractions at S1 during the season could be as a result of high traffic volume and activities.

In sampling locations S4 and S5 the minimum $PM_{0.5}$ and PM_1 for both seasons which could be attributed to lesser haulage vehicle activities compared to the other locations. However, in the dry season S1 which is located at the median of the dual carriageway experiencing higher traffic volumes as compared to other sampling locations had the maximum particle concentrations for all the size fractions. The maximum concentrations of all the size fractions at S1 during the season could be as a result of high traffic volume and activities.

Table 1: Eight hour averaged ambient particulate number concentrations (Particle/m^3) in July, 2010 wet season

Location	Concentration Wet season		
	0.3 µm	0.5 µm	1.0 µm
Station 1	1.91 x 10^8	5.12 x 10^7	6.11 x 10^6
Station 2	2.23 x 10^8	4.38 x 10^7	6.89 x 10^6
Station3	2.52 x 10^8	5.65 x 10^7	8.86 x 10^6
Station 4	2.50 x 10^8	7.59 x 10^7	9.82 x 10^6
Station 5	2.10 x 10^8	2.66 x 10^7	3.17 x 10^6
Mean	2.25 x 10^8	5.08 x 10^7	6.97 x 10^6

Table 2: Eight hour averaged ambient particulate number concentrations (Particle/m^3) in December, 2010 dry season

Location	Concentration Dry Season		
	0.3 µm	0.5 µm	1.0 µm
Station 1	1.73 x 10^8	3.99 x 10^7	9.67 x 10^6
Station 2	1.37 x 10^8	3.32 x 10^7	7.38 x 10^6
Station 3	1.52 x 10^8	2.57 x 10^7	5.54 x 10^6
Station 4	1.22 x 10^8	1.58 x 10^7	3.74 x 10^6
Station 5	1.22 x 10^8	3.22 x 10^7	6.07 x 10^6
Mean	1.41 x 10^8	2.94 x 10^7	6.48 x 10^8

Using the ISO 14644-1 classification for airborne particulate cleanliness classes for clean rooms and zones as summarized in Table 4, all the sampling points breach the $PM_{0.3}$ standard during both rain and dry seasons as the concentrations at these points exceed the maximum ISO Class 6 permitted for a clean zone. For $PM_{0.5}$, sampling point S5 can be classified into Class 9 during the rainy season, while other sampling points breached the limit set for this faction. During the dry season, sampling points S2, S3, S4 and S5 can be classified into ISO Class 9 using $PM_{0.5}$. Also sampling points S1, S2 and S5 during the rainy season as well as sampling points S2, S3, S3, S4 and S5 during the dry season can be classified into Class 9 using PM_1. The result showed that Ogere road transport system has enormous PM loading in its ambient air which could be attributed to the influence of vehicular activities in the region.

In this study, result showed that particulate number concentrations of the fine particles ($PM_{0.3}$ and $PM_{0.5}$) were higher during the wet season as compared to the dry season. This observation could be linked to the variation in the meteorological conditions (Table 3) which were 64.21 %, 29 ^{0}C and 0.82 m s^{-1} for relative humidity, temperature and wind speed respectively during the rainy season, while those of the dry season were 51.41 %, 32.44 ^{0}C and 0.76 m s^{-1} respectively. Also vehicular count could be a contributing factor to the variation in the particulate concentrations in the airshed in both seasons. From the measured meteorological parameters, it was

observed that the relative humidity during the wet season was higher compared to the dry season. High relative humidity accounts for the presence of moisture in the ambient air of the haulage park which could aid particles coagulation during the season, hence this could be the reason for higher concentrations of fine particle during the season compared to the dry season. Also from the overall mean of particulate in Table 2 the study area could be classified into ISO Class 9 during the dry season using $PM_{0.5}$. For PM_1 the study region could be classified into ISO Class 9 during the two seasons.

Table 3: Overall mean and Standard deviations of Meteorological parameters measured during the sampling period.

Season	Relative Humidity (RH %)	Temperature (°C)	Wind speed (m/s)
Rain	64.21 ± 7.38	29.00 ± 1.68	0.82 ± 0.26
Dry	51.41 ± 7.77	32.44 ± 1.36	0.76 ± 0.21

Table 4: Selected airborne particulate cleanliness classes for cleanrooms and clean zones

Classification Number(N)	Maximum concentration limits (particles / m^3) for particles equal to and larger than the considered sizes shown below		
	0.3 µm	0.5 µm	1 µm
ISO Class 1			
ISO Class 2	10	4	
ISO Class 3	102	35	8
ISO Class 4	1020	352	83
ISO Class 5	10200	3520	832
ISO Class 6	102000	35200	8320
ISO Class 7		352000	83200
ISO Class 8		3520000	832000
ISO Class 9		35200000	8320000

Using these ISO Classifications for airborne particulate cleanliness, efforts need to be made at the haulage park to ensure that the particulates levels in the ambient environment of the park do not go beyond ISO Class 5.

The Particle number concentrations (PNCs) of the fine mode fractions (0.3µm, 0.5µm, 1.0µm) appeared to be in similar order of magnitude at each of the five sampling points. The average of the PNCs over the entire sampling duration indicated that 0.3µm, 0.5µm and 1.0µm constituted 80%, 18% and 2% respectively of the total PM during rainy season (Fig. 2) while 80%, 16% and 4% respectively during the dry season (Fig. 3). These particles could consist of soot since diesel combustion in the heavy trucks operating around the park was a major source of particulates (Dallaman *et al*., 2014).

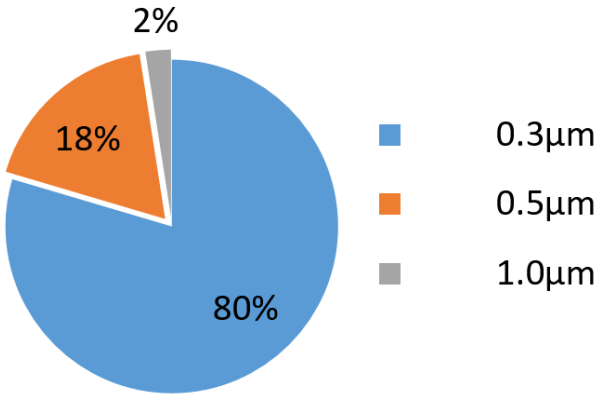

Fig. 2: Ambient Particle Concentration during Rainy Season.

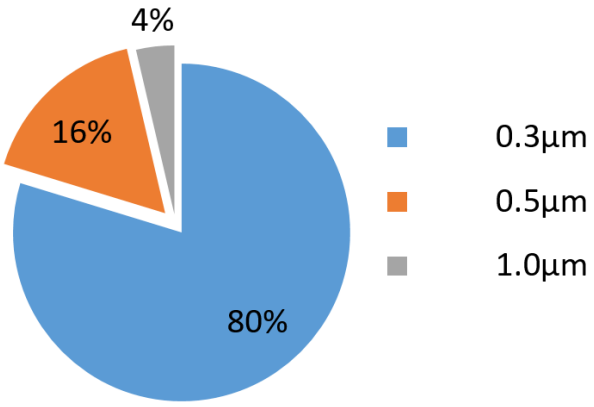

Fig. 3: Ambient Particle Concentration during Dry Season.

4. CONCLUSION

This work investigated the contribution of haulage vehicular activities to the air quality of Ogere's airshed based on PNC of fine mode particle. The particles with diameter of 0.3µm dominate the PNCs in the ambient air of the study area. The measured PNCs ranged between 1.91 x 10^8 - 2.52 x 10^8 particles/m^3, 2.66 x 10^7 - 7.59 x 10^7 particles/m^3, 3.17 x 10^6 - 9.82 x 10^6 particles/m^3 for particles with size fraction 0.3 µm, 0.5 µm, 1.0 µm respectively during the month of July, 2010 rainy season, while the ranges were 1.22 x 10^8 - 1.73 x 10^8 particles/m^3, 1.58 x 10^7 - 3.99 x 10^7 particles/m^3, 3.74 x 10^6 - 9.67 x 10^6 particles/m^3 respectively in the dry season in December, 2010. The percentage contributions of $PM_{0.3}$, $PM_{0.5}$ and PM_1 during the wet season were 80%, 18%, and 2% respectively, while that of the dry season were 80%, 16%, 4% respectively. Due to high concentration of the fine mode particle in the study area it is observed that the contribution of vehicular activities to the ambient air quality is significant hence it is imperative that control measure should be put in place in order to have an improved air quality. Control measure such as cleaner technology, the use of catalytic converters, the use of alternative fuel and clean fuel and the implementation of emission standard should be employed in order to control emission from vehicular activities.

REFERENCE

Atkinson, R., Bremner, S., Anderson, H., Strachan, D. and Bland, J. M. (1999). Short- term Association between Emergency Hospital Admissions for Respiratory and Cardiovascular Disease and Outdoor Air Pollution in London. Archives of Environmental Health; 54(6): 399-411

Bates, D. (1995). Particulate Air Pollution. American Journal of Respiratory and Critical Care Medicine; 151: 669-674.

Baveye, P (2008). 'Aggregation and toxicology of titanium dioxide nanoparticles', Environmental Health Perspectives, 116(4): A 152.

Cacciola, R.R., Sarva, M. and Polosa, R. (2002). Adverse respiratory effects and allergic susceptibility in relation to particulate air pollution: Flirting with disaster. Allergy 57: 281 – 286

Cheng, Y. H., Chao, Y. C., Wu, C. H., Tsai, C. J., Uang, S. N. and Shih, T. S. (2008). 'Measurements of ultrafine particle concentrations and size distribution in an iron foundry', Journal of Hazardous Materials, 158, 124-130.

Colvile, R.N., Hutchinson, E.J., Mindell, J.S. and Warren, R.F. (2001). The transport sector as a source of air pollution, Atmospheric Environment 35 (9): 1537–1565

Dallmann, T.R., Onasch, T.B., Kirchstetter, T.W., Worton, D.R., Fortner, E.C., Herndon, S.C., Wood, E.C., Franklin, J.P., Worsnop, D.R., Goldstein, A.H., and Harley, R.A. (2014) Characterization of particulate matter emissions from on-road gasoline and diesel

vehicles using a soot particle aerosol mass spectrometer. Atmospheric Chemistry and Physics 14: 7585-7599

DEH - Department of the Environment and Heritage (2004). Health Impact of Ultrafine _Particles; Desktop Literature Review and Analysis, Commonwealth of Australia, Canberra, ISBN 0642550557.

Donaldson, K., Li, X.Y. and MacNee, W. (1988). Ultrafine (nanometer) particle mediated lung injury. Journal of Aerosol Science, 29, 553 – 560

ECJRC – European Commission Joint Research Centre (2002). Guidelines for Concentration and Exposure – Response measurement of fine and ultrafine particulate Matter for use in Epidemiological Studies. European Commission, Italy. EUR 20238 EN 2002, L.M.D. Schwela D. Kotzlas.

Fakinle, B.S., Sonibare, J.A., Akeredolu, F.A., Okedere, O.B. and Jimoda, L.A. (2012). Toxicity Potential of Particulates in the Airshed of Haulage Vehicle Park. Global NEST Journal. In press.

Libby, M. (Adopt-a-Lake and Project WET Wisconsin). (2007). "North American Lake Management Society - Water-Words Glossary". Retrieved 2008-03-02

Masjuki, H.H., Karim M.R. and Mahlia, T.M.I. (2004). Energy use in the transportation sector of Malaysia. Economic planning unit of the Prime Minister's Department, Consultancy Unit, University of Malaya, Kuala Lumpur.

Maynard, A.D., Kuempel, E.D. (2005), 'Airborne nanostructured particles and occupational health', Journal of Nanoparticle Research 7, 587 - 614.

Morawska, L., Ristovski, Z., Jayaratne, E.R., Keogh, D.U. and Ling, X. (2008). Ambient nano and ultrafine particles from motor vehicle emissions: Characteristic, ambient processing and implications on human exposure. Atmospheric Environment, 42, 8113 – 8138.

Oberdörster, G. (2000). 'Toxicology of ultrafine particles: In Vivo studies', Philosophical Transactions of the Royal Society London A 358, Pope III, C. A., (2000). Review: Epidemiological basis for particulate air pollution health standards, Aerosol Science and Technology; 32, 4 – 14.

Ramachandran, G., Paulsen, D., Watts, W., Kittelson, D. (2005). 'Mass, surface area and number metrics in diesel occupational exposure assessment', Journal of Environmental Monitoring. 7, 728-735.

Saija, S. and Romano, D. (2002). A methodology for the estimation of road transport air emissions in urban areas of Italy, Atmospheric Environment 36 (34) 5377–5383.

Shee sley, R.J., Schaver, J.J., Zheng, M. and Wang, B. (2007). Sensitivity of Molecular Marker – based CMB models to biomass burning Source profiles. Atmospheric Environment 39, 9050 – 9063.

Soylu, S., (2007). Estimation of Turkish road transport emissions, Energy Policy 35 (8): 4088–4094.

Full Paper

ASSESSMENT OF THE PHYSICAL AND MECHANICAL PROPERTIES OF TREATED KENAF FIBRE CEMENT COMPOSITES

S.O. Amiandamhen
Department of Forestry and Wildlife Management,
Faculty of Agriculture.
University of Benin,
Benin City, Nigeria.

D.N. Izekor
Department of Forestry and Wildlife Management,
Faculty of Agriculture.
University of Benin,
Benin City, Nigeria.
david.izekor@uniben.edu

ABSTRACT

This study investigated the effect of pretreatment on the properties of kenaf fibre cement boards. Homogenous fibre cement boards were made from kenaf bast fibres, cement and water. The fibres were cut into smaller sizes, mixed with cement and water and formed in rectangular moulds. After demoulding, the boards were cured for 28 days. The boards were manufactured at three pretreatment levels which include hot water, 3% $CaCl_2$, hot water and 3% $CaCl_2$ and a control. The fibre cement boards were tested for Modulus of Rupture (MOR), Modulus of Elasticity (MOE), Internal Bonding (IB), Water Absorption (WA), Thickness Swelling (TS) and Linear Expansion (LE). Also nail ability and withdrawal resistance, termite, fungi and fire resistances were also assessed. The results showed that the mean MOR ranged from 1.31 to 8.25 N/mm^2; the mean MOE from 78.0 to 1636.3 N/mm^2 for all treated boards. Mean water absorption ranged from 27.52% to 67.64% and the mean thickness swelling from 14.51% to 48.01% for all treated boards. Statistical analysis showed that the effects of the pretreatments were significant on the properties evaluated ($p < 0.05$). The study concluded that hot water combined with $CaCl_2$ treated boards exhibited the best mechanical and physical properties.

Keywords: *Fibre cement boards, kenaf bast fibres, mechanical properties, physical properties, pretreatments*

1. INTRODUCTION

Composites are materials in which a homogeneous matrix component is reinforced by a stronger and stiffer constituent that is usually fibrous but may have a particulate or other shape (Gerstle, 1991). Fibre reinforced composites are composed of axial particulates embedded in a matrix material; the objective of which is to obtain a material with high specific strength and high specific modulus of elasticity good enough for its weight. The strength is obtained by having the applied load transmitted from the matrix to the fibres; hence, interfacial bonding is important. Therefore, a fibre reinforced composite is a building material that consists of three components; the fibres as the discontinuous or dispersed phase; the matrix as the continuous phase; and the fine inter-phase region also known as the interface (Cantwell and Morton, 1991). Fibre cement materials can offer a variety of advantages over traditional construction materials. When compared to wood, fibre cement products offer improved dimensional stability, moisture resistance, decay resistance and fire resistance. When compared to cement based materials without fibres, fibre cement products may offer improved toughness, ductility and flexural capacity as well as crack resistance and nail ability (Mohr *et al.*, 2006).

Synthetic fibres such as glass, roselle and a number of agricultural materials including coffee husk, maize husk, bagasse, and bamboo among others to reinforce cement composite boards (Mohr *et al.*, 2006). As the demand for composite board increases, researchers have to look at possible alternatives to reinforce cement such as natural fibres for the production of value-added composites. Natural fibres exist in abundance and are readily available at low cost being derivable from various parts of vegetable materials such as leaves, stems, fruits, or wood. These fibres can be incorporated into the cement matrix in discrete and discontinuous form. The major advantage of natural fibre reinforcement is to impart additional energy absorbing capacity in the end product. Natural fibres absorb large amounts of water and have high energy absorbing capacity resulting from their low modulus of elasticity (Ismail, 2007). This study investigated the effect of pretreatment of kenaf bast fibres on the mechanical and physical properties of cement composites while observing other durability properties.

2. MATERIALS AND METHODS

The kenaf bast fibres were obtained from the Institute of Agricultural Research and Training (IAR&T), Moore Plantation, Ibadan. The fibres were cut into smaller sizes of 3cm-4cm. This was done to avoid balling problem during mixing and to facilitate homogeneous mixing of the composite. Ordinary Portland cement was used as the binding material. Other materials used include: water, wooden rectangular mould, cellophane sheets, paper tape and calcium chloride ($CaCl_2$).

2.1. Sample Preparation

The fibres were divided into four portions, three were treated and the untreated was used as control. The treatments were hot water only; hot water + CaCl2; and CaCl2 only. The hot water treatment was carried out by soaking the fibres in aluminum bath at 100 oC for an hour. Thereafter, the water was drained and the fibres were air-dried to a moisture content of approximately 12%. The chemical treatment was applied by the addition of calcium chloride (at 3% of the cement weight) during the board manufacture. Each treatment and the control were repeated at least three times. The fibres and cement were weighed and packed in labeled polythene bags for ease of identification. The fibre cement mixing ratio was 1:1.5 (292.8 g kenaf

fibres to 439.2 g Portland cement). The weighed samples were placed in a plastic bowl and mixed properly. Water (316.224 ml) was added to the mixture and stirred thoroughly until homogenous slurry was formed. For samples treated with CaCl2, 13.18 g (3% of the cement weight) was dissolved in water prior to wet mixing. The quantity of water used for mixing was calculated from Equation (1) developed by Badejo (1988).

$$Q = 0.6Z + (0.3 - R)xH \quad (1)$$

Q = Quantity of water (ml)
Z = Mass of cement in the board (g)
R = Moisture content of the fibre material (%)
H = Mass of fibre in the board (g)

2.2. Board Formation

Wooden moulds of 350 mm x 350 mm x 6 mm were used. The mould was placed on a caul plate and covered with cellophane sheet in order to prevent the formed boards from sticking to the plate. The slurry was spread in the mould and was pressed to enhance uniform mat formation and to reduce the thickness of the board. The board formed was labeled using a paper tape to identify boards of different treatments. The labeled board was covered with another cellophane sheet and a wooden plate was placed on it. It was then compressed with a hydraulic cold press under a pressure of 1.28 N/mm^2 to a uniform thickness of 6 m. After 24 h, the boards were demoulded. The demoulded boards were arranged in an out-door environment and allowed to cure for 28 days.

2.3. Board Test

After curing, the boards were trimmed to avoid edge effects and then cut into smaller test sample sizes. The tests carried out on the boards are mechanical and physical properties. Durability properties assessed include termite resistance, fungi resistance, fire resistance, nail ability and withdrawal resistance.

2.3.1. Test for Mechanical Properties

The mechanical properties test carried out include modulus of rupture (MOR), modulus of elasticity (MOE) and internal bonding (IB). The mechanical properties of the board produced were determined using test samples of 50 mm (width) by 150 mm (length). Three test samples were randomly selected from the boards for each property test. The samples were tested with an automated universal testing machine at cross head speed of 5 mm/min.

2.3.2. Test for Physical Properties

Sample sizes of 50 mm (length) x 50 mm (width) were used to carry out the test for physical properties. The properties tested for include water absorption (WA), thickness swelling (TS) and linear expansion (LE). Samples were tested for weight and dimensional stability after 24 h and for durability in prolonged immersion in water for 48 h. Three test samples were randomly selected from the boards for each property test. These were completely immersed in distilled water at a temperature of about 20 ± 2 oC for 24 h. The initial weight and dimensions of the test samples were measured using an electronic balance and a digital caliper respectively. At the end of the immersion period, the samples were drained for about 10 minutes and re-measured. The procedure was repeated for another 24 h but the samples disintegrated on prolong immersion before the end of the period. Thereafter, water absorption, thickness swell and linear expansion after the first 24 h were calculated from the increase in weight and dimensions of the samples after immersion using Equation (2).

$$X(\%) = \frac{M1 - M0}{M0} X\ 100 \quad (2)$$

X = Measured physical property
M_1 = Final measurement after immersion (mm)
M_0 = Initial measurement before immersion (mm)

2.3.3. Nail ability and Withdrawal Resistance

This test gives an indication of the ease of nailing, nail holding capacity and nail withdrawal strength. Test samples were nailed at the centre and at the edges to a rod and the fastener were gradually withdrawn. The ease of nailing and withdrawal, ability to hold nails and occurrence of splits were visually observed.

2.3.4. Termites and Fungi Resistance

This test measures the ability of the fibre cement composites to resist attack by termites and decaying fungi. Test samples were inserted in active termite mound. In the latter test, samples were partially earthed in decaying organic humus. The samples were visually observed at monthly intervals for a period of 6 months. Presence or resistance to attack by termites and decaying fungi was physically assessed during the period of observation.

2.3.5. Fire Resistance

This test measures the ability of the composites to withstand sudden fire outbreak. Test samples were placed in burning flame heated with dry wood and were observed quarterly for a period of one hour. The ease or resistance to char by the burning samples was physically assessed at each time interval.

2.4. Statistical Analysis

The experiment was arranged in a completely randomized design (CRD) with three treatments and a control. The experiment was carried out in three replicates. Analysis of variance procedure was conducted to investigate the effect of the pretreatments on the mechanical and physical properties of the fibre cement boards. Duncan's Multiple Range test was used in the separation of means where significant differences occur.

3. RESULTS AND DISCUSSION

3.1. Effect of Pretreatment on Modulus of Rupture (MOR)

Fibre cement boards produced using pretreatments have high MOR than those without pretreatment, Table 1. The boards produced from hot water and additive chemical (3% $CaCl_2$) treatment have the highest mean MOR of 8.25 N/mm^2, followed by boards produced from hot water treatment only with a mean value of 6.94 N/mm^2. Boards produced with $CaCl_2$ treatment only have a mean value of 1.31 N/mm^2 while the untreated boards have the lowest mean MOR of 0.45 N/mm^2. This shows that pretreatments such as hot water and $CaCl_2$ have positive effect on the MOR of fibre cement boards. This result is in line with the findings of Olorunnisola (2007) that $CaCl_2$ treated samples generally have higher MOR than untreated samples. Ferraz *et al.* (2011) also submitted that $CaCl_2$ and hot water treated samples had high MOR values.

Table 1: Mechanical properties of kenaf fibre cement boards

Pretreatments	Mechanical properties		
	MOR(N/mm^2)	MOE (N/mm^2)	IB (N/mm^2)
Hot water only	6.94 ± 2.14	1636.30± 131.54	0.17 ± 0.01
$CaCl_2$ only	1.31 ± 0.81	78.00 ± 26.04	0.04 ± 0.02
Hot water + $CaCl_2$	8.25 ± 2.91	1429.20± 169.28	0.15 ± 0.08
No treatment	0.45±0.15	10.30 ± 5.29	0.02 ± 0.01

Each value represents mean data with standard deviation of 3 replicates

3.2. Effect of Pretreatment on Modulus of Elasticity (MOE)

The mean values of MOE of the fibre cement boards produced ranged from 10.3 N/mm^2 to 1636.3 N/mm^2 as shown in Table 1. Fibre cement boards produced from hot water treatment only have the highest mean MOE of 1636.3 N/mm^2, followed by those produced from hot water and $CaCl_2$ treatment with a mean value of 1429.2 N/mm^2.

Boards made of $CaCl_2$ treatment only have mean value of 78.0 N/mm^2 while boards produced with no treatment have the lowest mean MOE of 10.3 N/mm^2. This shows that pretreatment has a positive effect on MOE of fibre cement boards. This is similar to the report of Ferraz *et al.* (2011) with hot water treatment having the highest MOE value. However, Amiandamhen and Izekor (2013) reported an improvement in MOE with increase in fibre size. Furthermore, Clausen *et al.* (2001) and Li *et al.* (2004) reported that particle geometry has a greater control on stiffness of manufactured fibre boards.

3.3. Effect of Pretreatment on Internal Bonding (IB)

The mean values of IB of the fibre cement boards produced ranged from 0.02 N/mm^2 to 0.17 N/mm^2, Table 1. Fibre cement boards produced using hot water treatment only, hot water and $CaCl_2$ treatment, $CaCl_2$ treatment only and no pretreatment have mean IB values of 0.17 N/mm^2, 0.15 N/mm^2, 0.04 N/mm^2 and 0.02 N/mm^2 respectively. This result shows that pretreatment has a positive influence on the internal bonding ability of the fibre cement boards. It could be explained that pretreatments fibrillates the fibre surfaces, thereby enabling fibre-fibre bonding.

3.4. Effect of Pretreatment on Water Absorption (WA)

Fibre cement boards produced using different treatments have mean WA ranging from 27.52% to 90.62%. Boards produced with no pretreatment have the highest mean WA of 90.62%, followed by $CaCl_2$ treated boards with 67.64% and hot water treated boards with 33.29% while boards produced from both hot water and $CaCl_2$ treatment have the lowest mean WA of 27.52%. This result shows that fibre cement boards produced using different pretreatments have lower WA percentage compared to those produced with no pretreatment as a result of better bonding in the treated boards. This means that pretreated boards are more dimensionally stable.

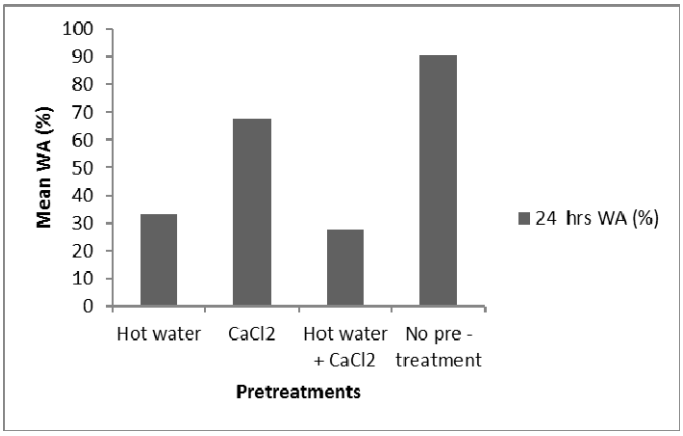

Fig. 1: Mean percentage water absorption of the boards

3.5. Effect of Pretreatment on Thickness Swelling (TS)

Fibre cement boards produced using different treatments have mean TS ranging from 14.51% to 48.01%. $CaCl_2$ treated boards have the highest mean TS of 48.01%, followed by the boards with no pretreatment with a mean value of 21.59%, then the boards treated with hot water only with a mean value of 16.55%. The boards treated with both hot water and $CaCl_2$ have the lowest mean TS of 14.51%. This result shows that pretreatments such as hot water only and both hot water and $CaCl_2$ are effective methods of reducing thickness swelling thereby making the boards more dimensionally stable. Also, pretreatment decreases thickness swelling by enhancing the bonding between fibers and cement. However, $CaCl_2$ treated boards exhibited highest TS percentage. This could be explained as a function of the hygroscopic nature of the additive which increased moisture migration at the edges.

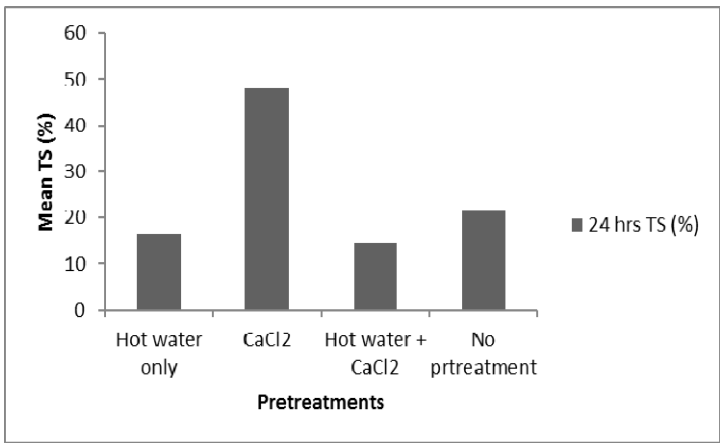

Fig. 2: Mean percentage thickness swelling of the boards

3.6. Effect of Pretreatment on Linear Expansion (LE)

Fibre cement boards produced using hot water only, $CaCl_2$ and hot water, $CaCl_2$ only and no pretreatment have mean LE of 2.69%, 4.43%, 4.99% and 6.62% respectively. Boards produced with no pretreatment have the highest mean LE of 6.62% while the boards produced with hot water treatment only have the lowest mean percentage of 2.69%. This observation shows that pretreatment helps to decrease linear expansion by embedding fibres into the cement matrix which restricts expansion of the fiber cement boards.

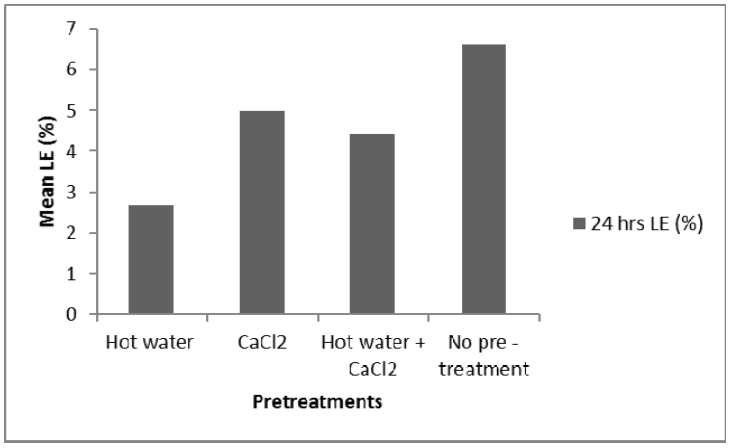

Fig. 3: Mean percentage linear expansion of the boards

Table 2 shows that all variables considered in the production of the fibre cement boards were significant on the mechanical properties and water absorption WA but the variables were not significant for thickness swelling TS and linear expansion LE ($p < 0.05$). This implies that pretreatments have significant effect on the properties assessed on the fibre cement boards. However, pretreatment effect was highly significant on WA.

Table 2: ANOVA Procedures for the properties of the boards

	Mechanical properties			Physical properties		
	MOR	MOE	IB	WA	TS	LE
F value	13.52	7.23	9.40	152.59	3.45	2.81
Pr > F	0.0017	0.0115	0.0053	< 0.0001	0.0715	0.108

Table 3 shows the mean separation of the pretreatments in the properties assessed. It would be observed that there is no significant difference in hot water only and hot water combined with $CaCl_2$ treatment on the mechanical and physical properties of the fibre cement boards. Also, there is no significant difference in $CaCl_2$ treatment and control on the mechanical properties of the fibre cement boards.

Table 3: Duncan's Multiple Range test for the fiber cement boards

Pre treatment	MOR	MOE	IB	WA	TS	LE
Hot water only	6.94[a]	1636.30[a]	0.17[a]	33.29[c]	16.55[b]	2.69[b]
$CaCl_2$ only	1.31[b]	78.00[b]	0.04[b]	67.64[b]	48.01[a]	4.99[ab]
Hot water + $CaCl_2$	8.25[a]	1429.2[a]	0.15[a]	27.52[c]	14.51[b]	4.43[ab]
No pretreatment	0.45[b]	10.3[b]	0.02[b]	90.62[a]	21.59[ab]	6.62[a]

Data in the same column with the same letter are not significantly different ($p \leq 0.05$)

3.7. Durability Properties

The durability of fibre cement boards in different conditions was also investigated. It was observed that the composites were highly resistant to fungi and termite attack within duration of six months for treated and non-treated boards (Table 4 and 5). This implies that the boards are structurally durable for outdoor applications. The boards were also moderately resistant to fire within a period of 30 minutes. However, the boards showed no resistance at 60 minutes exposure (Table 6). The properties observed in this study can be attributed to the constituents of cement like lime, silica, alumina and metal oxides which are intolerant to insects and fungi. Finally practical demonstrations revealed that the boards produced have high nail holding capacity and can withstand nail withdrawal with little or no splits at the edges.

Table 4: Fungi resistance properties of the composites

Period	Pretreatments			
(Weeks)	No treatment	$CaCl_2$ only	Hot water only	$CaCl_2$ + hot water
4	2	2	2	2
8	2	2	2	2
12	2	2	2	2
16	2	2	2	2
20	2	2	2	2
24	2	2	2	2

Table 5: Termite resistance properties of the composites

Period	Pretreatments			
(Weeks)	No treatment	$CaCl_2$ only	Hot water only	$CaCl_2$ + hot water
4	2	2	2	2
8	2	2	2	2
12	2	2	2	2
16	2	2	2	2
20	2	2	2	2
24	2	2	2	2

Table 6: Fire resistance properties of the composites

Period	Pretreatments			
(Minutes)	No treatment	$CaCl_2$ only	Hot water only	$CaCl_2$ + hot water
15	1	1	2	2
30	0	1	1	1
45	0	0	1	1
60	0	0	0	0

0 – Not resistant
1 – Moderately resistant
2 – Highly resistant

4. CONCLUSIONS

It can be concluded from this study that pretreatments have a positive effect on the properties tested on the fibre cement boards. Modulus of rupture (MOR), modulus of elasticity (MOE) and internal bonding (IB) were greater in treated boards than in the untreated boards while thickness swelling (TS), water absorption (WA) and linear expansion (LE) were lower in treated boards compared to untreated boards. Hot water combined with $CaCl_2$ pretreatment produced boards with the best mechanical and physical properties.

Fibre cement boards are generally resistant to fungal and termites attack. Pretreated boards are more resistant to fire compared to untreated boards. Fibre cement boards have high nail-holding capacity and can withstand nail withdrawal with little or no splits at the centre and edges.

REFERENCES

Amiandamhen, S.O. and Izekor, D.N. Effect of wood particle geometry and pretreatments on the strength and sorption properties of cement bonded particle boards. Journal of Applied and Natural Science 5 (2): 318-322, 2013.

Badejo, S.O.O. Effect of flake geometry on properties of cement-bonded particle board from mixed tropical hardwoods. Journal of Wood Science and Technology 22:357-370, 1988.

Cantwell, W.J. and Morton, J. The impact resistance of composite materials, a review. Composites 22 (5): 347-362, 1991.

Clausen, C.A., Kartal, S.N. and Muehl, J. Particleboard made from remediated CCA-treated wood: evaluation of panel properties. Forest Products Journal 51(7/8): 61-64, 2001.

Ferraz, M.J., Menezzi, H.S., Teixeira, D.E. and Martins, S.A. Coir fiber cement composites. Bioresources 6(3): 3481-3492, 2011.

Gerstle, F.P., Composites. Encyclopedia of polymer science and engineering, Wiley, New York, 1991.

Ismail, M.A., Compressive and tensile strength of natural fibre-reinforced cement based composite. Al-Rafidain Engineering 15 (2): 42-45, 2007.

Li, W., Shupe, T.F. and Hse, C.Y., Physical and mechanical properties of flake board produced from recycled CCA-treated wood. Forest Products Journal 54(2): 89–94, 2004.

Mohr, B.J., El-Ashkar, N.H., and Kurtis, K.E., Fibre cement composites for housing construction, state of the art review. 112-125, 2006.

Olorunnisola, A.O., Effects of particle geometry and chemical accelerator on strength properties of Rattan cement composites. African Journal of Science and Technology 8 (1): 22-27, 2007.

Full Paper

DESIGN MODIFICATIONS OF GAS COOKER BURNER FOR OPTIMAL THERMAL EFFICIENCY

T.A. Morakinyo
Department of Food Science and Technology,
Obafemi Awolowo University,
Ile-Ife.
morakzotec@yahoo.com

B.V. Omidiji
Department of Mechanical Engineering,
Obafemi Awolowo University,
Ile-Ife.

H.A. Owolabi
Department of Mechanical Engineering,
Obafemi Awolowo University,
Ile-Ife.

ABSTRACT

Design modification of gas cooker burner for domestic cooking is highly important to enhance acceptability of gas cooking facility globally. Typical material of existing burner was modified by increasing its thickness and also by changing the material of the product from mild steel to galvanize steel to eradicate corrosion at minimum cost. A progressive combination die coupled with drilling fixture for the production of burner were designed, manufactured and evaluated. The die and fixture were used for blanking, piercing and forming of four different burners of port sizes: 2.0, 2.5, 3.0 and 3.5 mm. The most effective burner port size was determined using response surface 3D to generate curves between cooking period, burner head temperature and food cooking temperature against port sizes. Uni-axial compressive test was carried out on cooked rice and beans to investigate their rheological properties. The rice and beans cooking temperatures were found to be: 170 and 180; 150 and 165; 140 and 160; 140 and 160 ^{o}C for 2.0, 2.5, 3.0 and 3.5 mm burner port sizes respectively. These results have shown that, burner port size of 2.0 mm exhibited optimum thermal efficiency than any other port sizes. The poison ratios of cooked rice and beans were found to be: 0.25, 0.28, 0.30 and 0.35, 0.23, 0.26, 0.28 and 0.31 for 2.0, 2.5, 3.0 and 3.5 mm burner port sizes respectively. Likewise, the poison ratios of cooked beans were measured to be: for 2.0, 2.5, 3.0 and 3.5 mm burner port sizes, respectively.

KEYWORDS: *Progressive combinations die, press tool, material utility percentage, forming and stripping forces. rheological properties.*

1. INTRODUCTION

Fossil fuels are thought of as cornerstones of our modern age. They generate our electricity, heat homes in temperate countries, fuel our cars, and even form plastics from which many of our modern utensils are made. More so, fossil fuels have played key roles for hundreds of years of our history, driving our transition from a primitive and pre-industrial society to one capable of both encircling this world and reaching beyond (Energy Aware Organization, 2006). Its history begins nearly three centuries ago. Before its exploration, wood and animal fats were common fuels, used primarily for cooking and heating. Fossil fuel originated in the late 18th century, they were formed from the remains of tiny sea plants and animals that died millions of years ago. Over time these organic debris sank into the bottom of the oceans and were buried by thousands of feet of sand and sediment, which turned into sedimentary rock. As the layers increased, they were subjected to high temperature and pressure. The heat and pressure eventually changed the remains into petroleum.

Petroleum is classified as a nonrenewable energy source, because it is depleting and irreversible. Today, we drill through the layer of sedimentary rock to reach the rock formations that contain oil and gas deposits. The crude oil is a liquid fuel mixture of hydrocarbons consisting roughly six parts of carbon and one of hydrogen, with some impurities such as salt sulphur, oxygen, metals and nitrogen. Refining of crude oil is a process in which mixture is heated in a vacuum to 600 ^{o}C by injecting superheated steam and pumped through the bottom of a vertical distillation column. As the vapour rises up the column, separation occurs by cooling. The column has trays at different heights with holes. Hence, the cooled fractions with different boiling points liquefied, collected and drained off. The principal products with their corresponding boiling points, are liquefied petroleum gas (LPG) (20 ^{o}C), petrol (70 ^{o}C), naphtha (40 ^{o}C), diesel (200 ^{o}C), kerosene and jet fuel (120 ^{o}C), lubricant (300 ^{o}C), and furnace oil (370 ^{o}C). Solid petroleum coke will be collected after liquid fractions were drained (USDE, 2003; GEPI, 2014). LPG consists of propane, propylene, butane, and butylenes. The product used for domestic heating is composed primarily of propane. LPG has two origins: 60% is recovered during the extraction of natural gas and oil from the earth, and the remaining 40% is produced during the refining of crude oil. LPG can be classified under three major grades; commercial-grade butane, engine fuel-grade propane and the commercial-grade butane. It is heavier than air, and liquefies under pressure, which is an added advantage for its haulage. It is generally use as household cooking gas, internal combustion engine fueling, furnace, oven and refrigerant. More than 4 million vehicles are estimated to be powered by LPG in the world. Different improvements had been made in gas cooking from time to time overcoming various challenges. The domestic device with which gas cooking can be achieved is the gas stove/cooker. It refers to as a kitchen appliance that can be used either to generate warmth during cooking (Howell et al., 1996). Gas cooker became a huge commercial success with some 90,000 units sold in the last 30 years, as reported by Gotrinity (2012). In Nigeria, most of this very important energy source is often subjected to flaring, where adequate storage facilities and pipelines were not provided (LPG Exceptional energy, 2012). The Information Age (1999) reported that James Sharp in Northampton, England, was first engineer that patented a gas stove in 1826 and opened a gas stove factory in 1836. More so, during London world fair in 1851, this company exhibited a gas stove, but this invention was not commercialized till 1880s, due to delay in gas pipeline installation. Travis, 1998 reported that, gas stove of enamel wares production started 1910 to eliminate corrosion and for easy cleaning. A high-end gas stove called the AGA cooker was invented in

1922 by Swedish Nobel prize winner. It is considered to be the most efficient design, despite the heavy price tag (Merriman, 2011). Gas stoves had been modified to certain extent by eliminating burner corrosion, through the use of non-metallic materials such bronze, brass, copper and zinc (Hardesty and Weinberg, 1974; Muthukumar, 2011; Michelle 2011). Other modifications were chrome plating of burners, cylinder cum burner design, and burner tripod stand for more air mixture to enhance combustion (Sathe et al., 1990; Zhang, 1997; Worgas, 2011). Even though gas stove had been in existence for years there are still various researches going on to improve its performance efficiency and to reduce emissions (Nelson, 1991; USEPA, 1999; Ashok, 2009).

In Nigeria, there are very few companies that embark on the production of LPG cooker burners such as Nigeria Gas Cylinder, Ijoku Ibadan and Midland Gas Cylinder Abeokuta (formerly located at Isolo Lagos). With the rapid growth in the technological development of our country and in collaboration with World Bank finance project, the laying of gas pipelines has commenced. This necessitated for design modification of exiting gas burner to enhance thermal efficiency and eliminate the incomplete combustion, which can result to environmental pollution. Furthermore, it was observed during preliminary survey that replacing the LPG gas burner was an expensive task and there was limited production, since most cookers are foreign products. This factor was the major reason, why many people could not embark on the use of LPG cooker. Therefore, the objective of this study was to modify the existing gas burner, by varying port sizes (circumferential pierced holes) for gas flaming to determine the best size that will support optimum thermal efficiency. Furthermore, this innovation will increase demand of LPG cooker that will eventually increase utility of LPG. More importantly, it will support generation of court-yard industries and mass production of LPG cookers at minimal cost to meet the crucial need of our society at large.

2. MATERIALS AND METHODS

The existing gas burner sample Fig.1 was obtained from Oshodi Market, in Lagos, Nigeria, of 3.0 mm port size. Adequate measurements of its dimensions were taken to avoid errors. The galvanized sheet was of 1.5 mm thickness was selected for the modify burner to replace the existing gas burner made from mild steel plate to eliminate corrosion. The blank profile was generated using Eq. (1) depicted below to be produced from the strip profile dimensions of 115 x 1240 mm. The material utility percentage was evaluated. Likewise scrap percentage was reduced to the minimal by adopting design procedures of Hinman (1950). The operational parameters of a Single stroke mechanical press of 25 Ton capacity were taken, such as its day light, short height, shoe holder diameter and bed slotted grove dimensions. A combination die for blanking and forming operation was designed and fabricated as described below.

2.2. Design Calculations

2.2.1. Determination of burner blank size.

The burner blank diameter was determined by making use of an existing old burner shown as Fig.1 shown above. For standardization purposes, all dimensions of the old burner were taken with the use of vernier calliper and radius gauge. The blank diameter was generated using Eq. (1)

$$D = a + \left(R_1 + q_1 + \frac{s}{2}\right)\frac{\pi\alpha_1}{180} + b + \left(R_2 + q_2 + \frac{s}{2}\right)\frac{\pi\alpha_2}{180} + c \quad (1)$$

source: ASTME (1959).

Where,

D = Diameter of blank

a = c = height of burner = 10.0 mm

b = Length of burner base = 80.0 mm

R_1= R_2 = Radius of curvature = 6 mm

s = Thickness of material = 1.5 mm

q_1= q_2 = Coefficient of material = 0.6 mm

α_1 = α_2 = angle of curvature to the horizontal plane = 90^0

The diameter of the burner calculated from the equation = 110 mm

2.2.2. Determination of blanking force

The blanking force was determined using Eq. (2) as shown below:

$$P = Lts \quad (2)$$

Source: Frank et al, (1965) and Morakinyo (2009)

Where,

L = forming circumference = πD = 345.71 mm

t = plate thickness = 1.5 mm

s = shear strength of steel = 350 MPa = 350 M N/m ^{2} = 350 N/mm^2 (Khurmi and Gupta, 2005; Morakinyo, 2009).

Therefore, the blanking force was calculated to be 181,497 N/10 = 18,149 kg = 18.2 tons

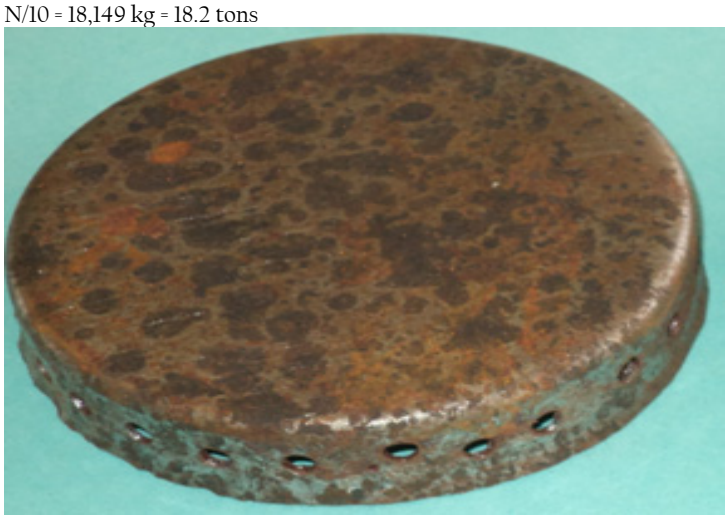

Fig. 1: Exiting Old Gas Burner
Scource: Oshodi market, Lagos

Power press of 25 tonnes was recommended by considering factor of safety of 35% for steel material (Khurmi and Guptal, 2006). The available power press at IFECO, Ketu, Lagos was preferred having these following configurations: Stroke of 80 mm, Adjustable heights facility of 75 mm, short height 150 mm, the day light 220 mm and the shank/ shoe holder was found to be 50 mm diameter with height of 60 mm.

2.3. Determination of ejector stripping force

The ejector stripping force was determined to facilitate appropriate selection of compression spring load for an effective ejection of both blank and formed gas burner after piercing operation. Frank et al. (1965) reported the collective submission of representatives of die makers and fabricators, that stripping pressure/force vary from 2.5 to 20% of blanking / punching force. Hence, 10% of the calculated blanking force was recommended as stripping force. Therefore, ejector stripping force = 2.5 ton. The corresponding compression spring that has the load capacity of 2.5 ton was selected having these dimensions: SWG 5/0, wire diameter 10.97 mm, free length 170 mm, and allowable stress of 364 MPa (Khurmi and Gupta, 2005).

2.3.1. Determination of forming force

The amount of forming force required for an effective interaction between punch and die was calculated using this mathematical expression shown below as Eq. (3).

$$F = \frac{KLSt^2}{W} \quad (3)$$

Source: Frank et al. (1965).

Where F = Bending force required at one side of the burner (ton)

K = Die opening factor influencing the spring back which varies from 1.2 for a die opening of 16 times metal thickness and above to 1.33 for a die opening of 8 times metal thickness. In this case, die opening was 81.5 mm equal to the outer diameter of old burner, which was more than 16 × 1.5 = 24 mm Therefore, K selected was 1.2.

S = Ultimate tensile strength of tons/in^2.The ultimate tensile strength of steel reported by Frank et al. (1965) was 40 tons/in^2. Blank area = 14.74 in^2

T = metal thickness = 1.5mm = 0.059 in,

W = Die opening = 81.5 mm = 3.33 in.

L = Blank diameter = 110 mm = 4.33 in

$$F = \frac{1.2 \times 4.33\ in \times 40\ tons \times 0.059\ in^2 \times 14.74}{3.33\ in \times in^2} = 3.33 \text{ tons.}$$

$$\text{Forming force} = 2 \times F + (\text{Blank area} \times 0.15) \quad (4)$$

Source: Frank et al. (1965).

Hence Forming force = 8.87 tons. This can be adequately delivered by selected mechanical powered press of 25-ton capacity.

2.4. Construction of press tools

The production of LPG gas burner for domestic cooking of food produce, involved design and construction of two separate dies, namely: progressive and combination die and blank piercing fixture. In this study, only a progressive combination die will be discussed in details. The progressive combination die was a pillar guided type of 200 mm vertical height. The explosive view of this die is shown in Fig. 2, while working components were listed on Table 1 with their corresponding dimensions.

2.4.1. Description of progressive and combination die

Upper bolster: This was made of low carbon steel of 40 × 270 × 230 (mm). At the centre of it was located a shoe holder with the help of M12 × 60 Allen bolt. Diagonally, two bushes/guides pillar were fixed such that both upper and bottom bolster will be concentric. The bushes were made of high carbon steel with hardness value of 45 HRC.

Die holder: This was made of medium carbon steel of 36 × 120 × 110 (mm). It was located at the bottom of upper bolster guided with two dowel pins for centrality and concentricity in coupled with combine die. It was heat treated to 40 HRC to avoid deformation of combine die.

Combine Die: The combine die was made of tool steel material of θ 110 mm outer and stepped turned to 81.5 mm inner diameter. It was hardened to 60 HRC and tempered to avoid cracking. This was coupled to the die holder with the help of dowel pins and fasteners. This die performed two functions of blanking with outer diameter of 110 mm and while the inner diameter of 81.5 mm was used for forming operation.

Bottom bolster: The bottom bolster was made of low carbon steel of 40 × 360 × 280 (mm). Two guided pillars of θ 30 mm x 195 mm were force fitted at a distance corresponding to centre distance observed on upper bolster. The blanking die was located at the centre of this bolster.

Blanking die: This was made of tool steel material of outer diameter of θ 160 mm and inner diameter of θ 110.25 mm It was hardened and tempered to the hardness value of 60 HRC. It was encasing pressure plate suspended with the help of ejector pins. These ejector pins were guided with spring upper plate, followed by the compression spring, located at the bottom bolster. The compression spring was retained by spring bottom plate with help of stud threaded at centre of the bottom bolster. The height of pressure plate was adjusted through the fastening of hexagonal bolt located below spring bottom plate, until its height was at parallel to blanking die.

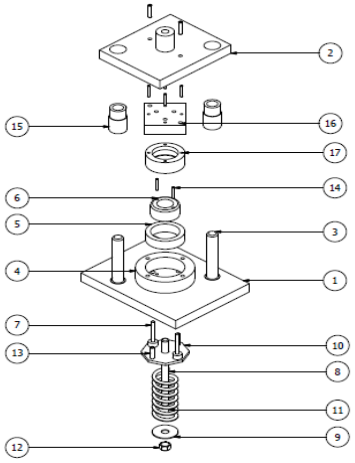

PARTS LIST			
S/N	QTY	PART NAME	MATERIAL
1	1	LOWER BOLSTER	Steel
2	1	UPPER BOLSTER	Steel
3	2	PILLAR	Steel
4	1	REVERSED PUNCH	Steel
5	1	PRESSURE PLATE	Steel
6	1	FORMING DIE	Steel
7	2	EJECTOR PIN	Steel
8	1	STUD	Steel
9	1	SPRING UPPER PLATE	Steel
10	1	SPRING LOWER PLATE	Steel
11	1	SPRING	Steel
12	1	Nut	Steel
13	8	Hex Stud-01	Steel
14	6	Hex Stud-02	Steel
15	2	BUSH	Steel
16	1	DIE HOLDER	Steel
17	1	DIE	Steel

Fig. 2: Exploded View of Combination Die for LPG Gas Burner Manufacturing

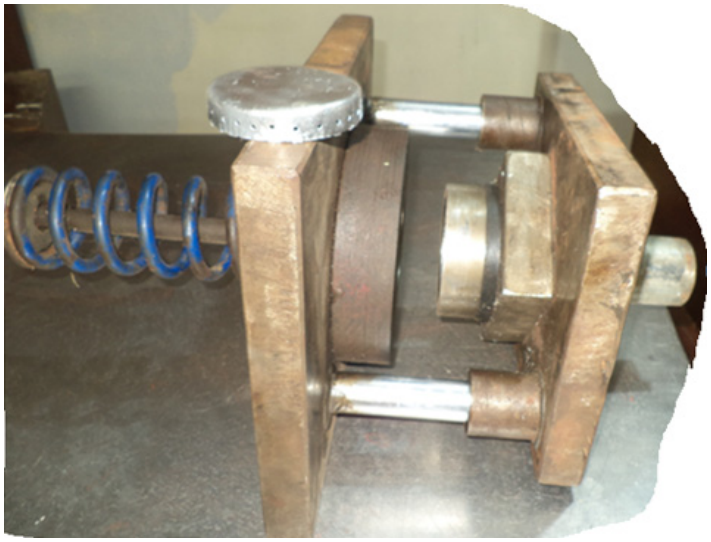

Fig. 3: Progressive and Combination Die with a sample of 2.0 mm Port Size Burner.

2.4.2. Blank piercing fixture

The production of gas cooker burner was done sequentially to reduce the cost of production. After the blanking operation, blanks were loaded inside piercing fixture at rate of five numbers at a time. The piercing fixture consists of blank holder of cylindrical shape, threaded externally to allow the fastened of cover plate that compressed drilling insert dies of different port sizes namely: 2.0, 2.5, 3.0 and 3.5 (mm). This drilling insert was made of tool steel of 10 mm thickness, having 30 holes (ports) at circumferential diameter of 78.0 mm and of equal diameter to blank size. To produce a set of burner of a particular port size, the corresponding insert die was loaded while the same size of drill bit was fitted on pillar drill machine chuck to pierce blank circumferentially. Thereafter, the pierced blanks were returned back to the progressive and combination die for forming operation by adjusting the stroke of mechanical powered press down ward till complete formation of gas burner was produced.

2.5. Performance Evaluation of Burners

The LPG burners produced with varying port sizes (circumferential pierced holes) were used extensively to determine optimum thermal efficiency. Two food items; rice and beans were

cooked with individual type of gas burners port sizes: 2.0, 2.5, 3.0 and 3.5 (mm) under the same regulatory gauge pressure of 2.0 Bar. Three dependent cooking variables were considered, namely: cooking period, burner head temperature and rice/beans boiling temperature measured against an independent variable (port size). The interactions of these variables were subjected to response surface 3D XYZ Plot for better interpretation. Finally, textural and rheological properties of both cooked food materials were subjected to uni-axial compression test for thorough investigation.

3. RESULTS AND DISCUSSION

The response surface 3D XYZ plots generated from the experimental data were shown as Fig. 3 to 10. The result indicated that, burner of port size 2.0 mm diameter has the shortest cooking times during the rice and beans cooking. Likewise, it exhibited the highest values of the cooking temperature for both food items. It was observed to be the best burner port size that converted the heat content of LPG as input energy into thermal energy efficiently with maximum cooking temperature. Furthermore, the optimum performance of burner port size 2.0 mm may be attributed to the fact that it has minimum diameter through which the gas atomized effectively which enhances blue flame generation. The performance evaluation data collected for 2.0, 2.5, 3.0, 3,5 mm port size burners were shown as Fig. 4, 5, 6 and 7 response surface diagrams respectively during rice cooking process. From the Fig. 4, the optimum burner head temperature of 92 °C commenced at 15 min and remained constant till the end of cooking period of 40 min, which generated ultimate rice cooking temperature of 170 °C. Considering Fig. 5 of burner port size 2.5 mm, its optimum burner head temperature of 92 °C arrived at 22.5 min and remained steady till the end of 40 min with maximum rice cooking temperature of 150° C. However, burner of 3.0 mm port size commenced its optimum burner head temperature of 92 °C at 35 min out of 40 min to produce rice cooking temperature of 140 °C. Generally, it was observed as burner port sizes increased the burner head and rice cooking temperature decreased. The same trends of observations were obtained during cooking of beans using port size burners of 2.0, 2.5 3.0 and 3.5 mm as demonstrated in Fig. 8, 9, 10 and 11 response surface diagrams. Fig. 8, depicted the performance evaluation diagram of 2.0 mm port size. The maximum burner head temperature of 92 °C occurred at 22 min and increased linearly to 95°C at the shortest period of 50 min during beans cooking with optimum temperature of 180 °C. Hence, in Fig. 9 of 2.5 mm burner port size, the maximum burner head temperature of 92 ° C commenced at 30 min and increased steadily to 93 °C at 55 min of beans cooking with optimum temperature of 165 °C.

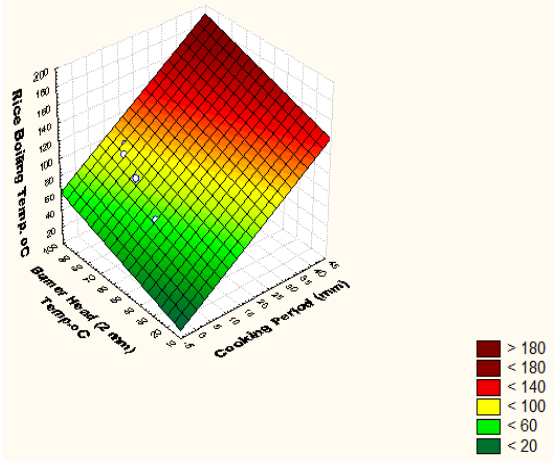

Fig. 4: Thermal Efficiency of 2.0 mm Burner size for Rice Cooking

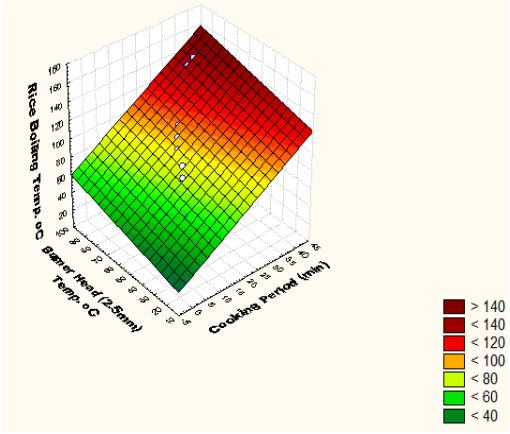

Fig. 5: Thermal Efficiency of 2.5 mm Burner size for Rice Cooking

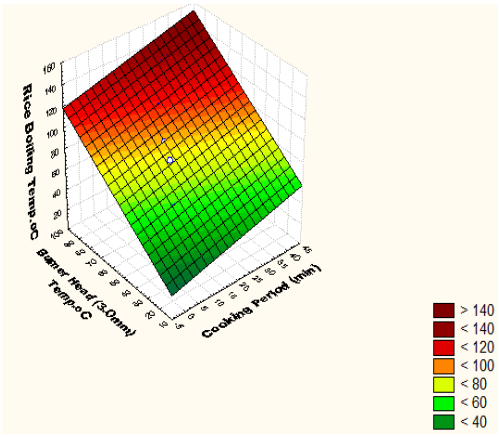

Fig.6: Thermal Efficiency of 3.0 mm Burner size for Rice Cooking

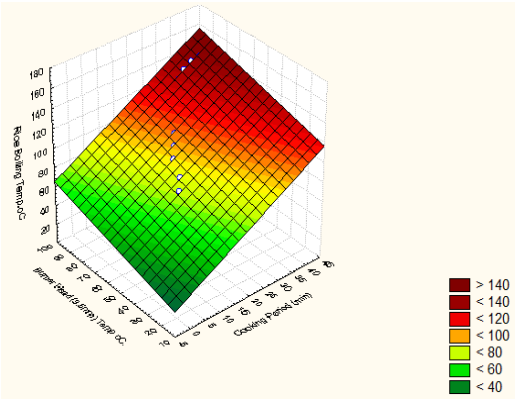

Fig.7: Thermal Efficiency of 3.5 mm Burner size for Rice Cooking

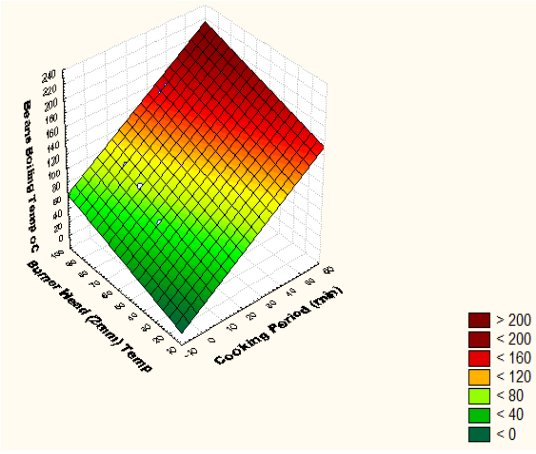

Fig. 8: Thermal Efficiency of 2.0 mm Burner size for Beans Cooking

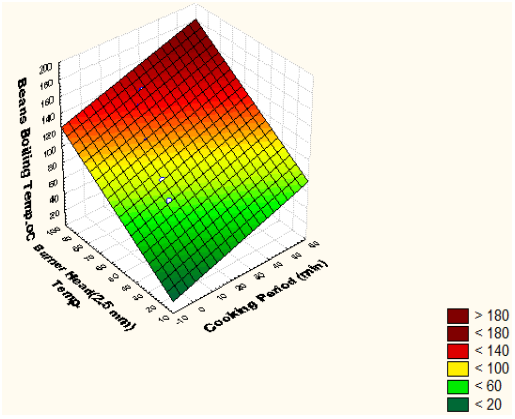

Fig. 9: Thermal Efficiency of 2.5 mm Burner size for Beans Cooking

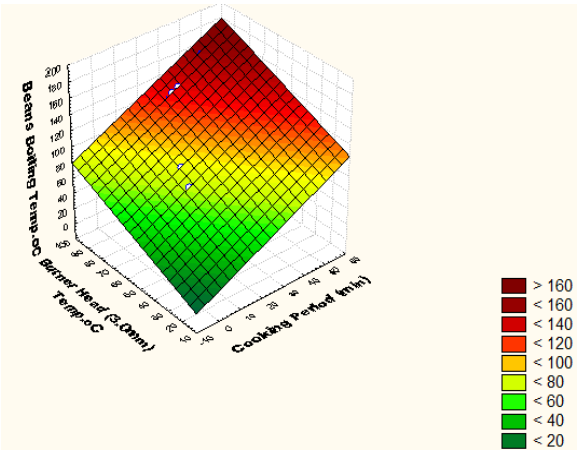

Fig. 10: Thermal Efficiency of 3.0 mm Burner size for Beans Cooking

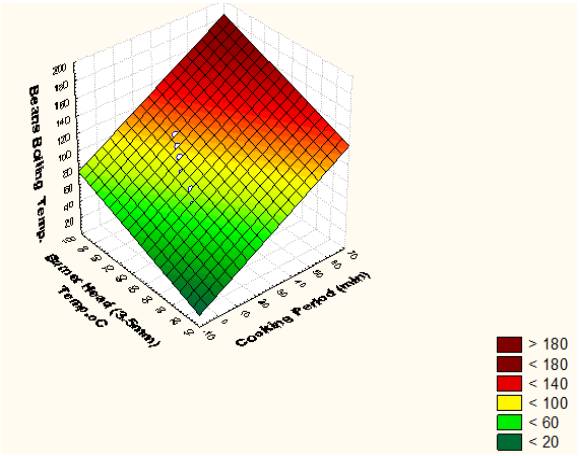

Fig. 11: Thermal Efficiency of 3.5 mm Burner size for Beans Cooking

Considered Fig. 10 of 3.0 mm burner port size, invariably, the maximum burner head temperature of 92 °C occurred at 35 min and remained constant till the end of beans cooking period of 57.5 min with optimum cooking temperature of 160 °C. Finally, Fig. 11 demonstrated performance evaluation of beans cooking on 3.5 mm burner port size, the maximum burner head temperature of 92 °C, commenced at 40 min and remained constant till longer period of 60 min was observed, which generated the optimum temperature of 160 °C. The results shown that during the cooking of rice and beans at separate period, gas burner of port size of 2.0 mm arrived at 92 °C earlier than any other gas burner port size. More importantly, cooking of both food materials were completed at minimum period and at higher temperature with gas burner of port 2.0 mm than remaining gas burner sizes. Since liquefied gas flow rate remain constant during the performance evaluation, it can be deduced that gas burner of 2.0 mm port size has higher thermal efficiency and more timely and economical than others.

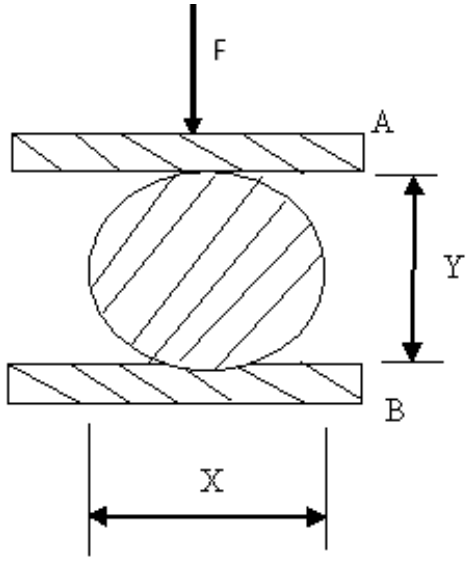

Fig. 12: Uni-axial compression test of Cooked Rice and Beans

Fig. 12, shown below, demonstrated the loading of the cooked food material during uni-axial compression test. Considered Fig. 13, 14, 15 and 16 of poison ratio, shown the axial and lateral strains curves of cooked rice and beans respectively during compression test. The results indicated that rice and beans cooked with 2.0 mm port size burner exhibited maximum values of axial and lateral strains under minimum application of compressive force, while rice cooked with 3.5 mm port size has minimum values of both axial and lateral strains. The poison ratios of cooked rice were calculated as: 0.25, 0.28, 0.30 and 0.35 for 2.0, 2.5, 3.0 and 3.5 mm burner port sizes respectively. Likewise, the poison ratios of cooked beans were also calculated as 0.23, 0.26, 0.28 and 0.31 for 2.0, 2.5, 3.0 and 3.5 mm burner port sizes respectively. These experimental results were compared favourably with other values reported by previous researchers on uni-axial compression test of grains and fruits. Moshsenin (1986) reported that most food materials exhibited poison ratio between: 0.2 to 0.5. The variability in their rheological properties validated differences in burners' thermal energy efficiency. It was also observed during uni-axial compression test, those samples of rice and beans cooked with burner of 2.0 mm port size arrived at their corresponding bio-yield point faster than those sample cooked with other burners. This relationship between the bio-yield point, compressive stress and sterilization were reported by Fellow (2000) and Sirisomboon et al. (2007).

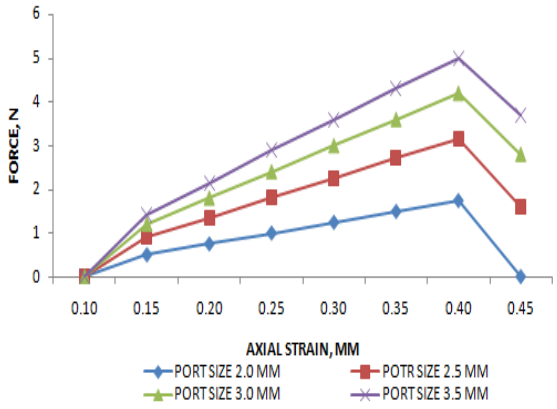

Fig. 13: Axial Strain of Cooked Rice Under Compression Test

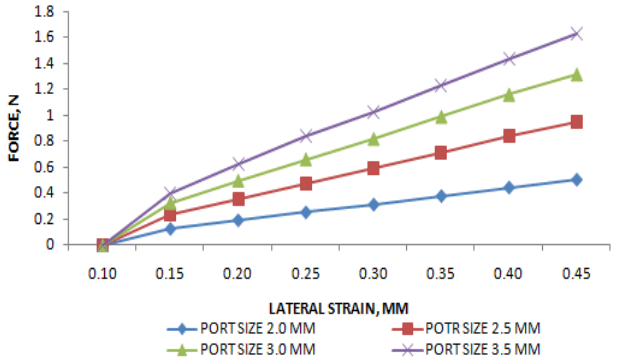

Fig. 14: Lateral Strain of Cooked Rice Under Compression Test

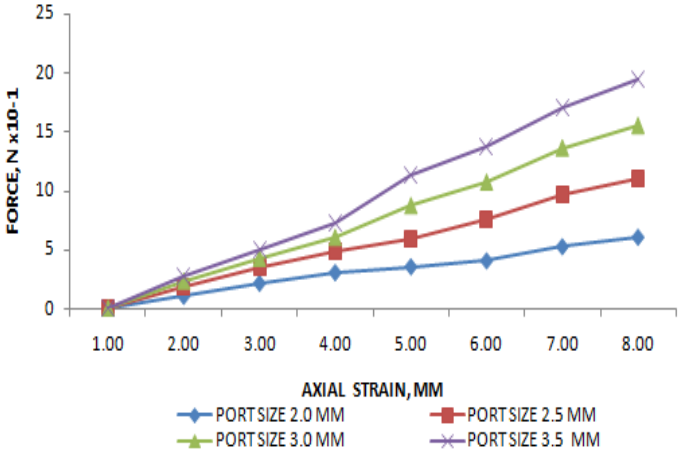

Fig. 15: Axial Strain of Cooked Beans Under Compression Test

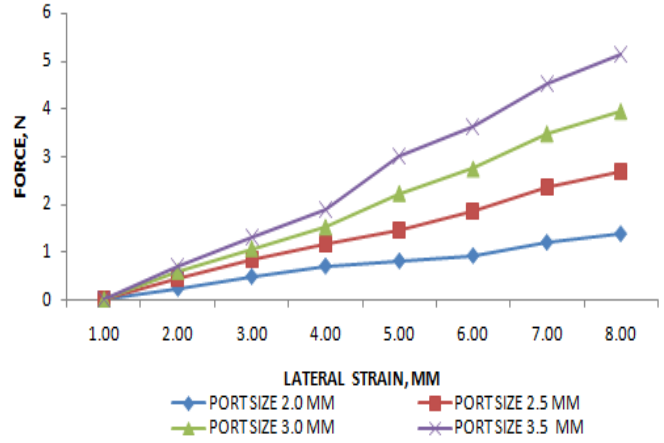

Fig. 16: Lateral Strain of Cooked Beans Under Compression Test

4. CONCLUSIONS

There are many areas in the gas industry where there is a definite need to bridge the gap between fundamental concepts and engineering application. The design of atmospheric gas burners for domestic and commercial appliances requires a judicious balance of characteristics. Knowledge of quantitative effects of all pertinent variables is therefore, necessary to achieve a desired balance in design. When designing a burner for domestic cooking, it is concluded that the use of smaller port sizes for gas burner when low gas supply is needed is advisable. This will enhance lean mixture, effective gas flame propagation and complete combustion to attain greater thermal efficiency. Gas cooker burner design research is a continuing process that involves fundamental concepts, the engineering design and metal forming technology.

REFERENCES

American Society of Tool and Manufacturing Engineers, Tool Engineers Handbooks, 2nd edition, McGraw-Hill Book Company, New York, 1959.

Ashok, S., "Domestic gas stove burner – old & new – a case study" www.energymeasuretosave.com, 2012.

Energy Aware Organization, "Fossil Fuels: Natural Gas", Retrieved from http://www.getenergyaware .org/energy-natural-gas.asp, 2006.

Fellows, P. Food Processing Technology. (2nd Edition) Wood head Publishing Limited, Abington Hall, Granta Park Cambridge. CB21 6AH, England, 2009.

Frank W.W, Phillip D. H and Charles B.G, JR, Die Design Handbook, McGraw-Hill Book Company, New York, 1965.

Gotrinity, W. Stoves, http://www.stoves.gotrinitywealth.com/gas-castiron-stoves. 2012.

Growth and Evolution of Petroleum Industry, Management Essay, www.uk essay.com, 2014.

Hardesty D.R., Weinberg F.J. Burners producing large excess enthalpies, Combustion Science and Technology. 8: 201-214, 1974.

Hinman, C.W., Press working of Metals, 2nd Edition, McGraw-Hill Book Company, New York, 1950.

Howell J.R., Hall M.J., Ellzey J.L. Combustion of hydrocarbon fuels within porous inert media. Prog Energy Combust Sci. 22: 121-145, 1996.

Khurmi, R.S. and Gupta, J.K. Machine Design First Multicolor. Publisher; Eurasia Publishing House (PVT) ltd. New Delhi, India. Revised Editionvol.2. 510 – 531, 632 – 640, 830 – 1040, 2005.

LPG Exceptional energy, "What is LPG". Retrieved from http://www.exceptionalenergy.com/en_GB/what-is-lpg/origin.html. July, 2012.

Merriman, O. "Gas Burner." Retrieved from http://www.gutenberg.org/files/37928/37928-h/37928-h.html, 2011.

Michelle S. Differences between open and sealed gas burner. http://www.ehow.com/info_8761950_difference-sealed-burner-gas-ranges.html, 2011.

Mohsenin N.N., Physical Properties of Plant and Animal Materials. Gordon and Breach Press, New York, USA, 1986.

Morakinyo, T.A. Strength of Material, Published by Lead Ventures, Auchi Polytechnic, Auchi, Edo State, Nigeria. 1st edition, 43-44, 2009.

Muthukumar P., Piyush A. and Prateek, S. Performance analysis of porous radiant burners used in LPG cooking stoves". International Journal of Energy and Environment, 2, 367-374, 2011.

Nelson, L.P., "Global Combustion Sources of Nitrous Oxide Emissions", Research Project 2333-4 Interim Report, Radian Corporation, Sacramento, CA, 1991.

Sathe, S.B., Peck R.E., Tong T.W., Flame stabilization and multi-mode heat transfer in inert porous media, a numerical study. Combust Sci. and Tech. 70: 93-109, 1990.

Sirisomboon, P., Kitchaiya, P., Pholpho, T., Mahuttanyavanitch, W. Physical and mechanical properties of Jatropha curcas L. fruits, nuts and kernels. Biosyst. Engineering. 97: 201–207, 2007.

The Information Age, "Gas and Electric Stove", http://www.edinformatics.com/inventions_inventors/electric_stove.html. 1999.

Travis, I. D., "Oxygen-gas fuel burner and glass fore hearth containing the oxygen-gas fuel burner," U.S. Patent 5,814,121, 1998.

U.S. Department of Energy, "Just the Basics: Liquefied Petroleum Gas",. Retrieved from ‹http://www1.eere.energy.gov/vehiclesandfuels/pdfs/basics/jtb_lpg.pdf

U.S. Environmental Protection Agency., Area Source Method Abstract (Washington, D.C., p. 1. (Computer printout.), May 1999.

Worgas., "Gas Burner Technology and Gas Burner Design for Application". ASGE 2011 – Worgas-G-Berthold, 2011.

Zhang, X. G., "Corrosion and Electrochemistry of Zinc", Book, Plenum Publication Co., New York, 1997.

Full Paper

DUCTILE IRON PRODUCTION TECHNOLOGY: A REVIEW

B.I. Imasogie
Department of Materials Science and Engineering,
Obafemi Awolowo University,
Ile-Ife, Nigeria.
imasogie@oauife.edu.ng, imasogie@gmail.com

ABSTRACT

Ductile iron castings have proven to be the cost-effective materials of choice and/or potential alternatives to other competing materials (e.g. malleable iron, steel and aluminum castings) and manufacturing processes (forgings, fabrications, etc.) with either an improvement in service performance or lower production cost or both. The outstanding growth in the use of ductile iron castings in engineering applications including those in which the casting properties are critical to lower energy utilization, safe operations and in safety related components such as automobile steering knuckles and brake calipers, gears, valves, pumps, etc., has occurred because of the tremendous improvement in production capabilities resulting in quality consistency and freedom from imperfections, obtained through stringent microstructure control. This paper is a review of the production technology and development (in terms of the metallurgical, chemical composition, heat treatment, microstructure and mechanical properties and design parameters) of this unique class of engineering purpose cast irons and highlights niche applications where ductile irons excel over conventional materials.

1. BACKGROUND INFORMATION ON DUCTILE IRON

The increased demand for improved performance output and fuel efficiencies, decreasing noise and pollution and reduced costs in automobiles and other dynamic-load bearing systems have led to the development of novel cast iron materials with superior strength to weight ratios that add up to more strength for less expense. In recent years, ductile (also known as spheroidal or nodular graphite) cast iron, the base material for the uniquely versatile austempered ductile iron (ADI), has become one of the most important engineering materials, in view of its excellent combination of good castability, machinability and mechanical properties with significant savings in cost and weight compared with equivalent steel components. The material can be tailored to fit an unusually broad diversity of needs, which remarkably, has opened new vistas for its application in the manufacture of automobile, construction, agricultural, mining, heavy-machine, military and railroad components, which are traditionally produced by expensive forging and fabrication processes involving high grade alloy steels (crs-latestream.pdf, 1999; Lerner, 2004; Bockus and Dobrovolskis, 2006; Palmeira *et al*., 2006; Ductile Iron Data for Designers – Section 2, 2010).

Ductile irons have strength, impact toughness and ductility comparable to those of many grades of steel, while exceeding by far those of standard gray irons. It has the same advantages of design flexibility and low-cost casting procedures of gray irons (Nicoletto *et al*., 2002). Their corrosion resistance is equal or superior to that of gray cast iron and cast steel in many corrosive environments. The wear resistance is comparable to some of the best grades of steel and superior to gray iron under heavy load or impact situations. Ductile irons are considerably less expensive than cast steels to produce and only moderately more expensive than gray cast irons since the production procedures are similar. Ductile iron has a clear advantage over malleable iron for applications where low solidification shrinkage is required or where the section is too thick to permit uniform solidification as white iron (Ductile Iron Data for Designers – Section 2, 2010).

Ductile iron castings have advantages of isotropy of properties and homogeneity without laminations as in the case of steel forgings and fabrications. Ductile iron offers substantial cost savings, particularly with respect to the reduced requirement for feed metal, production cost (in terms of material and energy requirements) and mechanical properties. Again, the use of the most common grades of ductile iron "as-cast" eliminates heat treatment costs, thus offering a further advantage.

The most important single step in the production of ductile iron is the addition of graphite nodularizing agents in the treatment of the iron melt. This gives an as-cast structure containing graphite in the form of small rounded, "spheroidal", "globular" or "nodular" particles in a ductile metallic matrix (Figs. 1(a)-(d): (Imasogie, 1994; Imasogie *et al*., 2000; Adetunji *et al*., 2008; Olusunle, 2008). Ductile iron results from a suitable treatment of the molten iron with magnesium and/or calcium containing treatment agents, prior to casting, which causes the graphite to precipitate as tiny spheroids or nodules rather than as flakes, as obtains in the case of gray cast iron.

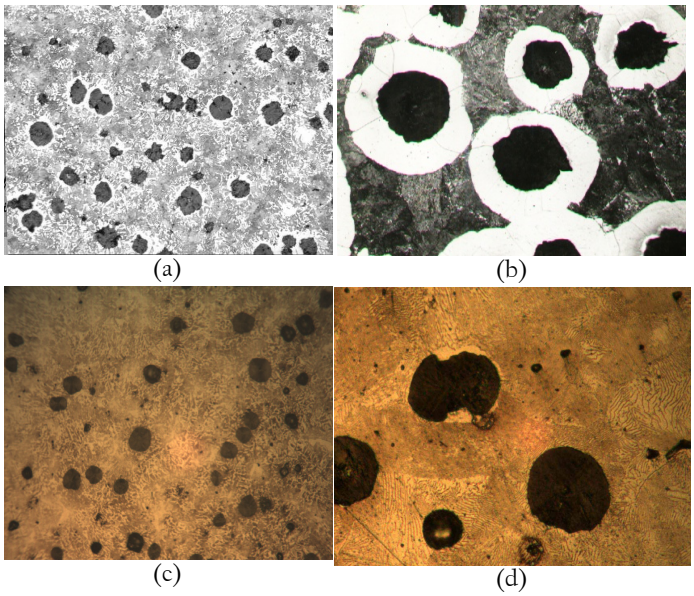

Fig. 1: Micrographs of nital etched, as-cast ductile irons: (a) Mg-Ca-Fe-Si treated iron, graphite nodules (dark grey) in ferrite envelopes, in fine pearlite matrix with some free carbides, x70 (Imasogie, (1994); (b) the enlarged form of (a) showing the 'bull's-eye" graphite nodule-free ferrite pair, x 500; (c) Rotary Furnace-Melted FeMgSi treated iron; graphite nodules (dark grey) in fine pearlite matrix, x70 (Adetunji et al., 2008); (d) Ni-Cr alloyed FeMgSi treated iron, showing graphite nodules in fine pearlite matrix with free carbide (light irregular particles), x 500 (Olusunle, 2008).

The graphite spheroids or nodules in ductile iron, unlike the random lamellae of graphite flakes in ordinary gray cast iron, create much fewer and less severe discontinuities in the metal matrix, thus producing a stronger, more ductile cast material. Thus, the spherical shape of the graphite removes its "crack" effect, while as spheroids, they act as "crack-arresters" in the system. A number of variables including chemical composition (charge and alloying, graphite nodularizing treatment and inoculating agents, etc.), melting conditions and practice, graphite nodularizing treatment and inoculation method and practice, temperature, cooling rate, section size, etc., affect the graphite and matrix structures. It has been established that all of the mechanical and physical properties characteristic of ductile iron are as a result of the graphite being substantially or wholly in the spheroidal/nodular shape. The bulk mechanical properties are thus determined primarily by the steel-like matrix and any departure from this shape/form or in the proportion of the graphite will cause a drastic deviation from these properties (Fuller *et al*., 1980; Emerson and Simmons, 1976; Fuller, 1977; Imasogie *et al*., 2000; 2001).

The presence of graphite contributes directly to lubrication of rubbing surfaces and provides reservoirs to accommodate and hold lubricants. This means good resistance to mechanical wear. Graphite also contributes to machinability because it acts as a lubricant during cutting and also tends to break up chips. Like gray iron, ductile iron has inherent corrosion resistance. In addition, the nodular graphite has desirable lubricating and crack arresting effects in the system (Imasogie, 1994; Imasogie *et al*., 2000; 2001)).

Ductile iron is a eutectic alloy, which means that it has a low melting point, high fluidity and good castability especially for intricate, complex-shape castings with light sections. Expectedly, the automotive industry has expressed its confidence in ductile iron through the extensive use of the material in safety related, functional and structural components such as steering knuckles, brake calipers, etc., which are used mostly as cast.

This paper reviews developments in ductile iron production technology and highlight some notable applications of the material. Section 2 describes briefly, the major types of ductile irons and their applications. The graphite nodularizing action can be regarded as a simultaneous desulphurization and deoxidation treatment where elements with strong affinity for sulphur and oxygen are added (Anderson and Kaysay, 1985; Heine, 1987; Imasogie, 1994; Imasogie *et al*., 2000; Imasogie, 2003). A detailed review of graphite nodularizers and theories of nodularization mechanisms is presented elsewhere (Imasogie *et al*., 1991, 2001). Section 3 reviews ductile iron production metallurgy in terms of the evolution of graphite nodularizing treatment and post treatment inoculation methods and practices (open ladle, sandwich, tundish cover, in-mold, plunger, converter, injection, etc.,). The choice of a treatment method depends to a large extent on prevailing circumstances such as the level of technological advancement (expertise and installed capacity) and available foundry equipment. Section 4 highlights recent improvements in ductile iron technology and describes briefly how to achieve high-volume-continuous-casting production of near-net-shape high quality casts. Section 5 discusses the microstructure in relation to the fracture characteristics of ductile irons. Section 6 highlights niche areas of applications where ductile iron materials compete and are even preferred to conventional engineering materials such as forged steels, wrought steels, aluminum, etc.

2. TYPES OF DUCTILE IRONS

There are three major types of ductile iron castings (Ductile Iron Society, 2010):

i. Ferritic Ductile Iron (60-40-18); with graphite spheroids in a matrix of ferrite. It has high impact resistance, relatively good thermal conductivity, high magnetic permeability, low hysteresis loss, good corrosion resistance and good machinability.

ii. Pearlitic-Ferritic Ductile Iron (80-55-06); with graphite spheroids in a mixed matrix of ferrite and pearlite. It is usually produced in a normal production of ductile iron and it is less expensive to the ferritic grade. It has good machinability.

iii. Pearlitic Ductile Iron (100-70-03); with graphite spheroids in a matrix of pearlite (i.e. a fine aggregate of ferrite and cementitie (Fe_3C)). It is relatively hard, with moderate ductility, high strength, good wear resistance, moderate impact resistance, relatively lower thermal conductivity, magnetic permeability and higher hysteresis loss. It has good machinability. Pearlitic grades of ductile irons are good candidates for applications requiring only high strengths and limited ductility and toughness and are generally not recommended for use in applications requiring impact toughness.

There are some other emerging special grades of ductile irons:

i. Martensitic Ductile Irons: these are tempered martensitic ductile irons having very high strength and wear resistance.

ii. Austenitic Ductile Iron; with outstanding features including good corrosion and oxidation resistance, magnetic properties, strength and dimensional stability at elevated temperatures. It is also known as Ductile Ni-Resist.

iii. Heat Resisting Ductile Irons: these are alloy ductile irons containing 4-6% silicon (Imasogie *et al*., 2001), Ductile Iron Data (2010)) developed to meet the increasing demands of high strength ductile irons capable of operating at high temperatures in applications such as exhaust manifolds, turbocharger casings, etc. The primary properties required for such applications are oxidation resistance, structural stability, strength and resistance to thermal cycling. Alloying with Si and Mo significantly improves the high temperature performance of ferritic ductile irons while maintaining many of the production and cost advantages of conventional ductile irons.

iv. Austempered Ductile Iron (ADI): This is the most versatile set of ductile irons. ADI offers a remarkable combination of strength, toughness and wear resistance; almost double the strength of conventional ductile iron, but with comparable percentage elongation (ε %) and toughness characteristics. It has exceptional wear resistance and fatigue strength and compared to equivalent high alloy steels, it offers reduced component weight, costs and improved service performance.

ADI is subjected to the austempering process to produce mechanical properties that are superior to conventional ductile iron, cast and forged aluminum and steel. In addition, ADI weighs only 2.4 times more than aluminum but it is 2.3 times stiffer. ADI is also 10% less dense than steel. For a typical component, ADI costs 20% less per unit weight than steel and half that of aluminum (Johansson, 1977).

3. DUCTILE IRON METALLURGY

3.1. Graphite Nodularization Treatment and Practices

The vital characteristic of ductile iron (DI); the base material for ADI, is the globular structure of the graphite component and this is traditionally produced by adding small quantities of magnesium

and/or cerium under highly controlled conditions. However, magnesium is expensive and dangerously reactive. Violent agitation of the molten metal causes undesirable pyrotechnics, splashing, and low recovery of reagent, the low boiling temperature and volatility of magnesium being the cause. The cerium process is even more expensive because of the very high cost of misch-metal used as an additive. A greater residual content of cerium than magnesium is needed for an equivalent nodularity and the iron produced is more susceptible to chilling (Davis and Magny, 1978). Also, the graphite spheres given by cerium treatment are in general not so perfect, while a heavy inoculation is essential for good nodularity in thick sections, where graphite flotation tends to be more serious. Thus, the growing interest of metallurgists in finding cheaper, safer, and equally effective substitutes is understandable.

Among other identified potential nodularizers, calcium and calcium containing compounds have been successfully used as modifiers before in-mould nodularizing treatment with magnesium (Horuichi, 1957; Krzemien, 1979; Kurganov *et al*., 1981; Petrichenko *et al*., 1981). However, only modest properties have been obtained for irons inoculated with Ca-CaC_2 (Imasogie, 1994; Umoru *et al*., 2005) and CaSi-CaF_2 (Imasogie *et al*., 2001) as primary nodularizers. An extensive study was carried out by the present author working with the ductile iron research group based at the Department of Materials Science and Engineering, Obafemi Awolowo University, Ile-Ife, and at the Engineering Materials Development Institute, EMDI, Akure, Nigeria, to find a cost-effective treatment route for the production of standard ductile irons using locally available materials and foundry equipment. The research was focused on the possibility of harnessing the positive and additive aspects of appropriate calcium alloy combinations used together with magnesium; that is as master alloys with the added advantage of better treatment control and ultimately improved ductile iron. The research effort yielded a special Ca-CaC_2-Mg master-alloy formulation, selected on the basis of optimum results (Imasogie, 1994, 2002, 2003; Imasogie *et al*., 2000). Results of investigations of the effectiveness of the multiple calcium-magnesium based master alloy nodularizer and the properties of the ductile iron produced have been extensively reported (Imasogie, 1994, 2002, 2003; Imasogie *et al*., 2000; Imasogie and Afonja, 2003).

One of the emerging hypotheses of the mechanism of nodularization of graphite in cast iron is based on the removal or neutralization under special conditions, of some surface active elements such as sulphur, phosphorus, oxygen, etc. Results of the above mentioned research (Imasogie, 1994, 2002, 2003), established that the removal and/or neutralization of both sulphur and phosphorous in particular, in the iron melt through reactions with the nodularizers employed, is indeed necessary for the production of ductile iron. Sulphur, phosphorus and to some extent oxygen are known to be surface active and by reducing the graphite/iron interfacial energy, through their segregation on the graphite/iron interface and selective adsorption on the graphite prism planes, can promote the extended interfacial characteristics of flake graphite (Franklin and Stark, 1984; Takita and Ueda, 1979; Imasogie, 2002). The nodularizers ensure that the graphite basal planes would now have the lower surface energy in contact with molten iron and nodular graphite is formed. It was observed that the degree of this apparent neutralization of the surface active elements was relatively higher with the multi-material Ca-CaC_2-Mg master-alloy treatment than with the traditional Mg or Mg-FeSi treatment (Imasogie, 2002). Figs. 2(a) – (d) show typical photomicrographs of two sets of as-cast ductile iron specimens obtained using the multi-material Ca-CaC_2-Mg master-alloy and the conventional FeMgSi nodularizers. Figs. 2(a) and 2 (b) illustrate the microstructural features of the two irons in the as-cast conditions; respectively.

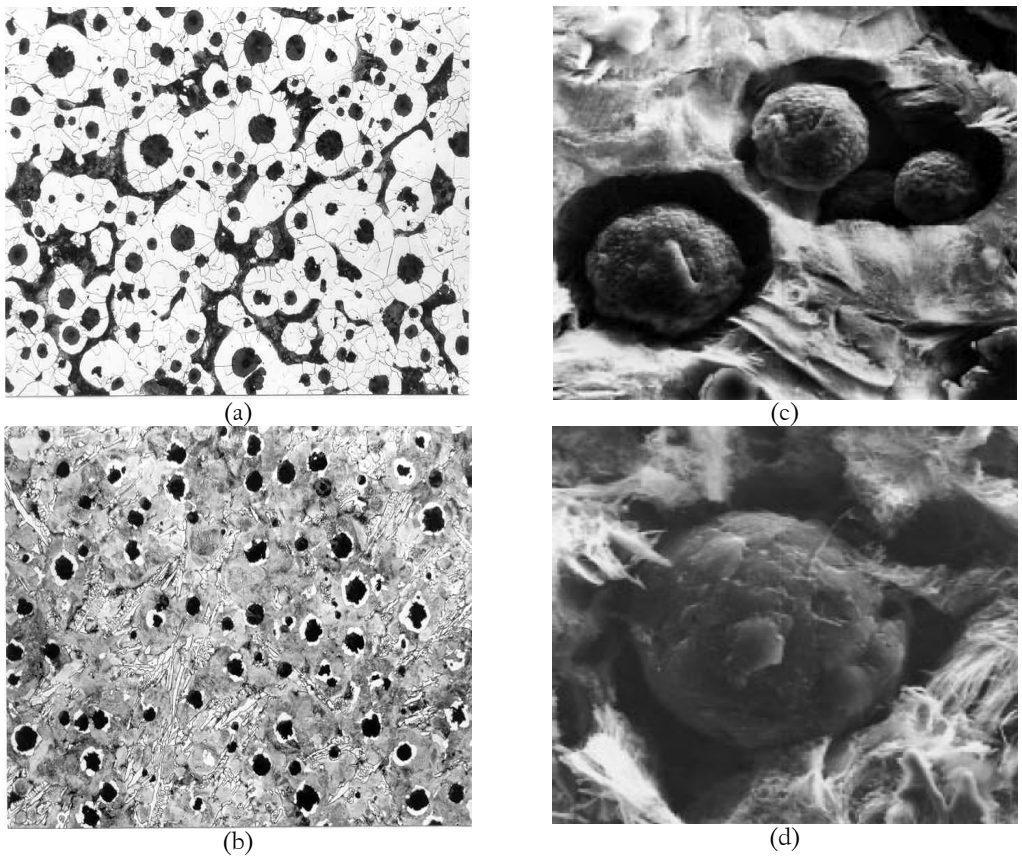

Fig. 2: Micrographs of irons in the as-cast state, nital etched; (a) Ca-CaC_2-Mg masteralloy treated iron; showing graphite nodules (dark grey) and some fine pearlite (irregular dark areas) in a ferrite matrix; (b) FeMgSi treated iron; showing excessive amount of free carbide (light columnar particles), other phases, with graphite nodules enveloped in ferrite, in a pearlite matrix; (c) and (d): irons in ((a) and (b), respectively, showing SEM of the as-cast specimens with matrix etched away to show the different 3-D graphite nodule forms (Imasogie, et al 2000).

The iron treated with MgFeSi (Fig. 2(b)) has a much larger pearlitic phase, confirming the tendency of magnesium to stabilize carbide. The microstructure also exhibits significant phosphide eutectic and other hard phases. However, in the iron treated with the special masteralloy nodularizer (Fig. 2(a)), the graphite spheroids appear almost uniform in size and distribution in the matrix, which appears to have none of these hard phases. Up to 96% nodularity was obtained using the special Ca-CaC_2-Mg masteralloy compared with 98% using magnesium alone. The mechanical properties were also comparable. Figs. 2(c) and 2(d) illustrate SEM observations of the form and/or morphology of graphite in these specimens, respectively, where the matrix has been etched away. Here, striking distinctions exist between graphite morphologies obtained using the aforementioned master-alloy (Fig. 2(c); which shows colonies of graphite spheroids each of which appears to be built up of several tiny spherulites), compared with that produced using the conventional magnesium ferrosilicon (Fig. 2(d); which shows the graphite as lumpy and solid with a relatively rough surface).

The first step in the production of a sound ductile iron is the careful selection of charge materials as well as graphite nodularization treatment process parameters. The amount of each alloying elements required should be such as will give castings that are free of carbides as much as possible; particularly in as-cast ferritic ductile irons (Bockus and Dobrovolskis, 2004). For instance, manganese and chromium should be in the range 0.5 and 0.1 % respectively. Manganese and chromium usually come in from steel scrap, iron units and returns or they can be deliberately added as alloying elements. In particular, the graphite structure as well as the matrix is affected by the carbon content and/or C/Si ratio (as increasing this ratio decreases the proportion of ferrite to pearlite phases in the system). Generally, to achieve a ferritic casting in as-cast condition, chemical composition of charge material should not contain more than 0.01%Sn, 0.02%As, 0.1% Σ(V + Mo), 0.04%Cr, 0.02%S and 0.05%P (Bockus and Dobrovolskis, 2004).

In all cases, the sulphur content must be kept below 0.02% through melting and desulphurization processes for the treatment to be effective with the above mentioned nodularizers. In the case of the use of the traditional pure magnesium, the material is introduced into the molten iron either in the open-ladle (or in-ladle) method or the pressure-container (converter) method. In both cases, special (mostly proprietary) techniques have been developed and numerous patents have been taken out regarding most of the techniques.

Lerner and Panteleev (2002; 2003) have carried out a comprehensive review of magnesium and magnesium-based-alloy treatment agents in ductile iron production. Fig. 3 presents a typical classification of Mg-treatment alloys and treatment methods currently in use for producing ductile iron castings.

In general, apart from the deployment of special equipment or devices to control the violent reaction rate and maximize Mg recovery, the use of pure magnesium as a treatment agent presents several challenges. Most of these have had something to do with the undesirable effects of significant undercooling, high chill rate and Mg "fading". Its major advantage is the fact that the necessary desulphurization process can be carried out in the same ladle before or during treatment.

Two of these traditional processes; the 'plunging' and the sealed pressure/autoclave ladles (Figs. 4(a) and (b)), have stood the test of time. Apart from its simplicity, the plunging process can utilize the full range of nodularizing materials and has the ability to treat iron with relatively high sulphur content. However, it suffers from considerable temperature losses, as a result of plunging the large cold plunging bell with the nodularizing agent, as well as a significant pyro-effect. In addition, due to the extreme working conditions of the plunging bell, it is seldom reusable. On the other hand, the pressure ladle/autoclave technique has a pneumatically or hydraulically operated pressure head that plunges the Mg billet into the ladle and finally seals it. Since the magnesium is introduced into the liquid iron under excessive air pressure, it melts, but does not vaporize. A special stirring device mixes the liquid metal layers, resulting in improved nodularizing treatment. The advantages of this latter process include up to 70% Mg recovery and an adequate residual Mg content. Nowadays, the process is fully automated and environmentally safe. However, the process still suffers from significant temperature losses, a relatively high cost of equipment and the necessity for regular maintenance during operations.

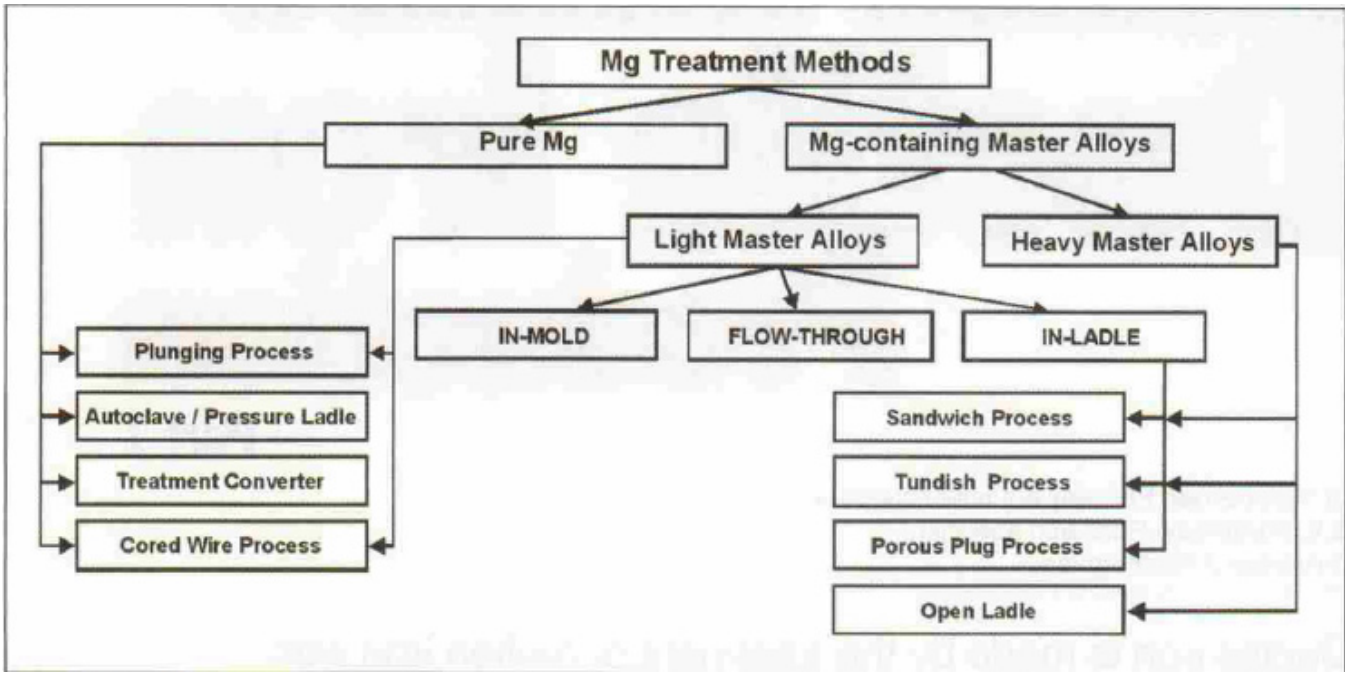

Fig. 3: Classification of Mg treatment alloys and methods currently used for ductile iron castings (Lerner and Panteleev, 2002)

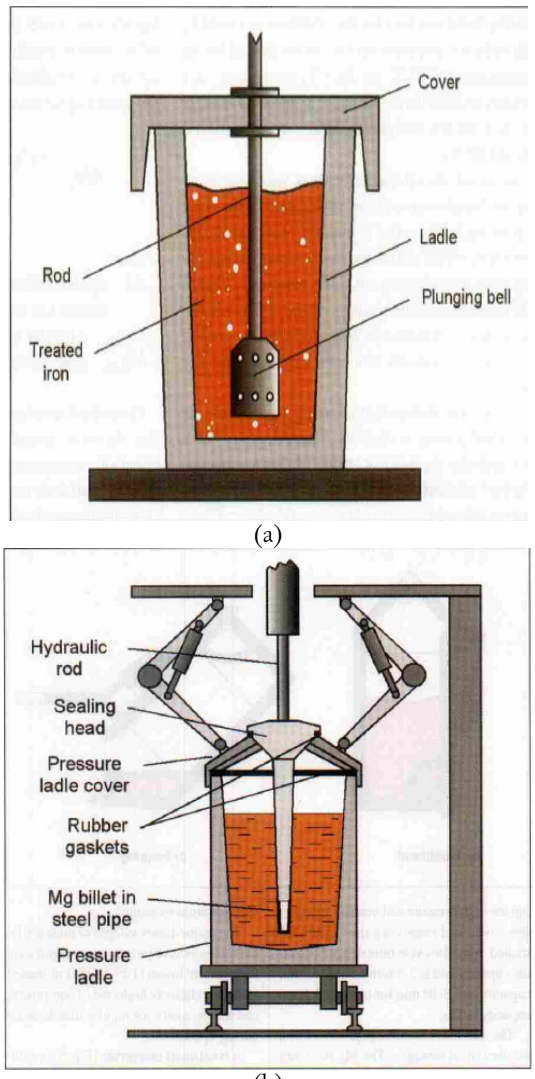

Fig. 4: Schematic of (a) Plunging and (b) sealed pressure ladle processes (Lerner and Panteleev, 2002)

The treatment converter shown in Fig. 5 (Lerner and Panteleev, 2002), is a latter development over the plunging and pressure ladle/autoclave process. It is a tilting cylindrical vessel lined with a refractory material, with a simple reaction chamber at the bottom of the vessel, above the liquid iron surface, when the converter is in a horizontal position, to avoid a premature Mg contact with the iron. This is a more efficient and safe design, compared with the plunging and pressure ladle/autoclave processes. It provides effective desulphurization and makes possible the use of cupola-melted high sulphur base iron. Although an Mg recovery of up to 50-55% is possible, the process suffers from a relatively long treatment cycle involving post-inoculation, etc. It requires a high financial investment in equipment and ancillary devices.

In modern graphite nodularizing treatments, magnesium still forms the base treatment agent, used in combination with other nodularizing elements (as masteralloys), or as Fe-Mg-Si alloys. In these cases, the modes of introduction of the nodularizer in molten iron to be treated are significantly different from the techniques reported above for pure magnesium treatment. Recent research on the use of multiple nodularizing elements as a substitute for pure magnesium has been aimed primarily at the need to reduce the smoke and flare produced by addition of magnesium or magnesium-ferrosilicon, to achieve higher magnesium recovery and minimal fading, and to reduce the susceptibility to chilling inherent in both magnesium and cerium treatments (Imasogie, 1994, 2002, 2003; Takita and Ueda 1979; Lerner and Panteleev, 2003). With this shift, came several notable melt treatment techniques using multiple-element treatment alloys (masteralloys) and Fe-Mg-Si alloys.

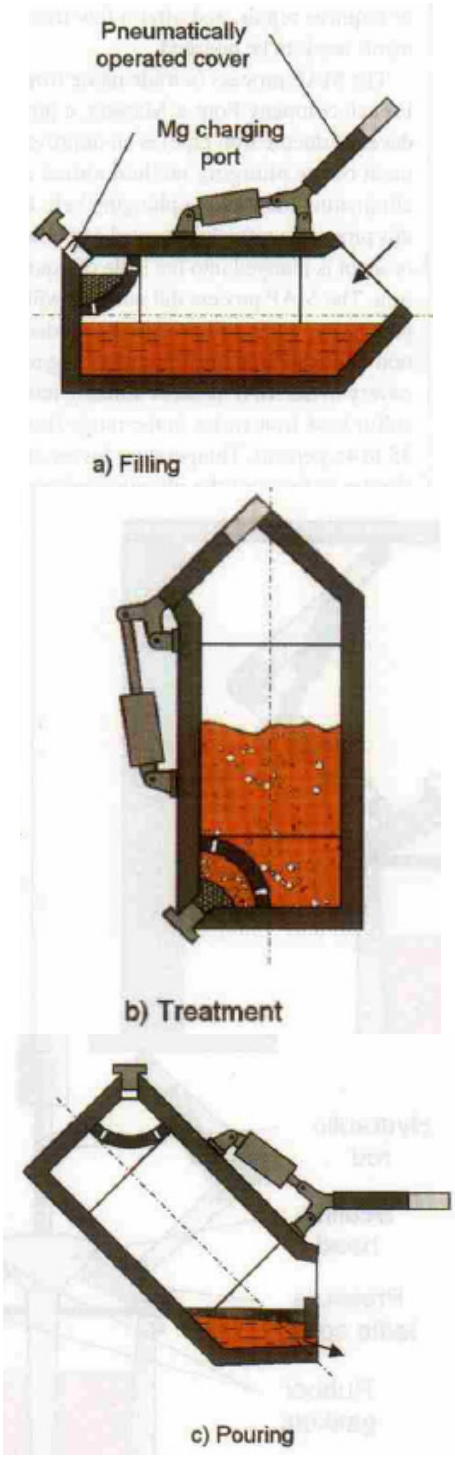

Fig. 5: Schematic of the treatment converter illustrating the treatment sequence (Lerner and Panteleev, 2002)

Generally, these techniques are classified into two main groups; namely, "In-Ladle" and "In-mold". The in-ladle techniques include the "open-ladle" process, of which the well-known "sandwich process" (Figs. 6(a)), is a special case.

It is pertinent to mention here that the OAU/EMDI DI-ADI research group has been able to adapt the sandwich method to successfully treat Rotary Furnace melted cast iron. To achieve this, a pre-heatable treatment ladle was designed and fabricated in-house, to offset any temperature loss during and after treatment. An easily removable wire-gauze sheath mechanism was used to secure the iron-

filings cover material and the treatment alloy in place in the chamber at the bottom of the ladle, prior to tapping. The sheath is steadily withdrawn, while a slight toggling-stirring action is applied, when the ladle is about three-quarter filled with molten metal, an action which effectively triggers the release, dispersal and reaction of the nodularizing agent as the sheath is taken up through the melt. In this way, a higher treatment agent recovery was achieved.

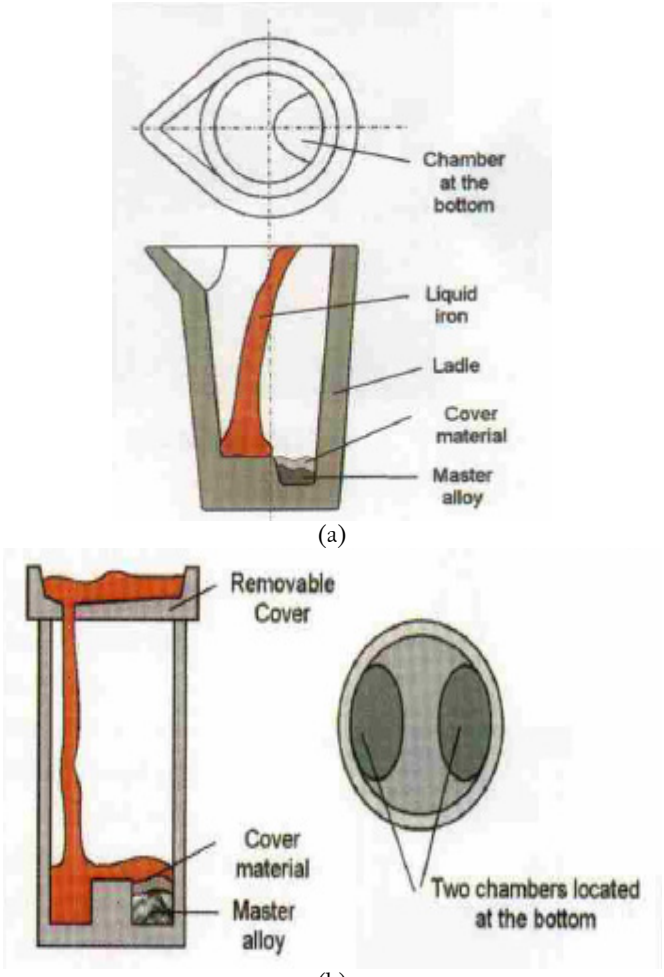

Fig. 6: Schematic of (a) Sandwich method, (b) Two-chamber tundish ladle with removable cover (Lerner and Panteleev, 2003).

A latter modification to the open ladle sandwich process makes use of the "tundish ladle" with a lifting and/or removable cover (Fig. 6(b)). In fact, the "tundish process" is an improvement on the sandwich method aimed at reducing the oxygen level inside the ladle (Lerner and Panteleev, 2003). The tundish ladle with lifting cover (Fig. 7(a)) and the tundish "converter" (Fig. 7(b)) are the most modern Mg-Fe-Si and master-alloy treatment equipment. The latter is a further modification of the sandwich process, which is a combination of a conventional tundish ladle and Mg-Fe-Si/master-alloy treatment converter (Lerner and Panteleev, 2003). This device contains a reaction chamber attached to the bottom of the ladle to hold pure Mg or master alloys. Liquid iron is tapped through the tundish cover and then through the orifices, located at the bottom, enters the reaction chamber and reacts with the nodularizer preloaded in the chamber before tapping. A crane or monorail delivery system allows for the use of the tundish-converter also as a transfer ladle to tap ductile iron into a pouring ladle or autopour (Lerner and Panteleev, 2003). About 30% of the world's ductile iron is currently produced by this method. Mg recovery (with little or no fading) in the tundish process may reach up to 75%.

Another advantage of the tundish converter is the relatively low cost of tundish ladles, coupled with its environmental safety and low emission levels. The only disadvantage is the inherent temperature losses and the relatively long treatment cycle.

The "In-mold" treatment process and the flow-through Mg-based master alloy treatment process are the major technological revolutions in the graphite nodularizing processes for the mass production of ductile iron automotive parts, since the last quarter of the last century (Figs. 8(a) and (b), respectively) (Lerner and Panteleev, 2003; Dremann, 1983; Hummer, 1985).

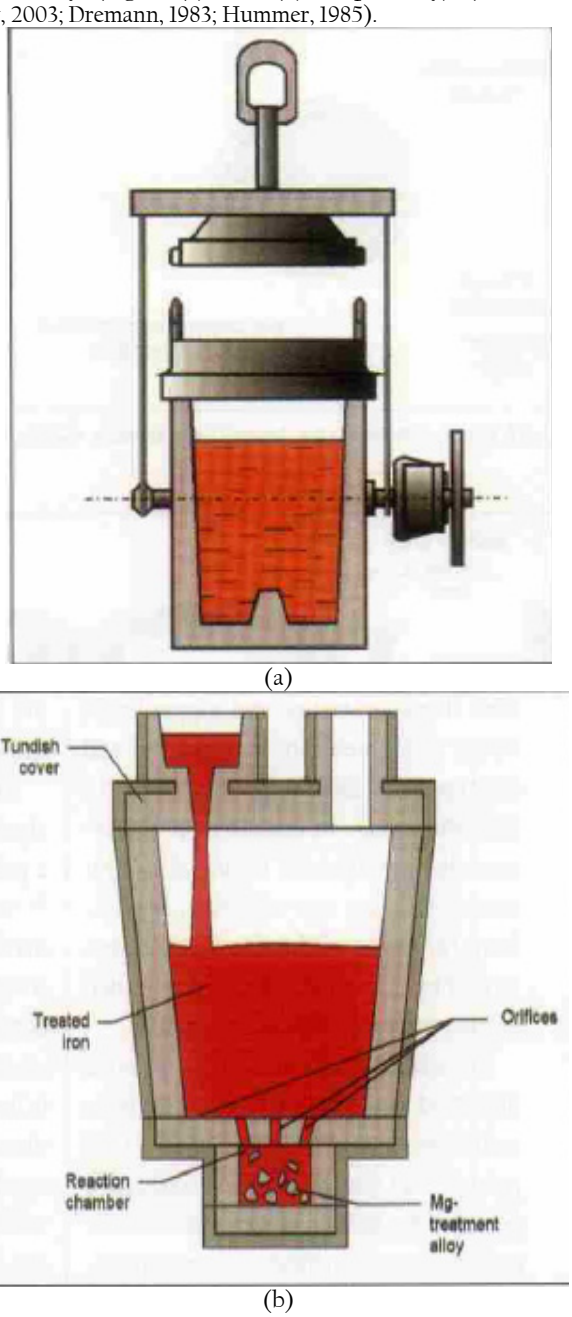

Fig. 7: Schematic of (a) the tundish ladle with lifting cover, (b) tundish converter (Lerner and Panteleev, 2003).

In the in-mold process (Fig. 8 (a)), the nodularizer; typically, the FeMgSi or Mg-based master alloy with 3-5% Mg content is placed into the reaction chamber of each mold during mold assembly (Lerner and Panteleev, 2003). The liquid iron is treated by passing it over the reaction chamber that is a part of the running system of the mold. The process allows Mg recoveries of 70-80%, while temperature losses and pyro-effects are minimized. However, its major disadvantage is the high risk of impurities and slag build-up in the casting. Nowadays, extremely low-sulphur irons are treated using this technique to avoid slag build-up and its penetration into the castings.

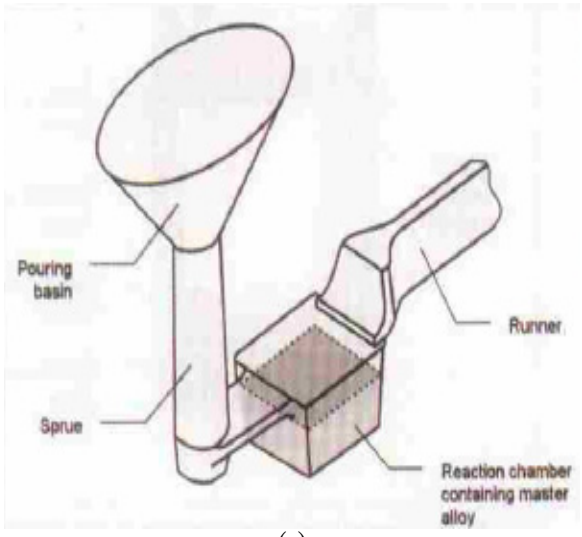

(a)

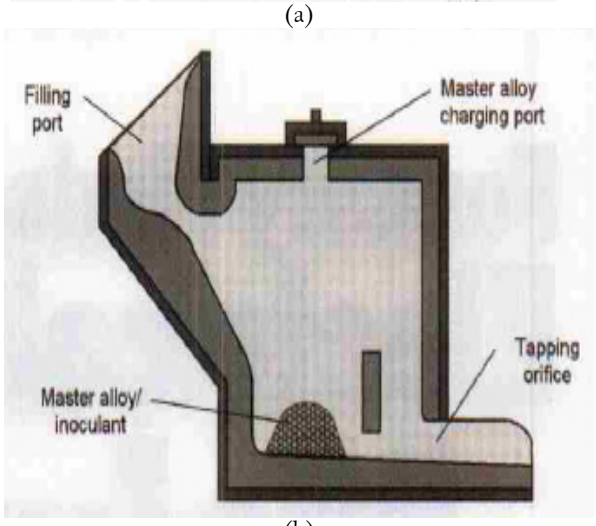

(b)

Fig. 8: Schematic of (a) In-mold process and (b) Flow-through Mg-based master alloy treatment process, for the mass production ductile iron (Lerner and Panteleev, 2003)

The flow-through (Fig. 8 (b)) is an improvement on the in-mold treatment process and it is made up of a device/unit located between the source of liquid iron and the target ladle. Oxygen access is prevented by the sealed charging orifice linked to the reaction chamber. The process has a high Mg recovery of 60-70%, with low temperature losses and low smoke, flare or pyro-effect levels. The entire unit is cheap and offers a cost-effective production route for high quality and quantity ductile iron.

Finally, for continuous casting of ductile iron (e.g. as in ConCast mold-lines), the cored-wire treatment process (Fig. 9) stands out. The Mg-containing wire is introduced into liquid iron by a special automated feeding device that gradually delivers wire into the closed ladle. The automation allows for precise control of residual Mg content, flexibility with respect to the required capacity, base sulphur content and temperature ranges. As a continuous casting process, the cored-wire method is suitable for making ductile iron concurrently with its production on a horizontal casting machine.

As mentioned above, previous work (Imasogie, 1994, 2002, 2003; Imasogie *et al*., 2000, 2001; Umoru *et al*., 2005; Adetunji *et al*., 2008; Olusunle, 2008), pertinent to the sandwich nodularization process have been carried out by the OAU/EMDI DI-ADI research group, to enhance our local understanding of the graphite nodularization process, to establish optimum production parameters and evaluate the as-cast and heat treated properties of DI produced.

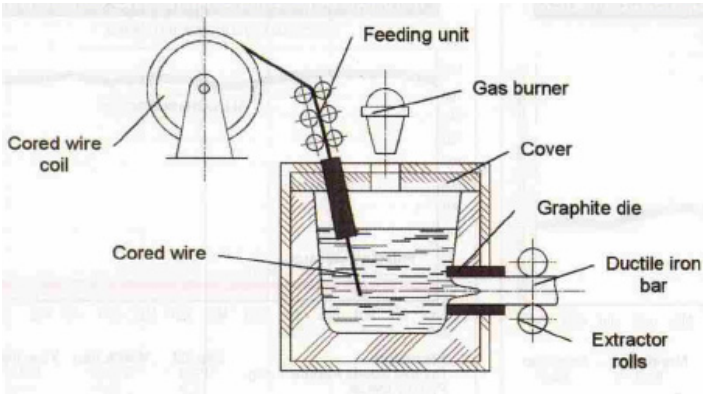

Fig. 9: A schematic of the cored-wire treatment process for horizontal continuous casting of ductile iron (Lerner and Panteleev, 2003)

3.2. Post Treatment Inoculation of Ductile Iron

Post treatment inoculation is required to promote graphitization. There are three common methods of post-treatment inoculation, which may be used individually or in combination; namely, in the ladle, in the stream while pouring and in the mold (in-mold). Most commercial inoculant grade FeSi contains elements in relatively low concentrations which are active inoculants such as Ca, Al, Zr, Ba, Sr, Ti, etc.

Research has shown that late-stream inoculation produces a dramatically higher nodule count thereby increasing the strength of the iron produced (crs-latestream.pdf, (2006)). However, late-stream inoculation also increases the potential for producing nodule populations with distinctly large and small nodule sizes. Generally, large nodules are believed to reduce fatigue strength, while nodules above a critical size have been observed to significantly reduce fatigue properties. It has been reported that an increase in fatigue strength of 10 % or greater can be achieved by improvements in the control of graphite nodule size distribution with late-stream inoculation. It is believed that fatigue life failures are often initiated at large graphite nodules, nodule clusters, non-metallic inclusions and micro-shrinkage porosity (Nicoletto *et al*., 2002).

4. RECENT IMPROVEMENTS IN DUCTILE IRON PRODUCTION TECHNOLOGY

A number of other recent but proprietary processes are now available for producing ductile irons including the Georg Fischer converter, for which bespoke alloys have been developed to operate in conjunction with some specific techniques and in-mold processes mentioned above. In fact, "Inmold" is the trademark of Materials and Methods Limited, and "Flotret" and "Sigmat" are among their patented processes. "Imconod" is a patented process of International Meehanite Metal Co. The NovaCast PQ Inmold process (Fig. 10; Sillen, (2006)) was specifically designed to solve the problem of magnesium based nodularizers' "fading" and low recovery in treatment. The method is used for both compacted graphite iron (CGI) and ductile iron production. The fading is due to a gradual vaporization of magnesium and to agglomeration of nucleation particles, which makes them too large to act as graphite nodule nucleation sites. This results in unwanted deterioration of graphite shape and form.

Measured in terms of magnesium level, fading in a normal sized ladle is approximately 0.0005% per minute. In the PQ Inmold method, there is little or no fading since the reaction occurs in an oxygen-free environment. The time span between the reaction and the filling of the mold cavity is very short, often less than 2 seconds. The treatment temperature is the same as the pouring temperature, usually about 100 ^{o}C lower than with conventional methods. This means that the magnesium level remains virtually the same in every casting. The magnesium recovery is equally very high compared with the conventional methods.

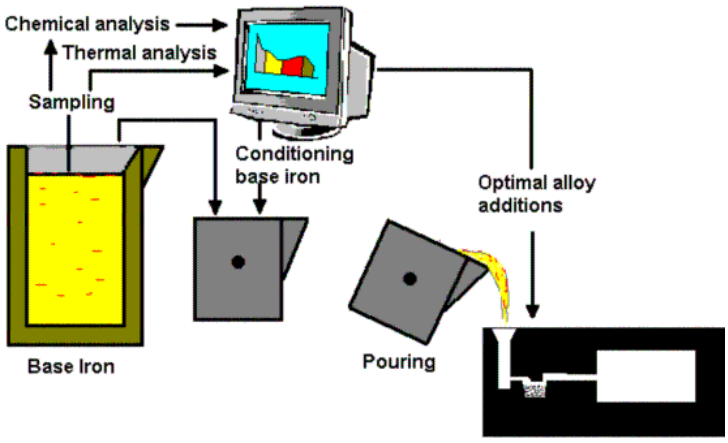

Fig. 10: A schematic of the NovaCast PQ Inmold method.

The process requires much fewer operational steps before the mold cavity is filled, since all critical steps are made fully automated. Also, the need for costly investment in specialized production equipment is very low and no extra ventilation is required. There is no need for any separate inoculant or inoculation, since there is already high magnesium recovery and no fading. Thus, low magnesium levels can be used, with the added advantage that the risk of defects such as dross, carbide, microshrinkage and variations in graphite shape and in the matrix is minimized. The process is environmentally friendly, with no white smoke and pyrotechniques from the magnesium reaction and it is energy efficient. There is also much less slag and used refractories can be recycled.

The PortCast-Intermet Porto Foundry now routinely cast several high-volume general types of automobile family castings, such as brake components, suspension arms, different cases, bearing caps, etc., for most renowned end user car producers in their ConCast unit (Palmeira *et al*., 2006). They use a very powerful and new informatics tool - DataPro® in combination with CAD and CAE softwares to model, adapt and simulate the different production layouts in order to have the Intergovernmental Panel on Climate Change (IPPC) compliant installations operate in an efficient, competitive and environmentally friendly manner.

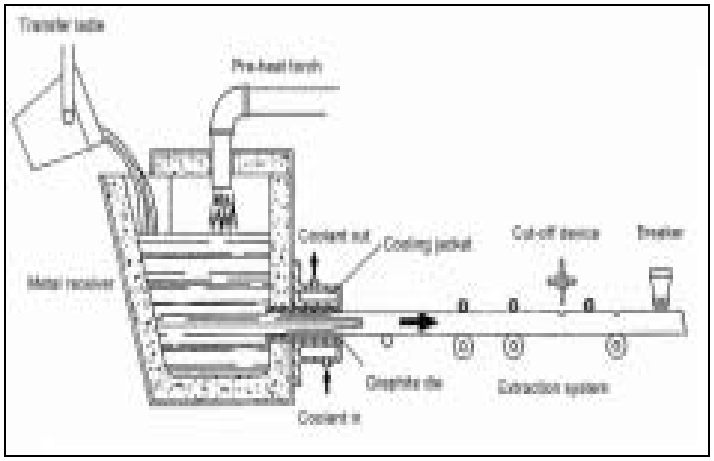

Fig. 11: A Schematic View of Horizontal Continuous Casting (HCC) Process.

The goal of high-volume production of ductile iron can be achieved by Horizontal Continuous Casting (HCC); a relatively new but promising method of producing near-net-shape high quality cast bars (Lerner, 2004). Fig. 11 presents a schematic view of HCC. Molten iron is tapped from the transfer ladle into a heatable metal receiver (as shown), to maintain the required temperature range and compensate for temperature losses during drawing process. Following a sequence of operations and upon complete solidification, a special mechanism cuts and breaks the bars to required lengths. The major advantages of HCC for ductile iron process include:

i. High casting yield of 92-95%, since it eliminates traditional feeder needs due to the fact that molten metal in the receiver plays the role of a pre-heated riser that continuously supplies liquid metal to feed the bar during solidification and also compensate for shrinkage.
ii. The absence of casting defects, usually associated with sand molding (sand inclusions, dense gas and shrinkage porosities, etc.), makes the product ideal for hydraulic and pneumatic components' applications.
iii. For the same reasons, and a very uniform grain structure, HCC bars have excellent machinability.
iv. Optimal balance between iron chemistry, melt temperature, iron level in the receiver, drawing and cooling parameters, ensures production of defect-free high quality bar stocks.

The method of informational macrodynamics (IMD) is used for a systematic informational solidification modeling and optimization of the HCC of the ductile iron process (Lerner and Lerner, 2000).

Over the last few decades, design engineers have been able to optimize casting quality, integrity and performance with increased speed and confidence by using CAD/CAM, solid modeling and finite element analysis (FEA) techniques to achieve accurate analysis of stress distributions and component deflections under simulated operating conditions (Ductile Iron Society, (2010)). In addition to enhancing functional design, the analytical capabilities of CAD/CAM have enabled foundry engineers to maximize casting integrity and reduce production costs through the optimization of solidification behavior. Furthermore, the mechanization and automation of casting processes have significantly reduced the cost of high volume castings, while new and innovative techniques such as the use of Styrofoam patterns and CAD/CAM patterns production have substantially reduced both development times and costs for prototype and short-run castings. These developments have led in many cases, to the replacement of multi-part (e.g. in planetary gear system), welded and/or fastened steel assembly by a single ductile iron casting, thus offering significant savings in production costs. In addition, inventory costs are reduced, close-tolerance machining required to fit parts together is eliminated, assembly errors are less and engineering, inspection and administrative costs related to multi-part assemblies are significantly reduced.

5. MICROSTRUCTURE AND FRACTURE CHARACTERISTICS OF DUCTILE IRONS

Ductile iron is a prime example of engineering materials where the properties achieved depend upon the characteristics of the microstructure (graphite form and distribution and matrix features). The microstructure is determined in part during solidification (graphite shape, size and distribution) and in part during solid-state transformation (matrix). The microstructures are normally characterized using the following numerical assessment indices: graphite nodule count, percentage nodularity or degree of nodularization, % ferrite, etc. The determination of the mechanical properties and failure characteristics, follow applicable ASTM, BSI or DIN specifications.

There is enough evidence to suggest that the overall fracture path is controlled by initial nodule decohesion and microcracking of the graphite/matrix interface of ductile iron. It is thus the graphite–nodule distribution that dictates the least energy propagation path. For example, in ferritic ductile iron, dimple pattern of fracture is found to be the predominant and operative mode of fracture as shown in Fig. 12a (Imasogie *et al*., 2000). But in ferritic-pearlitic matrix structures, two different fracture patterns are observed, (Fig. 12(b)). In the vicinity of the graphite nodules, the wider areas of the ferrite phase are deformed considerably and the overall fracture occurs in a ductile manner. On the other hand, brittle fracture with "river patterns" and "beach-markings", in pearlitic areas are observed. In fully pearlitic matrix ductile iron, a complex pattern of fracture is

observed, reflecting the low toughness of the material. Many cleavage facets are observed on the fracture surface; (Fig. 12(c)).

Impact toughness is known to increase with ferrite % and nodule count. Increase in % ferrite is found to modify the fracture micro-mechanisms from transcrystalline cleavage to transcrystalline ductile fracture with nodule decohesion and cavitation and final dimple formation. A fracture surface roughness parameter has been introduced (Nicoletto, 2002) and found to correlate linearly with impact toughness. However, in all cases, hardness decreases with increase in nodule count and ferrite content, while impact toughness increases with ferrite percent and nodule count. Therefore, optimization of the mechanical properties and/or performance while maintaining suitable melting, treatment and casting practice can be achieved by chemical composition, treatment practice, alloy content and matrix microstructure control.

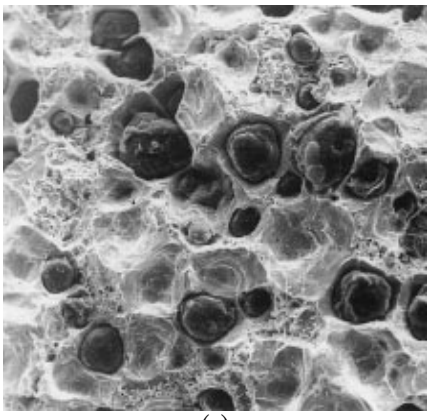

(a)

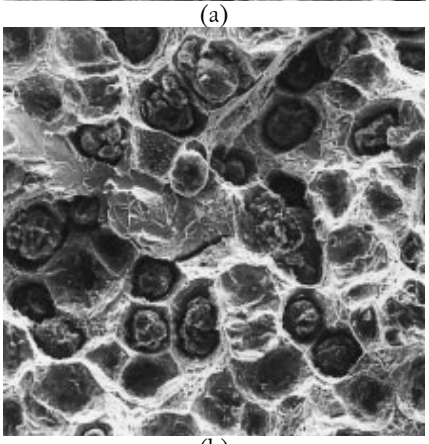

(b)

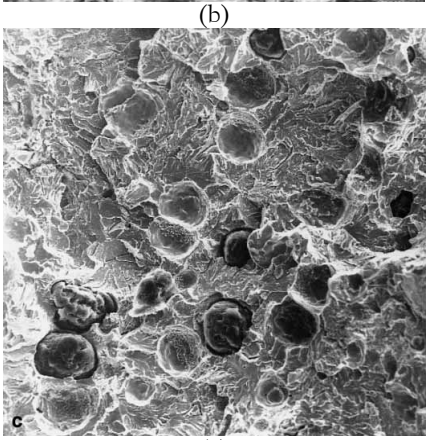

(c)

Fig. 12: Fractographs of as-cast (a) Ferritic ductile iron, showing predominantly ductile fracture; (b) Ferritic-pearlitic ductile iron, showing mixed mode fracture, with evidence of graphite as 'crack arrester'; (c) Fully pearlitic ductile iron, showing facets of intergranular brittle fracture and characteristic river markings (Imasogie, et al (2000)).

6. APPLICATIONS WHERE DUCTILE IRONS EXCEL

Many technological advances have been recorded by the Nigerian DI/ADI group and researchers globally in the last three decades, to improve production efficiency in the ductile iron founding industry, to enable it to continue to produce quality castings at costs which make their use economical compared with other materials and methods of manufacture. As products go, the ductile iron material can be tailored to fit an unusually broad diversity of needs. This is why ductile iron is termed versatile. It has in many instances been chosen over and above cast steel, steel forgings, high strength gray iron, and steel fabrications including weldments, in parts ranging from a fraction of a kilogramme (e.g. pump cylinder), to mill rolls. Designers are converting steel castings, forgings, and fabrications to ductile iron castings to gain the following benefits *(http://www.steelinc.com.au/ADI/ADIbenefits.htm)*:

i. Improved strength to weight ratio
ii. Better surface detail and finish
iii. Improved machinability
iv. Reduced machining allowance
v. Lower component cost
vi. More strength per dollar
vii. Reduced component weight

Fig. 13 shows a picture of some of the ductile iron castings used in a Japanese automobile. Virtually all functional component parts in Japanese cars are now made from DI and ADI castings. Other steel castings, forgings, and fabrications have been converted to Ductile Iron castings at lower cost with equal or superior performance.

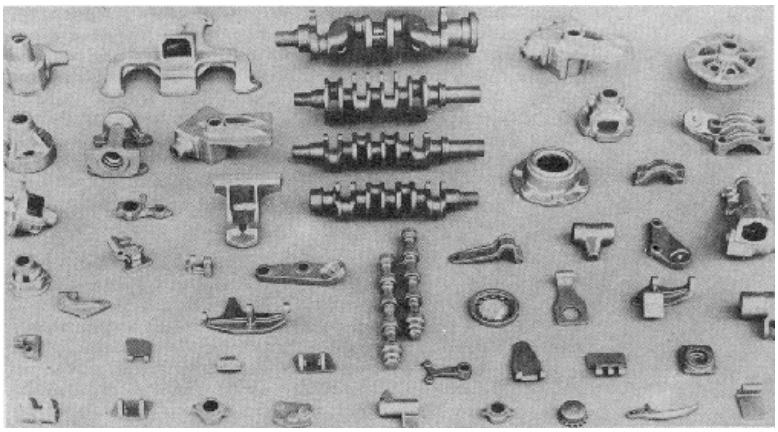

Fig. 13: A Picture of some of the Ductile Iron Castings Used in a Japanese Automobile (http://www.steelinc.com.au/ADI/ADIbenefits.htm)

According to Chandler (1977), conversion - cost reduction is a common motive for switching to ductile iron castings. For example, manufacturing costs were slashed 69% in converting a two-piece fabrication; a steam turbine governor case, to a one-piece ductile iron casting. Formerly, steel bar stock 10.16 cm in diameter and 6.45 cm steel tubing were joined by welding and machined in eight separate operations. Remarkably, the one-piece casting exceeds maximum engineering requirements. Another notable case involved a conversion from a steel forging. Primarily, as a forging, the part, a wire rope clamp for conveyor idler and support stand, cost $2.31 per unit to manufacture. But by going to a sand-cast clamp of an 80- 55- 06 grade of ductile iron, it became possible to shave part cost by 91%. Also, the ductile iron castings had more than adequate strength and toughness; and machining was eliminated because functional surfaces had sufficient accuracy in the as-cast condition. Another special case, involves the use of the 65-4-12 grade of ductile iron casing lined with Teflon. The complex plug valve, which controls the flow of extremely corrosive liquids in chemical processing plants, was formerly made of a variety of exotic materials, including Type 316 stainless steel, Monel, Hastelloy B, titanium and tantalum. In some specific cases, unit costs ran as high as $229. The item is now down to $79. Cast recessor and

machined grooves in the body and plug lock the Teflon in place. It will not collapse in a high vacuum or during thermal cycling.

In addition to cost, other considerations such as mechanical properties' requirements, corrosion resistance, weight and thermal (spalling) qualities, recommend ductile irons over and above all other materials. Specifically, the oil manifold for earth-moving equipment is presently made of ductile iron because the application called for a combination of high strength and good ductility. Ductile iron piston for diesel locomotive engines is stronger and has more wear resistance than previously used types. Reduction in weight (by 50%) also means less stress on other parts, such as bearings. Drive sleeves for automatic torque control devices were formerly steel castings or made from solid steel billets. Service conditions range up to 6.67 x 10^5 N of thrust and 5700 Nm of torque. The drive shaft for farm equipment was formerly gray iron. Full-length, heavy-duty ductile iron pipe have now replaced sand core for hub, which simplifies machining and assembly. The high – strength part weighs 32.84 kg. Ductile iron planetary carriers for earth-moving equipment combine high strength, dimensional stability, and resistance to wear, shock and sudden loading. The weights range from 3.4 to 126.3 kg. Ductile iron suspension link for railroad track scale transmits 3.1 x 10^5 N of force from platform to a lever. Bending movements in the lever system were reduced by 50% because a smaller link is possible. Final drive housing for earth-moving equipment (118 kg) was switched from gray iron to get more strength to handle unusual shock loads. Existing pattern for gray iron was used. The base for rubber impeller in centrifugal slurry pumps was a six-part steel weldment. On introducing ductile iron, the casting trimmed 12% from component weight and reduced per-part cost from $ 69.40 to $ 32.35. The front wheel casting for heavy machinery was switched from steel to ductile iron primarily to bring about a reduction in costs. This rather complex part weighs 73 kg. Door mechanism for bomber aircraft, formerly an eight-part steel weldment, was converted because it had a tendency to warp. Ductile iron casting reduced part cost from $182 to $41. Tool storage index for a numerically controlled machining center formally required 2, 115 manufacturing operations. Conversion to one-piece casting cut number to 24. Drive gear for tyre changer was formerly machined from steel. A smooth finish on ductile iron casting cut per-part machining cost from $4.55 to 23 cents. Part cost dropped from $9.00 to $3.50. The compression discharge casting was switched from a cast-weld structure that called for 200 manufacturing operations to a one-piece casting that requires only ten. Bi-directional valve bodies were made from carbon steel. Now, tapered body bore does not require machining or lapping. Per-unit cost of machining is now $2.00; from $ 14.00 (Chandler, 1977).

Other notable applications of ductile iron where cost has been reduced and properties improved, include bull rings, sinter pallets, cams, cylinders, liners, burring discs, drawing dies, drawing wheels, mining knives, asphalt mixer liners, hot-forming dies, rock jaw crushers, coal pulverizer rings, bridge bearings, impellers for outboard diesel engines, heavy section sheet metal dies, pulp press rolls, hot air valves, pump castings that carry coal- containing mud, wire straightening dies, drop balls, compressor valves, bearing cages, auto-body dies, explosive-forming dies, sprockets, bushings, piston rings, hydrospin mandrels, grinder rolls, oil – well pump beams, sheet and ball mill rolls, and grooved rolls for finishing stands (as compiled in Table 1 (Chandler, (1977), O'Rourke, (2004), Keough and Hayrynen (2000), US Pipe and Foundry Company, (2013). Guesser *et al.* (2012) discussed the potential of using ADI for gears in replacing conventional induction hardened steels. The ADI gears were produced from continuous cast iron bars and heat-treated to achieve a grade 3 of ASTM ADI Standard A897M-06 (UTS > 1200 MPa).

In particular, there have been recent developments in trenchless piping applications with ductile iron that can be used for horizontal directional drilling (HDD) and pipe bursting (US Pipe and Foundry Company, (2013). This pipe has the same great qualities of being rugged, durable and dependable in extreme trenchless conditions with conventional steel pipes, but has the added advantage of not requiring the rather expensive special piping cladding and long lead times.

The Table can be split to 2 (i.e Table 1(a), 1(b)) because of its length. The update of the Table with more recent additions, say up to 2013 is recommended.

7. CONCLUSION

In the last half century, ductile iron (DI) has earned what can be described as a unique position among engineering materials. Although it is not a cure-all material, it is generally agreed that no other ferrous material can match its combination of castability, mechanical properties and design flexibility at low cost, while allowing the manufacturer to obtain a wide range of properties in a component. There is no doubt that we have made giant strides in our understanding of the production, characterization and applications of ductile iron and austempered ductile iron (ADI). But what is required now is to harness this knowledge and to bring these special purpose engineering materials to the fore, in terms of their large scale production capacity, to meet specific needs (in transportation, construction, agricultural mechanization, oil and gas and allied industries, etc.) of the country. To do this successfully, there is an urgent need through research and development, to obtain more practical information on their dynamic properties such as fatigue strength, impact toughness, sliding-friction-wear resistance, micro-mechanism of fracture and/or failure, etc. This will require serious funding and commitment from relevant agencies and institutions, to research and development of this class of engineering materials.

REFERENCES

Adetunji, A. R; Imasogie, B. I; Olasupo, O. A; Alasoluyi, J. A; Olusunle, S. O. O; Babatope, B. and Adewoye, O. O. Current Production Trends of Ductile Iron with the Rotary Furnace at Engineering Materials Development Institute, Akure, Nigeria. Unpublished work at EMDI, Akure, Nigeria, 2008.

Anderson, J. V. and Kaysay, S. I. Pouring Rate, Pouring Time and Choke design for SG Iron Castings. Brit. Foundryman 78 (10): 492-498, 1985.

Anon. A Design Engineer's Digest of Ductile Iron. 8th Ed. RTZ Iron and Titanium America Report, 2004.

Anon. Technical information. Salt bath furnace heated by high-frequency current for small-scale and individual manufacturing. Metal Science and Heat Treatment, Springer Link, 1573-8973, p104, 2004.

Bockus, S. and Dobrovolskis, A. Effect of Melting Techniques on Ductile Iron Castings Properties. METABK, 45 (1): 13-16, 2006.

Caine, J. B. In Ductile Iron Castings. Design of Ferrous Castings, American Foundrymen's Society, Des Plaines, IL. USA, 1984.

Chandler, H. E. Iron Castings. Source Book on Materials Selection. Vol. 1. ASM Engineering Bookshelf. ASM Metals Park. Ohio, 44073: 268-302, 1977.

Charkaluk, E and Constantinescu, A. Energetic Approach in Thermomechanical fatigue for Silicon-molybdenum Cast-iron. Mater. High Temp. 17: 373-380, 2000.

Davis, K. G. and Magny, J. G. Effect of Hydrogen Charging on Nodularization Efficiency of a Rare-earth Alloy used in Treating Cast Iron. Metal Science, 12: 51-55, 1978.

Delbrugge, V. Ausform Finishing for Bulk Strength and Ductility - in Focus on Mechanical Drive Transmission Technologies, iMAST Quarterly, 1: 3-7: 1999.

Dremann, C. E. New Alloys for Making ductile Irons in the Mold. Trans. American Foundrymen's Society, 91: 263-264, 1983.

Ductile Iron Society. Ductile Iron Data for Engineers –Section 2. www.ductile.org/ ductile_iron.html. (assessed 14 Feb. 2013), 2010.

Emerson, P. J., and Simmons, W. "Final Report on the Evaluadion of t`e Graphite Form in Ferritic Ductile Iron by Ultrasonic and Sonic Testing, and the Effect of Graphite Form on Mechanical Properties". AFS Trans. No. 76-26: 109-128, 1976.

Franklin, S. E. and Stark, R. A. Application of Secondary Ion Mass Spectroscopy to Study of Graphite Morphology in Cast Iron. Metal Science, 18: 187-200, 1984.

Table 1: Examples of Conversions to Ductile Iron (Caine, 1984)

COMPONENT	CONVERTED FROM	CONVERTED TO	COST SAVINGS	OTHER DESIGN IMPROVEMENTS
Off-road Truck Suspension Cylinder	Welded Steel Fabrication	BS2789 420/12	›20%	Reduced machining costs. Reduced inventory and stock control costs.
Backhoe Loader Stabilizer Foot	Steel Weldment	ASTM A-536 80-55-06	49%	Used as-cast. All machining and fabricating costs eliminated.
Rope Clamp and Eye Nut	Steel Forging	ASTM A-536 80-55-06	82%	Stronger. Improved appearance.
Crankshaft for Supercharged Engine	Steel Forging	ASTM A-897 ADI	39%	Lighter/stronger/improved wear resistance. Improved sound dampening.
Diesel Engine Timing Gears	Carburized Steel Forging	ASTM A-897 ADI	30%	Increased machine shop productivity. Reduced wt. & noise. Rapid "break-in."
Aircraft Towbar Head	Steel Weldment	ASTM A-536 80-55-06	76%	Improved mech. properties. Reduced machining. Improved appearance.
Worm Gear and Post Screw	Bronze and Steel Fabrication	ASTM A-536 60-40-18	46%	Improved performance. Simplified final assembly.
4WD ATV Wheel Hub	Aluminum Casting	ASTM A-536 65-45-12	50%	Light weight. Increased strength and safety. Improved aesthetics.
Fertilizer Injection Knife	Steel Forging and Weldment	ASTM A-897 ADI	44%	Excellent wear resistance. Eliminated all fabrication costs.
Stainless Steel Banding Jig	Tool Steel Inv. Casting	ASTM A-897 ADI	77%	Significant reduction in machining costs achieved with equal performance.
Wire Rope Clamp	Steel Forging	ASTM A-536 80-55-06	92%	Close tolerance as-cast. High strength. Marketing advantages.
Aircraft Door Fixture	Steel Weldment	ASTM A-536 65-45-10	78%	Solved warpage problem. Increased strength. Reduced number of parts.
Gas Turbine Casing	Steel Castings	BS2789 400/12	›30%	Additional savings in machining costs. 17% less wt. Better vibration damping.
Truck Drive Shaft U-Joint Slip Yoke	Steel Forging	ASTM A-536 100-70-03	47%	Reduced material and machining costs for equivalent reliability.
Tractor Brake Anchor	Steel Fabrication	ASTM A-536 80-55-06	44%	Equivalent mechanical properties with reduced machining costs.
Air Compressor Block	Steel Weldment	ASTM A-536 65-45-12	46%	Improved sound damping and product integrity. Reduced manufacturing operations.
Automobile Steering Knuckle	Eleven-part Assembly	ASTM A-536 60-40-18	large	Reduced manufacturing operations, parts inventory. Improved reliability.
Photometer Housing	Steel Fabrication	ASTM A-536 65-45-12	45%	Weight reduction. Improved appearance. Improved performance.
Truck Cab Mount	Steel Fabrication	ASTM A-536 80-55-06	31%	Improved fatigue life. Two-part casting replaced 34 parts and 25 welds.
Cam for Cotton Picker	Hardened Tool Steel	SAE J-434C D5506	68%	Reduced surface loads. Increased picking speeds. Improved efficiency.
Backhoe Loader Swing Pivot	Steel Weldment	ASTM A-536 65-45-12	31%	Reduced manufacturing time. Better machining. Improved wear properties.
Tractor Transmission Hydraulic Lift Case	Gray Iron Casting	BS2789 420/12	40% (vs Steel)	Updated design required. Stronger. Steel casting 40% more, plus pattern change
Plug Valve	SS, Monel and Titanium	ASTM A-536 &0-40-18	66%	Close dimensional tolerances. Enabled installation of plastic liner.
Air Compressor Crankcase	Steel Weldment	ASTM A-536 60-40-18	82%	Improved sound damping and shock resistance.

Fuller, A. G. Evaluation of the Graphite Form in Pearltic Ductile Iron by Ultrasonic and Sonic Testing and the Effect of Graphite Form on Mechanical Properties. AFS Trans. No. 77-102: 509-526, 1977.

Fuller, A. G., Emerson, P. J., and Sergeant, G. F. A Report on the Effect Upon Mechanical Properties of Variation in Graphite Form in Irons Having Varying Amounts of Ferrite and Pearlite in the Matrix Structure and the Use of Nondestructive Tests in the Assessments of Mechanical Properties of such Irons, AFS Trans, No. 80-09: 21-50, 1980.

Grigy, C and Le Gal, J (1981). Surface Fatigue of Spheroidal Graphite Cast Iron. Atempted Improvement by Mechanical Heat treatments. Fonderie-Fondeur d'Aujourd'hui, 8, 21-29.

Guesser, W. L; Koda, F; Martinez, J. A. B. And da Silva, C. H. Austempered Ductile Iron for Gears, SAE International, adi-engrenagens.pdf. 2012-36-0305, 2012.

Hafiz, M. Mechanical Properties of SG-iron with Different Matrix Structures. Journal of Materials Science, 36: 1293-1300, 2001.

Heine, H. J. An Overview of Magnesium Treatment Processes which have stood the test of Time in America. Paper 9, BCIRA Conf. SG Iron – the next 40 Years, Univ. Warwick, UK, April 1987.

Hornung, K. and Hauke, W. Cast Iron Materials for Highly Stressed Automobile Components such as Gears. VDI-Zeitschrift, 123 (4): 16-24, 1981.

Horuichi, Y. Study on the Production of Spheroidal Graphite Cast Iron by Calcium Treatment. Testu-to-Hagane, 43: 903-908, 1957.

Imasogie, B. I. Development and Characterization of Isothermally Heat-Treated Nodular Cast Irons. Ph.D. Thesis, Obafemi Awolowo University, Ile-Ife, Nigeria, 1994.

Imasogie, B. I; Afonja, A. A. and Ali, J. A. Properties of Ductile Cast Iron Nodularised with a Multiple Calcium-Magnesium Based Master Alloy. Materials Science and Technology. 16(2): 194-201, 2000.

Imasogie, B. I; Afonja, A. A. and Ali, J. A. Properties of As-cast and Heat-treated Nodular Graphite Cast Irons, Melts Treated with CaSi-CaF_2 Alloy. Scandinavian Journal of Metallurgy, 30(2): 91-102, 2001.

Imasogie, B. I. Microstructural Features and Mechanical Properties of Compacted Graphite Iron Treated with Calcium-Magnesium Based

Masteralloy. Journal of Materials Engineering and Performance, 12(3): 239-243, 2003.
Imasogie, B. I. Optimum Ca-CaC_2-Mg Masteralloy Concentration Requirements in Graphite Nodularising Treatments of Cast Iron. Materials Engineering. 14(1): 77-86, 2003.
Imasogie, B. I. and Wendt, U. Characterisation of Graphite Particle Shape in Spheroidal Graphite Iron Using a Computer-based Image Analyzer. Journal of Minerals and Materials Characterization and Engineering, 3(1): 1-12, 2004.
Johansson, M. Replacing Steel Components with ADI Castings. International ADI and Simulation Conference, May 28-30, 1997, Karkkila, Finland, 1997.
Krzemien, E. Cast Iron Spheroidization in Casting Mould; Zesz. Nauk. Politech. Slask [Hutn.] 2:123-130, 1979.
Kurganov, V. A; Taran Yu. N. Krause, L. A; Lesovoi, V. V. and Sofonov, V. F. Use of Complex Inoculants in the Production of High Strength Cast Iron Ingot Molds. Liteinoe Proizvod., 1: 8-10, 1981.
Lerner, V. and Lerner, Y. A new approach to the Solidification Modeling of Casting Processes. Proceedings of the First International Conference on Mathematical Modeling of Metalworking Processes. NMT-2000, pp. 351-360, 2000.
Lerner, Y. S. and Panteleev, G. V. Magnesium Treatment in Ductile Iron Production. Part I. Foundry Management and Technology, www.foundrymag.com, 25-31, 2002.
Lerner, Y. S. and Panteleev, G. V. Magnesium Treatment in Ductile Iron Production. Part 2. Foundry Management and Technology, www.foundrymag.com, 24-26, 2003.
Lerner, Y. S, Continuous Casting of Ductile Iron, FMT 221608 – ductile iron.pdf, 40-67, 2004.
Keough, J. R. and Hayrynen, K. L. (2000) Automotive Applications of Austempered Ductile Iron (ADI) – A critical Review. Society of Automotive Engineers. 2000-01-0764. Document.pdf. (accessed 12 October 2014).
Metal Casting: Project Fact Sheet. Consistent Casting of High Strength Ductile Iron. Crs-latestream.pdf (assessed 20 Feb. 2010), 2006.
Nicoletto, G.; Konecna, R; Hadzimova, B and Collini, L. Microstructure and Mechanical Strength of Nodular Cast Irons, Associazione Italiana per L'Analisi delle Sollecitaziani, XXXI Convegno Nazionale, 18-21 September, 2002, Parma, Italy, 206.pdf, 2002.
Olusunle, S.O. Evaluation of Microstructural and Mechanical Properties of Austempered Rotary-Furnace-Melt Treated Ni-Cr Ductile Irons. Unpublished work at EMDI, Akure, Nigeria, 2008.
O'Rourke, R. F. www.gearsolution.com, 22 – 30; 2004-05-01_The_details_of_Ductile_Iron.pdf, 2004, (Accessed 23 December, 2014)
Palmeira, M; Oliveira, M; Cunha, A and Ribeiro, S. Process Measures Implemented into an IPPC Nodular Iron Foundry, Large Series Automotive Casting Producer, to Increase Energy Efficiency Use, ribeiro-ductile iron.pdf, 2006 (assessed 08 Sept. 2008).
Petrichenko, A. M. Priymak, V. A. Mozharov, M. V. Use of Complex Inoculants for the Production of Spheroidal Graphite Cast Iron. Liteinoe Proizvod. 1: 7-8, 1981.
Sillen, R. The PQ-CGI Inmold Process. NovaCast AB Bulletin, 2004.
Takita, M. and Ueda, Y. Influence of Interfacial Energy on the Shape of Graphite in Cast Iron. Trans. Japan Institute of Metals, 20: 569-576, 1979.
Umoru L. E; Ali, J. A. and Afonja, A. A. Effect of Calcium on the Degree of Nodularization of Graphite in Cast Iron. NSE Technical Transactions, 2: 33-42, 2005.
US Pipe and Foundry Company (2013). Trenchless Applications with Ductile Iron Pipe. US Pipe and Foundry Company, 866.Dip. Pipe/www.USPIPE.COM. 20133211.627360.pdf 2013 (accessed 27 December, 2014).

Full Paper

FUNCTIONAL AND SENSORY PROPERTIES OF FERMENTED LOCUST BEAN SEEDS USING OPTIMIZED PRE-FERMENTATION CONDITIONS

A. O. Koledoye
Department of Food Science and Technology, Obafemi Awolowo University, Ile-Ife, Nigeria.
princesskols@gmail.com

C. T. Akanbi
Department of Food Science and Technology, Obafemi Awolowo University, Ile-Ife, Nigeria.

ABSTRACT

This study is a continuation of previous work set to establish optimal processing conditions for the production of fermented locust bean seeds. The effect of employing these already determined conditions (First cooking at 50 kPa for 54 min per 100 g of seed and second cooking time of 15 min per 90 g of seed) on anti-nutritional factors, functional and sensory properties of the product was determined. The functional properties investigated were water and oil absorption capacity, emulsion capacity and solubility while tannin, phytate and oxalate were the anti-nutritional factors determined. Water absorption capacity and emulsion capacity decreased with dehulling but were increased by fermentation and drying while the oil absorption capacity and solubility decreased with processing. There was significant reduction in all anti-nutritional factors investigated. The consumer preference for taste and mouth-feel of both the traditionally and optimally processed *Iru* were significantly comparable ($p<0.05$). There was a significant difference in the preference for colour, aroma, texture, and overall acceptability. The study concluded that processing locust bean seeds under optimized conditions yields a product with acceptable nutritional benefits.

Keywords: *Fermented Locust Bean, Functional and Sensory Properties, Anti-nutrient*

1. INTRODUCTION

Locust Bean seeds provide an alternative source of protein in local food systems especially in West Africa. The fermented seed is prominently used in the preparation of stews and soups as condiment to enhance flavour and nutritional values. This condiment is referred to as *iru* in Yoruba, *dawadawa* in Hausa and *ogiri-igala* in Igbo. It is also referred to as *kinda* in Sierra-Leone and *Kpalugu* in Ghana (Odunfa, 1981).

Processing techniques may be employed to reduce or destroy the anti-nutrients present in them and to improve the nutritional quality or organoleptic acceptability of leguminous seeds. Some of the commonly used processing techniques include soaking in water, boiling at high temperatures in water, alkaline or acidic solutions, sprouting, autoclaving, roasting, dehulling, microwave treatment, steam blanching and fermentations (Christiana and Marcel, 2008). Omafuvbe *et al*., (2004) reported an increase in the moisture content of "*dawadawa*" when compared with the unprocessed seed and this may probably be due to boiling and subsequent soaking in water. It may also be as a result of metabolic activities of microorganism during fermentation period which gave out moisture as one of their end products. Several other researchers have come up with appropriate fermentation conditions such as pH, temperature and humidity (Odunfa and Adewuyi, 1985; Obeta, 1985; Ogbadu and Okagbue, 1988) for *iru* processing but there is dearth of information on the effects of optimization of pre-processing conditions such as dehulling and re-cooking on the functionality of the seeds.

Seed proteins are required to possess the essential requisite functional properties for successful utilization in various food products. These functional properties are intrinsic physico-chemical characteristics which affect the behaviour of properties in food systems during processing, manufacturing, storage and preparation. The properties include emulsion capacity, activities and stability. It also includes foam capacity and stability. Other paramount functionalities are proteins solubility, water and fat absorption capacity, organoleptic properties and bulk density (Aremu *et al*., 2007).

The quality and technological usability of food proteins are determined by their nutritional and functional properties (Ulloa *et al*., 2011). When protein is not considered as the main food component but as one of many constituents, its functionality can be an even more important evaluation criterion than its nutritional value. Owen (1996) reports that the sensory attributes of foods are achieved by complex interactions among various functional ingredients and since proteins possess a multitude of physical and chemical properties, it is difficult to delineate the role of each of these properties with respect to a given functional property. deMan (1999) agrees that in low and intermediate moisture foods, such as bakery and comminuted meat products, the ability of proteins to bind water is critical to the acceptability of these foods.

In a previous work by Koledoye and Akanbi (2013), optimum conditions for cooking and dehulling locust bean seeds prior to fermentation was established. But the study did not investigate the effect of employing these conditions on the anti-nutritional factors, functionality and sensory properties of the fermented product. This study therefore seeks to use the established conditions to achieve this purpose.

2. EXPERIMENTAL PROCEDURE

2.1. Sample preparation

Fresh locust bean seeds were processed using optimal conditions for dehulling and re-cooking established by Koledoye and Akanbi (2013). About 100 g of seeds were cooked in 4 L of water at 50 kPa (using a Prestige Pressure Cooker) for 54 min and re-cooking 90 g of seeds in 3 L of water for 15 min. Dehulling was carried out using a hand-held Russell Hobbs mixer set at a determined speed. The dehulled seeds were fermented following a modified method of Abiose *et al.* (1986). The seeds were transferred hot into calabashes lined with

banana leaves and incubating at 30 °C for 48 h. A portion of the fermented seeds was dried in a hot air oven at 65 °C for 24 h. The dried seeds were packaged as such in polythene bags.

2.2. Determination of Functional Properties

Sample solubility, emulsifying capacity, water and oil absorption capacity determinations were carried out on both the raw and dried fermented locust bean seeds. Solubility of the products was carried out using the method of Beuchat (1977), Emulsifying capacity was determined using the method of Neto *et al.* (2001). Water and oil absorption capacity was carried according to the method of Hayta and Naysar (2002).

2.3. Determination of Anti-nutritional factors

The anti-nutritional factors investigated in this study were Tannin, Phytate and Oxalate. The tannin content was determined using the method of Makkar and Goodchild (1996), Phytate content was determined using the method described by Haugh and Lantzsch (1993) while determination of oxalic acid content was according to the method of Oke (1966).

2.4. Sensory Evaluation of the Optimally Processed *Iru*

The processed *Iru* was assessed by presenting both traditionally and optimally processed *Iru* samples at random to a 10 member panellists who are familiar with the product and asking them to score the following attributes: colour, taste, aroma, mouth feel, texture and overall acceptability using a 7-point Hedonic scale.

2.5. Statistical Analyses

The data collected were expressed as Mean ± standard deviation of three experiments, and subjected to statistical analysis using one-way analysis of variance to determine significant differences between means ($\alpha = 0.05$). Tukey's Least Significant Difference test was used to compare means. All statistical procedures were carried out using PlotIT 3.2 software.

3. RESULTS AND DISCUSSION

3.1. Effect of Processing on the Functional Properties of the Raw and Fermented Locust Bean Seeds

The functional properties of the raw and fermented locust beans seeds are shown in Table 1. The water absorption capacity of the dehulled seeds was lower than that of the raw seeds but it significantly increased with fermentation. The reduction in the water absorption capacity of the dehulled seed may be due to the loss of insoluble fibre (Cadden, 1987) but the water absorption capacity increased with fermentation and dehydration. The water absorption capacity for the dehydrated *Iru* was significantly higher than that of the wet *Iru*. Choonhahirun (2010) reports that water absorption capacity describes the flour-water association ability under limited water supply and it is also used as an indication of performance in several food formulations (Circle and Smith, 1972). Therefore, the dehydrated seeds when ground to flour will be of great use in soups and gravies as a thickener.

Abbey and Ibeh (1988), reported that heat processing increases water absorption by about 52%. According to Eke and Akobundu (1993); Narayana and Narasigan Rao (1984); during heat processing gelatinization of the carbohydrate and swelling of the crude fibre occur which could also lead to increased water absorption. The higher water absorption capacity may be due to the presence of high polar amino acid residues of proteins having affinity for water molecules (Yusuf *et al*., 2008). The major chemical components that enhance the water absorption capacity of flours are proteins and carbohydrates, since they contain hydrophilic parts such as polar or charged side chains (Lawal and Adebowale, 2004).

The oil absorption capacity also decreased with processing i.e. fermentation and dehydration but the dehydrated product had a higher oil absorption capacity than the wet fermented product. Oil absorption is an important property in food formulations because oil improves the satiety, flavour and mouth feel of foods (Kinsella, 1976). The high values of oil absorption capacity agree with the findings of Ibrahim *et al.* (2011) for roasted and defatted cashew nut flour. Obatolu *et al.* (1995) reported that oil absorption was attributed to the physical entrapment of oil which is related to the number of non-polar side chains in the protein that bind hydrocarbon chains of the fatty acid. Lawal (2003) attributed this behaviour to the presence of non-covalent bonds, such as hydrophobic, electrostatic and hydrogen bonding forces that are involved in lipid-protein interactions. The major chemical component affecting oil absorption capacity is protein which is composed of both hydrophilic and hydrophobic parts. Non-polar amino acid side chains can form hydrophobic interactions with hydrocarbon chains of lipid (Jitngarmkusol *et al*., 2008). In addition, Adebowale and Lawal (2004) reported that variations in the presence of non-polar side chains, which might bind the hydrocarbon side chains of oil among the flour explains difference in the oil binding capacity.

The solubility of the seeds after dehulling increased with fermentation and dehydration by 28% and 73%, respectively. This implies that the fermented seed is capable of going into solution in the dehydrated form much more than the wet form.

The high emulsion activity suggests that the product can be useful as an additive for stabilization of fat emulsions in food formulations. The results agree with Jitngarmkusol *et al*., (2008)'s report that processing contributes to the emulsifying capacity of protein. According to Vioque *et al.* (2000), limited hydrolysis improves the emulsifying properties of protein owing to the exposure of hydrophobic amino acid residue that may interact with the oil while the hydrophilic residues interact with water. This thus explains the improved emulsifying properties observed in the dehydrated product. Obatolu *et al.* (1995) reported that no observable emulsion activity in fermented locust bean seeds and attributed it to the length of time in boiling before fermentation which led to protein denaturation. It then suffices to say that the short cooking time employed in this study enhanced emulsion activity in the product.

3.2. Effect of Processing on Anti-Nutrient Activity of the Raw and Fermented Locust Bean Seeds

The anti-nutrient activity levels of the raw and fermented seeds are shown in Table 2. There was a significant reduction in the tannin content from the raw state to the fermented state by 78% while there was a 54% decrease in the tannin content of the dried fermented seeds as compared with the raw. This reduction is similar to that obtained in a similar study by Esenwah and Ikenebomeh (2008) who reported a 59% reduction in hydrolysable tannin content. Helsper *et al.* (1993) reported that condensed tannins were responsible for the testa-bound trypsin inhibitor activity of faba beans. They also have the ability to form complexes with vit B_{12} (Liener, 1980). A reduction in tannin content of legumes due to processing has been reported by several authors. A 48.0 to 50.1% reduction was reported by El-Adawy (2002) during the processing of chickpea using different cooking methods. Esenwah and Ikenebomeh (2008) also asserted that the loss of tannin may be due to its solubility in water and its sensitivity to heat during processing.

The phytic acid content also reduced significantly by 92% in the wet fermented seeds and 88% in the dehydrated seeds. This reduction also agrees with a similar study by Mbajunwa (1995) although on another variety of locust beans. Phytic acid has been reported by Hendricks and Bailey (1989) to chelate metal ions such as calcium, magnesium, zinc, copper, iron and molybdenum to form insoluble complexes that are not readily absorbed from the gastro-intestinal tract. It also inhibits the action of some gastro-intestinal enzymes such as tyrosinase, trypsin, pepsin, lipase and α-amylase. Martinez (1977) also reported that in oilseeds which contain little or no endosperm, the phytates are distributed throughout the kernel found

within the subcellular inclusions called aleurone grains or protein bodies.

A 30% decrease was observed in the oxalic acid content of the dried fermented seeds while the decrease in the wet seeds was just 50%. These observations imply that fermentation and heat processing reduce the anti-nutrient content of locust beans. According to Olomu (1995), oxalic acid binds calcium and forms calcium oxalate which is insoluble. Calcium oxalate adversely affects the absorption and utilization of calcium in the animal body.

The significant decrease in all anti-nutrient levels checked makes the product safe for consumption either in the raw form or as a condiment in soups.

3.3. Sensory Evaluation

As shown in Table 3, the optimally and traditionally processed *Iru* samples had comparable consumer preference for taste and mouthfeel while there was a significant difference in the preference for colour, aroma, texture and overall acceptability.

The colour of the optimally processed sample was brown and wasn't different from the colour of the unfermented seeds unlike the traditionally processed sample which was black as a result of prolonged cooking and soaking that allowed the bleaching of the colour of the hull into the cotyledon. This agrees with Sadiku (2010), who reported that the cooking of seeds in water, especially pre-dehulling cooking has a relationship with changes in colour of seeds.

The fermentation period of the optimally processed sample was longer than the traditionally processed one and this resulted in it having a slightly marshy texture thus agreeing with the report of Omafuvbe *et al.* (2004) that the amount of water absorbed by the cotyledons during cooking primarily determines how marshy the product will be while the bacterial (mainly Bacillus and Staphylococcus) activities during fermentation enhance it.

The significant difference in overall acceptability can be attributed to the consumers being accustomed to the conventional fermented locust bean found in the market.

Table 1: Functional Properties of the Raw and Fermented Locust Bean Seeds

	Water Absorption Capacity (%)	Oil Absorption Capacity (%)	Solubility (%)	Emulsion Capacity (%)
Raw Seeds	145.5 ± 0.68^{c}	117.25 ± 0.43^{d}	48.47 ± 0.18^{c}	55.56 ± 0.49^{c}
Dehulled Seeds	97 ± 1.52^{a}	85.06 ± 0.21^{a}	12.04 ± 0.20^{a}	24.85 ± 0.63^{a}
Fermented Seeds	119.5 ± 0.65^{b}	73 ± 1.44^{b}	16.71 ± 0.14^{b}	39.04 ± 1.18^{b}
Fermented and Dehydrated Seeds	191 ± 0.50^{d}	101.75 ± 0.09^{c}	39.80 ± 0.11^{c}	60.09 ± 0.51^{d}

**Means within the same column having the same superscript are not significantly different at 5% level*

Table 2: Anti-nutrient Composition of the Raw and Fermented Locust Bean Seeds

	%Oxalate	%Phytate	% Tannin
Raw Seeds	0.086^{d}	0.57^{d}	0.065^{d}
Dehulled Seeds	0.078^{c}	0.250^{c}	0.055^{c}
Fermented Seeds	0.043^{a}	0.048^{a}	0.014^{a}
Fermented and Dehydrated	0.060^{b}	0.070^{b}	0.030^{b}

**Means within the same column having the same superscript are not significantly different at 5% level*

4. CONCLUSIONS

The study revealed that processing locust bean seeds under optimized conditions yields a product with acceptable nutritional benefits. The study also shows that reducing cooking time significantly causes a reduction in anti-nutrient activity which could have otherwise been a major draw-back in the utilization of *iru* as a food condiment. Conclusively, the conditions used in this study can be adapted in mechanizing the entire process of *iru* production without altering the functionality and consumer acceptability of the product.

Table 3: Sensory Qualities of the Optimally Processed and Traditionally Processed Iru

	Sensory Attributes*					
	Colour	Aroma	Taste	Mouthfeel	Texture	Overall Acceptability
TPI	6.8^{a}	6.4^{a}	6.4^{a}	5.8^{a}	6.6^{a}	6.6^{a}
OPI	5.6^{b}	5.2^{b}	5.6^{a}	4.6^{b}	4.8^{b}	4.6^{b}

**Means within the same column having the same superscript are not significantly different at 5% level*

TPI = Traditionally Processed Iru

OPI = Optimally Processed Iru

REFERENCES

Abbey, B. W. and Ibeh, G. O., Functional properties of raw and heat processed cowpea (*Vigna unguiculata*) flour, *Journal of Food Science*, 53: 1775 – 1991, 1988.

Abiose, S. H., Talabi, T. A., and Ajayi, L. O., Fermentation of African Locust Beans: Microbiological and Biochemical studies, *Nigerian Journal of Biological Science*. 1(2): 109 – 117, 1986.

Adebowale, K. O. and Lawal, O. S., Comparative study of the functional properties of Bambara groundnut (*Voandezia subterranean*), jack bean (*Canavalia ensiformins*) and mucuna bean (*Mucuna pruriens*) flour, *Food Research International*, 37(4): 355-365, 2004.

Amza, T., Amadou, I., Kamara, M. T., Zhu, K., and Zhou, H., Chemical and Nutrient Analysis of Gingerbread Plum, *Advance Journal of Food Science and Technology* 2(4):191 – 195, 2010.

Aremu, M. O., Olaofe, O. and Akintayo, E. T., Functional properties of some Nigerian varieties of legume seed flours and flour concentration effect on foaming and gelation properties, *Journal of Food Technology*, 5 (2): 109 – 115, 2007.

Beuchat, L. R., Functional and electrophoretic characteristic of succinylated peanut flour protein, *Journal of Agriculture and Food Chemistry*, 25: 258-261, 1977.

Cadden, A. M., Comparative effects of particle size reduction on physical structure and water binding properties of several plant fibers, *Journal of Food Science*, 52: 1595 – 1599, 1987.

Choonhahirun, A., Proximate composition and functional properties of (*Elateriospermun tapos* Blume) seed flour, *African Journal of Biotechnology*, 9(36): 5946-5949, 2010.

Christiana, N. E. and Marcel, J. I., Processing Effects of the Nutritional and Anti-nutritional content of African Locust Bean (*Parkia biglobosa* benth) Seed, *Pakistan Journal of Nutrition* 7: 214 -217, 2008.

Circle, S. J. and Smith, A. K., Functional properties of commercial edible soybean protein products, In: Seed Proteins. Inglet G.E (ed). Avi, Westport, CT. pp. 242 – 254, 1972.

Eke, O. S. and Akobundu, E. N. T., Functional properties of African yam bean (*Sphenostylis stenocorpa*) seed flour as affected by processing, *Food Chemistry*, 48: 337 – 340, 1993.

El-Adawy, T. A., Nutritional composition and anti-nutritional factors of chickpeas (*Cicer arietinum* L.) undergoing different cooking methods and germination, *Plant Foods and Human Nutrition*, 57: 83-97, 2002.

Esenwah, C. N. and Ikenebomeh, M. J., Processing Effects on the Nutritional and Anti-Nutritional Contents of African Locust Bean (*Parkia biglobosa* Benth.) Seed, *Pakistan Journal of Nutrition* 7 (2): 214-217, 2008.

Haugh, W. and Lantzch, H. J., Sensitive method for determination of phytate in cereals and cereals product, *Plant Foods for Human Nutrition* 44: 261 – 266, 1993.

Hayta, M. and Naysar, A., Effect of drying method on functional properties of Tarhana, Wheat flour, Yoghurt mixture. *Journal of Food Science*, 67(2): 740-744, 2002.

Helsper, J. P., Hoogendyk, J. M., Van Novel, A. and Burger-Meyer, K., Antinutritional factors in faba beans (*Vicia faba* L.) as affected by breeding toward the absence of condensed tannins, *Journal of Agriculture and Food Chemistry*, 41: 1058 – 1061, 1993.

Hendricks, J. D. and Bailey, G. S., "Adventitious toxins". In: Fish Nutrition. 2nd edition, Halver, J. E. (ed.). Academic Press inc., New York, USA. pp: 606-651, 1989.

Ibrahim, T. A., Omosuli, V., Oloye, D. A., Aladekoyi, G. and Ogundowole, O., Functional properties of roasted and defatted cashew nut (*Anarcadium occidentale*) flour, *Electronic Journal of Environmental, Agricultural and Food Chemistry*, 10(4): 2135 – 2138, 2011.

Jitngarmkusol, S., Hongsuwankul, J. and Tananuwong, K., Chemical composition, functional properties, and microstructure of defatted macademice flours, *Food Chemistry*, 110: 23 – 30, 2008.

Kinsella, J. E., Functional properties of food proteins: A review. CRC Crit. Rev. *Food Sci. Nutr.* 7:219 – 280, 1976.

Koledoye, A. O. and Akanbi, C. T., Optimisation of process conditions for dehulling and softening of locust bean (*Parkia biglobosa*, Jacq. Benth) seeds prior to fermentation in *Iru* production, *International Journal of Postharvest Technology and Innovation*, 3: 123 - 139, 2013.

Lawal, O. S., "Functionality of African locust bean (*Parkia biglobosa*) protein isolate: effects of pH, ionic strength and various protein concentrations", *Food Chemistry*, 86: 345–355, 2003.

Lawal, O. S. and Adebowale, K. O., Effect of acetylation and succinylation on solubility profile, water absorption capacity, oil absorption capacity and emulsifying properties of muncuna bean (*Mucuna prueins*) protein concentrate. *Nahrung/Food*, 48(2): 129-136, 2004.

Liener, I. E., "Heat labile antinutrient factors". In: Advanced Legume Science, (Editor: R. J. Sumerfield and A. H. Bunting), Kew London, Royal Botanical Gardens, pp: 157-170, 1980.

Makkar, A. O. S. and Goodchild, A. V., "Qualification of Tannins", A laboratory manual. International Centre for Agricultural Research in the Dry Areas (ICARDA) Aleppo, Syria. 25p, 1996.

Martinez, W. H., "Evaluation of Proteins for Humans", (Editor, C.E. Bodwell). Publishing Co. Inc., Westport, CT. 203p, 1977.

Mbajunwa, O. K., Effect of processing on some anti-nutritive and toxic components and on the nutritional composition of the African oil bean seed (*Pentaclethra macrophylla* Benth.), *Journal of the Science of Food and Agriculture*, 68: 153-158, 1995.

Narayana, K. and Narasinga Rao, M. S., Effect of partial proteolysis on the functional properties of sunflower meal product, *Journal of Food Science*, 49: 944 – 947, 1984.

Neto, V. Q., Narain, N., Silva, J. B., and Bora, P.S., Functional properties of raw and heat processed cashew nut (*anarcadian occidentale*, L.) kernel protein isolate, *Nahrung/Food*, 45, 258 – 262, 2001.

Obatolu, V. A., Osho, S. M. and Uwaegbute A. C., Comparative physicochemical properties of fermented soybean and locust bean, Post-harvest technology and commodity marketing. Proceedings of a post-harves conference. Nov 2nd - Dec 1st 1995, Accra Ghana.

Obeta, J. A. N., "A note on microorganism associated with the fermentation of African locust bean (*Parkia filicoidea*) during Iru preparation, *Plant Foods Human Nutrition* 5: 245 – 250, 1985.

Odunfa, S. A and Adewuyi, E. Y., Optimization of process conditions for the fermentation of locust bean (*Parkia biglobosa*). Effects of time, temperature and humidity, *Food Chemistry and Microbiology Technology* 9: 6 – 10, 1985.

Odunfa, S. A., Microorganisms associated with fermentation of African locust bean (*Parkia filicoidea*) during iru preparation, *Journal of Plant Foods* 3, 245 – 250, 1981.

Ogbadu, L. J and Okagbue, R. R., Fermentation of African locust bean (*Parkia biglobosa*). Involvement of different species of Bacillus species, *Journal of Food Microbiology* 5: 195 – 199, 1988.

Oke, O. L., Chemical studies on some Nigerian Vegetables, *Tropical Science*, 8(3): 128-132, 1966.

Okeoma, J. and Oyeleke, K., Nutritional consideration in the choice of flavour enhancer in Nigerian soups, *Nigerian Journal of Nutritional Sciences*, 9 (2): 87-95, 1988.

Oladunmoye, M. K., Effects of fermentation on nutrient enrichment of locust beans (*Parkia biglobosa*, Robert bam), *Research Journal of Microbiology*, 2: 185-189, 2007.

Olomu, J. M., Monogastric animal nutrition, principles and practice. Jachem publication, 320p, 1995.

Omafuvbe, B. O., Falade, O. S., Osuntogun, B. A. and Adewusi, S. R. A., Chemical and Biochemical Changes in African Locust Bean (*Parkia biglobosa*) and Melon (*Citrullus vulgaris*) Seeds During Fermentation to Condiments, *Pakistan Journal of Nutrition*, 3 (3): 140-145, 2004.

Sadiku, O. A., Processing Method Influence the Quality of Fermented African Locust Bean (iru/ogiri/dadawa), *Parkia biglobosa*, *Journal of Applied Sciences Research*, 6(11):1656-1661, 2010.

Ulloa, J. A., Rosas-Ulloa, P. And Ulloa-Rangel B. E., Physicochemical and functional properties of a protein isolate produced from safflower (*Carthamus tinctorius* L.) meal by ultrafiltration, *Journal of Science, Food and Agriculture*, 91(3): 572-577, 2011

Vioque, J., Sanchez-Vioque, R., Clemente, A., Pedroche, J., Bautista, J. and Millan, F., Partially hydrolysed rapeseed protein isolates with improved functional properties, *Journal of American Oil Chemist's Society*, 77; 447 – 450, 2000.

Yusuf, A. A, Ayedun, H. and Sanni, L. O., Chemical composition and functional properties of raw and roasted Nigerian benniseed (*Sesamum indicum*) and Bambara groundnut (*Vigna subterranean*)-, *Food Chemistry*, 111: 277-282, 2008.

Full Paper

STATISTICAL TEXT ANALYSIS FOR YORÙBÁ SPEECH GENERATION USING ZIPF'S LAW

A.R. Iyanda
Computer Science and Engineering Department
Obafemi Awolowo University, Ile-Ife, Nigeria
abiyanda@oauife.edu.ng

ABSTRACT.

The practical challenge of creating a Yorùbá text-to-speech synthesis has initiated our work on statistical text analysis. Language and speech technology applications have gained an increasingly wide-spread use in several languages/countries, and this has necessitated the importance of examining how much difference exists between English (in most cases the first language for most technologies and applications) and tone languages, specifically, Yoruba. These differences are studied and described in detail in linguistics but they rarely quantified and used by technology developers. In this paper, Yoruba language was described using text corpora from textbooks and newspapers. Other texts from Internet sources were also used. The corpus size was 291,392 word forms and the data was analyzed using Zipf. Based on the statistical analysis, it was found that the coverage of corpora by the most frequent words follows a parallel logarithmic rule for all languages in coverage range, known as Zipf's law in linguistics.

Keywords: *Text corpora, Data analysis, Standard Yoruba, Text-to-speech synthesis*

1. INTRODUCTION

As Text-To-Speech (TTS) systems find application in varied fields such as (i) computer assisted language learning (CALL) system; (ii) text-to-speech synthesis for Linguistic and Psycholinguistic Experimentation; (iii) telecommunication services (such as mobiles, multimedia, man machine Communication); and (iv) automatic text read aloud system and so on (Ngugi *et al.*, 2005). There is a need to create an adequate language resource which requires inter-disciplinary efforts amongst phoneticians, linguists as well as the use of powerful speech processing software.

A TTS synthesizer is a computer-based system that should be able to read any text aloud, whether it was directly introduced in the computer by an operator or scanned and submitted to an Optical Character Recognition (OCR) system. A text-to-speech system consists of two main parts: The first part is the natural language processing module, which produces a phonetic transcription of the input text, together with the prosodic information, that is information about say pitch, duration and phrasing (Dutoit, 1997). The second part is the digital signal-processing module, which transforms the information given by the natural language processing model into synthesized speech. Systems that simply concatenate isolated words or parts of sentences, denoted as Voice Response Systems, are only applicable when a limited vocabulary is required (typically a few one hundreds of words), and when the sentences to be pronounced respect a very restricted structure, as is the case for the announcement of arrivals in train stations for instance. In the context of TTS synthesis, it is impossible (and useless) to record and store all the words of the language. It is thus more suitable to define Text-To-Speech as the automatic production of speech, through a grapheme-to-phoneme transcription of the sentences to utter (Dutoit, 1997).

1.1. Standard Yorùbá

Yorùbá is classified as a Niger-Congo language of the Yoruboid branch of Defoid, Benue-Congo (Riddle and Stahlke, 1991). Although Yorùbá has several dialects with linguistic variations, all speakers can communicate effectively using the Standard Yorùbá (SY) (also known as Yorùbá Koine (Fagborun, 1994). SY is used in language education, the mass media and everyday communication (Odejobi, 2007). Yorùbá is a tone language in which a pitch of an utterance is used to express differences in meaning; or when a particular pitch or change of pitch constitutes an element in the intonation of a phrase or sentence, such as high, mid or low. The tone information in Yorùbá texts is indicated by diacritics - tone marking on top of vowels and syllabic nasals to give meaning to the contexts (Iyanda, 2014). Yorùbá alphabet comprises of 18 consonants (Bb, Dd, Ff, Gg, GBgb,Hh, Jj, Kk, Ll, Mm, Nn, Pp, Rr, Ss, Ṣṣ, Tt, Ww, Yy) and 7 vowels (Aa, Ee, Ẹẹ, Ii, Oo, Ọọ, Uu).

2. DATA

Data can exist in two forms: primary data and secondary data. Primary data are those collected by the researcher for the purpose of the survey in mind. They are always given in the form of raw materials and are originals in character. To be able to analyse and interpret such data, there is a need for the application of statistical technique. The data can be collected in three different ways such as by: (i) experiment, (ii) survey using structured questionnaires and (iii) interview, participant observation or focus group. Secondary data, on the other hand, is information that has been collected by somebody for other purpose. These are data collected through censuses, organisational records as well as through qualitative methodologies or qualitative research. Secondary data must possess the qualities of reliability, suitability and adequacy. For the purpose of our design, secondary data was used. In designing database, there are four major procedures to consider and these include; collecting databases, labelling, extraction of features and building models from the data (Black and Lenzo, 2007).

i. Collecting databases: Getting the right type of data is important when one is going to be using its content to build models. The quality of synthesized speech of data collected, for example a database of isolated words provide clearly articulated synthesized speech that will sound like isolated words, even when used for the synthesis of continuous speech. Both the acoustic properties and the prosodic properties of the database are important. In designing a database, the specific points worth to be considered are: phonetic coverage, dialect, voice quality, prosodic coverage as well as size.

ii. Labelling databases: In order for Festival to use a database it is most useful to build utterance structures for each utterance in the database. Festival is a multi-lingual TTS engine and a general purpose concatenative TTS system that offers a general framework for building speech synthesis systems. Generally, there is need for labels for: segments, syllables, words, phrases, intonation events, pitch targets.

iii. Extracting features: The easiest way to extract features from a labelled database is by loading in each of the utterance structures and dumping the desired features for training using the Festival script 'dumpfeats'.

iv. Building models: In this stage, model is built from data extracted from databases using the CART building program, 'wagon' which is available as with the Edinburgh Speech Tools Library.

2.1. Data Collection

The domain for the speech synthesis for this research is in language education, religious and mass media from various sources such as Internet, digitized printed material and existing digital materials from non-Internet sources. Two SY newspaper (Aláròyé and Yorùbá Gbòde) and two SY textbooks (Awobuluyi, 2008, Owolabi, 2011) were selected. The two newspapers were not toned mark, and Yorùbá Gbòde is without under dots. The texts selected from the newspaper for the text corpus were fully tone marked and under dotted. To increase the quality and coverage of the acquired materials, additional Yorùbá text data were gathered from existing printed materials by scanning through a process known as optical character recognition. The volume of textual data generated using this technique was about 291,392 words.

The texts were edited using a Tákàdá text editor (www.sourceforge.net/projects/takada) and were corrected for graphemic items (tone marks and under dots) using Àkotó Yorùbá. Àkotó Yorùbá is a software developed by Asahiah (2014) for restoration of Yorùbá diacritics. In this system, database of pre-selected units (syllables) was used. The creation of this database involved selecting a single unit, for inclusion in the system representing all possible occurrences. To cater for all possible segmental (auto and supra) contexts, the unit needs to be as neutral as possible.

For the Yorùbá TTS, the database contains syllable segments and their feature descriptions were translated into a data structure. The data (that is syllable segments and their feature descriptions) were stored in a hashtable using linked lists. The selection of a set of phonemically balanced sentences that contain the units was done by comparing the text corpus and the transcribed text. The choice of this unit is critical to realizing the selection of phonemically balanced sentences. The sample data collected is shown in Table 1. The data is based on the Yorùbá syllable structure. There are about 690 syllables (V=7x3, Vn=5x3, N=2x3, CV=126x3 and CVn=90x3) collected.

The concatenation of those syllables form a word and the concatenation of words produce a sentence. It should be noted that not all the syllables presented in Tables 1 are valid Yorùbá syllables. For example, "l" cannot precede a nasal vowel (for instance, **lan, lẹn, lọn, and lun,** do not exist in the Yorùbá words).

2.2. Data Analysis

Data analysis was done using Zipf which observed a phenomenon in human languages (and some other social structures) that indicated that there is a pattern in the distribution of tokens and that a few very frequent words make up a very large portion of any text or collection of texts, while the large majority of words occur relatively rarely. Zipf's law is an empirical law formulated using mathematical statistics. It refers to the fact that many types of data studied in the physical and social sciences can be approximated with a Zipfian distribution, one of a family of related discrete power law probability distributions (Chen, 2012).

The law is named after the American linguist George Kingsley Zipf (1902-1950), who first proposed it.

Zipf's law states that given some corpus of natural language utterances, the frequency of any word is inversely proportional to its rank in the frequency table. Thus the most frequent word will occur approximately twice as often as the second most frequent word, three times as often as the third most frequent word, etc (Sorell. 2012). For example, in the Brown Corpus of American English text, the word "the" is the most frequently occurring word, and by itself accounts for nearly 7% of all word occurrences (69,971 out of slightly over 1 million). True to Zipf's Law, the second-place word "of" accounts for slightly over 3.5% of words (36,411 occurrences), followed by "and" (28,852). Only 135 vocabulary items are needed to account for half the Brown Corpus (Manning and Schutze, 1999).

Table 1: Yorùbá syllable data for mid tone

Consonant (C)	Oral Vowel (V)								Nasal Vowel (Vn)				Syllabic Nasal (N)
	a	e	ẹ	i	o	ọ	u	an	ẹn	in	ọn	un	n, m
C				CV						CVn			
b	ba	be	bẹ	bi	bo	bọ	bu	ban	bẹn	bin	bọn	bun	Syllabic nasals can stand alone as a syllable not in combination with any consonant or vowel.
d	da	de	dẹ	di	do	dọ	du	dan	dẹn	din	dọn	dun	
f	fa	fe	fẹ	fi	fo	fọ	fu	fan	fẹn	fin	fọn	fun	
g	ga	ge	gẹ	gi	go	gọ	gu	gan	gẹn	gin	gọn	gun	
gb	gba	gbe	gbẹ	gbi	gbo	gbọ	gbu	gban	gbẹn	gbin	gbọn	gbun	
h	ha	he	hẹ	hi	ho	họ	hu	han	hẹn	hin	họn	hun	
j	ja	je	jẹ	ji	jo	jọ	ju	jan	jẹn	jin	jọn	jun	
k	ka	ke	kẹ	ki	ko	kọ	ku	kan	kẹn	kin	kọn	kun	
l	la	le	lẹ	li	lo	lọ	lu	lan	lẹn	lin	lọn	lun	
m	ma	me	mẹ	mi	mo	mọ	mu	man	mẹn	min	mọn	mun	
n	na	ne	nẹ	ni	no	nọ	nu	nan	nẹn	nin	nọn	nun	
p	pa	pe	pẹ	pi	po	pọ	pu	pan	pẹn	pin	pọn	pun	
r	ra	re	rẹ	ri	ro	rọ	ru	ran	rẹn	rin	rọn	run	
s	sa	se	sẹ	si	so	sọ	su	san	sẹn	sin	sọn	sun	
ṣ	ṣa	ṣe	ṣẹ	ṣi	ṣo	ṣọ	ṣu	ṣan	ṣẹn	ṣin	ṣọn	ṣun	
t	ta	te	tẹ	ti	to	tọ	tu	tan	tẹn	tin	tọn	tun	
w	wa	we	wẹ	wi	wo	wọ	wu	wan	wẹn	win	wọn	wun	
y	ya	ye	yẹ	yi	yo	yọ	yu	yan	yẹn	yin	yọn	yun	

The analysis of the data used in this study for frequency distribution was performed using a free concordance software Simple Text Analysis Tool (TextSTAT) version 2.9.0.0 (Hüning, 2014). TextSTAT was designed to be user friendly and provide simple Internet functionality. Texts can be combined to form corpora (which can also be stored as such). The program analyses these text corpora, displays word frequency lists, concordances, and keywords in context according to search terms. TextSTAT can be used to search large amounts of text. It can also help to learn how often a certain word occurs or in what contexts it is used. Word combinations can as well be examined.

TextSTAT) version 2.9.0.0 was used to generate the frequency count for the word tokens in the text data. It was also used to detect words that have incorrect forms such as wrong diacritics (tone marks and under dots). In the analysis of the words in the main text corpus, 6857 words appeared only once in the corpus and the word with the highest appearance in the data set (*tí*) occurs 8257 times, followed by *ni* with frequency of 6358 and followed by *àwon* with frequency of 5753. This pattern is expected of natural language (Sorell, 2012). Table 2 shows the distribution of some selected words in conformity with Zipf's law for linguistic data. The word n is in the tenth position and it occurred 4365 times, *ti* is in the twentieth position and occurred 2673 times and so on.

Table 2: Ranks and frequencies of the text data

Word Type	Rank (r)	Frequency (f)	Proportion (%)
n	10	4365	1.4978
ti (has)	20	2673	0.9173
fún (give)	30	2215	0.7601
gẹ (cut)	40	1560	0.5354
èdè (language)	50	1153	0.3957
o (you)	60	947	0.3250
ìṣe (doing)	70	786	0.2697
ìtàn (story)	80	694	0.2382
pọ	90	599	0.2056
ìmọ (knowledge)	100	524	0.1798
ìpínlẹ (state)	200	189	0.0649
àtijọ (former)	300	110	0.0377
yí (turn)	400	77	0.0264
ọjà (market)	500	57	0.0196
Adéyẹmí (Yoru□ba□ name)	600	44	0.0151
Ààyè (opportunity)	700	37	0.0127
Àgbàlagbà (adult)	800	30	0.0103
gbeyẹwò (consider)	900	25	0.0086
déésì (translated name)	1000	21	0.0072
kórìira (hate)	10000	1	0.0003

Zipf's law states that there is an inverse proportional relationship between the rank and frequency of words in a text. Rank is the position of a word in a table of words ordered by frequency of occurrence (rank one being the most frequent) (Sorell, 2012).

The general nature of Zipf's distribution as it applies to human language use whether in oral or written communication or discourse (Asahiah, 2014) is as highlighted below:

i. a few word tends to score very high on the frequency table meaning that they appear regularly in discourse;
ii. a medium number of words or linguistic tokens appears with relatively medium frequency indicating that they are regularly used;
iii. a huge number of words in a document have very low level of occurrence, indicating that they are rarely used.

With the proportion of these tokens in relation to the total token count, it means that these words (*tí* and *ni*) occurred in many contexts and are good features to be used in grapheme to phoneme conversion system for Yorùbá language. This agrees with existing work (Asahiah, 2014). The Zipf curve for the words whose rank ranges from tens to thousands (the regularly occur to the rarely occur), to have a wide coverage of the database is shown in Fig. 1. The shape of the curve justifies Zipf's law for linguistic data. This means that a few words appear regularly in discourse; a medium number of words or linguistic tokens appears with relatively medium frequency indicating that they are averagely used; a huge number of words in a document have very low level of occurrence, indicating that they are rarely used.

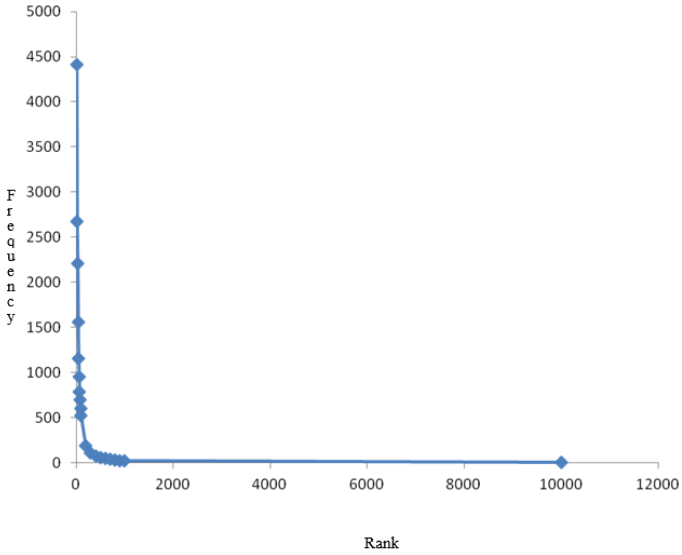

Fig. 1: Zipf frequency-rank curve for Yorùbá texts

Zipf also argued that the proportion of a text made up by words with a certain frequency should be equal (Sorell, 2012):

$$1=f\ (f+1) \qquad (1)$$

Where f is the frequency of each word in the database.

3. IMPLEMENTATION

R

Language resource such as specially prepared speech material (e.g. text and speech sound) has become a central issue in the development of a TTS for any language. The design, collection, recording and annotation of such materials depend on several factors. These factors include: the scope of the research, the linguistic features of the language, and the domain of application.

The data used in studies like this varies widely in scale and scope. The creation of an adequate language resource is a very complex task which requires inter-disciplinary efforts amongst phoneticians, linguists as well as the use of powerful speech processing software (Odejobi, 2005). There are no publicly available language resources for standard Yorùbá, so a small language resource was created for use in this research.

3.1. Speech Corpus

The analysis of the text database discussed earlier informed the selection of text for the speech corpus. Six hundred and ninety (690) syllables were used for the speech database. The following procedures are carried out:

i. Recording: 740 words and 690 syllables were read by two males and two females who are native speakers of SY. The age of the speakers ranges from 22 to 37 years old. Each speaker reads the text at his/her own pace, resulting in the average number of syllable per seconds ranging from two to three. The sounds were prepared by recording at a 44100 Hz sampling rate and 32-bit quantization. After that, they were down-sampled to 16 kHz for analyzing and use in the

implementation of the system in Festival TTS engine. All speech units were recorded in normal speaking rate.

ii. Recording equipment: The corresponding speech data for the Yorùbá syllables collected was recorded in a quiet environment with a noise cancelling microphone on a typical multimedia computer system using the Speech Filing System (SFS) software. Adobe Audition 3.0 was used to normalise and to reduce adaptive noise. SY which is the one being used in education, the mass media and everyday communication was chosen for the recording. The recorded speech data was analysed and annotated using the PRAAT speech processing software.

iii. Speech file annotation: Each file of the recording was loaded into PRAAT and annotated manually. For the annotation, TextGrid is created in PRAAT for each speech waveform file. The TextGrid and waveform files were selected for annotation and editing. There are two tiers in the annotation: word and syllable. The labelling was done to identify syllabic boundaries. In the annotation of the syllable speech files, only one tier was specified (the syllable tier). The syllable is labelled with its associated tone as shown in Fig. 2. In the annotation of the word speech files, two tiers were specified (the syllable and word tiers) as shown in Fig. 3. Both the spectrogram and the waveform were used in determining syllable and word boundaries.

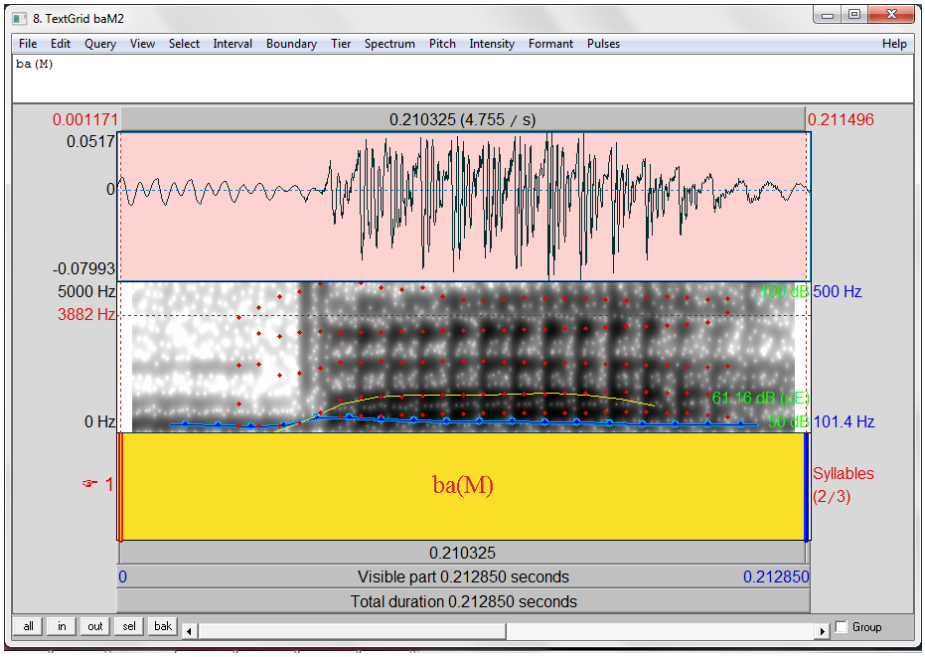

Fig. 2: Screen capture of annotation of the syllable bá

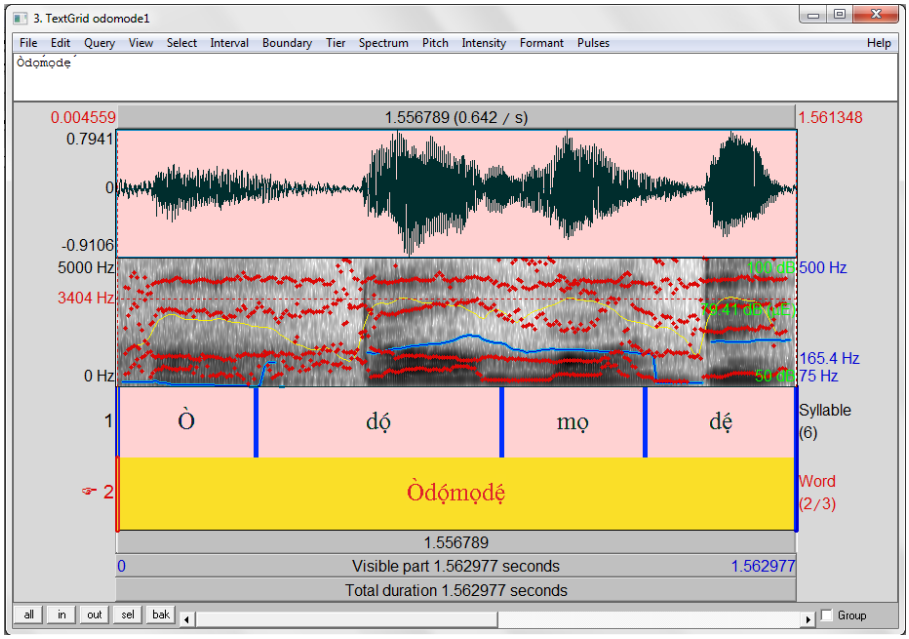

Fig. 3: Screen capture of annotation of the word Ọdọmọdé

4. CONCLUSION

The text corpus shows a very similar coverage distribution which can be well approximated by straight lines on a logarithmic scale. The shape of the curve conforms to Zipf's law for linguistic data and agrees with existing works (Lin *et al.*, 2014; Manning and Schutze, 1999). This means that a few words appear regularly in discourse; a medium number of words or linguistic tokens appears with relatively medium frequency indicating that they are averagely used; a huge number of words in a document have very low level of occurrence, indicating that they are rarely used. This work contributes significantly to the knowledge for natural language engineering for Yorùbá such as predictive text input, diacritic restoration, word hyphenation, language modelling in speech recognition, corpus-based speech synthesis, and so on.

REFERENCES

Asahiah, F. O. The Development of a Standard Yorùbá Diacritics Restoration System. PhD thesis,Obafemi Awolowo University, Ile-Ife, Nigeria, 2014.

Awobùlúyì, O. Èkó Ìsèdá-Òrò Yorùbá . Montem Paperbacks, Akure, Ondo State, 2008.

Black, A.W. and Lenzo, K. A. Building synthetic voices. available from festvox.org/bsv/bsv.pdf. 2007.

Chen, Y. Zipf's law, 1/f noise, and fractal hierarchy. Chaos, Solitons & Fractals 45.1: 63-73. 2012.

Dutoit, T. An introduction to text-to-speech speech system. isbn 0-7923-7923- 4498-7. Master's thesis, Kluwer Academic, 1997.

Fágborún, J. G. The Yorùbá Koiné: Its History and Linguistic Innovations, volume 6. LINCOM Europa, München, Newcastle, linguistics edition, 1994.

Hüning, M. Textstat - simple text analysis tool/ concordance software. available from http://neon.niederlandistik.fu-berlin.de/en/textstat/. visited: April, 2014.

Ìyàndá, A. R. Design and Implementation of a Grapheme-to-Phoneme Conversion System for Yorùbá Text-to-Speech Synthesis. PhD thesis, Obafemi Awolowo University, Ile-Ife, Nigeria, 2014.

Lin, R., Ma, Q. D. Y. and Bian, C. Scaling laws in human speech, Decreasing emergence of new words and a generalized model. arXiv preprint arXiv:1412.4846. 2014.

Manning, C. D. and Schutze, H. Foundations of Statistical Natural Language Processing, volume 999. MIT Press, 1999.

Ngugi, K., Okelo-Odongo, W., and Wagacha, P. W. Swahili Text-to-Speech System. African Journal of Science and Technology (AJST) Science and Engineering Series, 6(1):80-89. 2005.

Odéjobí, O. A. A Computational Model of Prosody for Yorùbá Text-to-Speech Synthesis. PhD thesis, Aston University, 2005.

Odéjobí, O. A. A quantitative model of yorùbá speech intonation using stem-ml. INFOCOMP Journal of Computer Science, 6(3):47–55, 2007.

Owólabí, K. Ìjìnlè Ìtúpalè Èdè Yorùbá (1): Fònétîkì ati Fonólojì. Universal Akada Books Nigeria Limited, 2011.

Riddle, E. and Stahlke, H. Linguistic typology and Sinospheric languages. First Annual Meeting of the Southeast Asian Linguistics Society. 1991.

Sorell, C. Zipf's law and vocabulary. The Encyclopedia of Applied Linguistics. Wiley Online Library 2012.

INSTRUCTION TO AUTHORS

Preamble: the manuscripts should be double-spaced and typed on not more than 20 pages of A4 paper. Four copies of the manuscript and originals of diagrams should be submitted. Three referees who have appropriate knowledge of the subject will be appointed for each paper. Our list of reviewers, who are drawn from the international academic and professional engineering community, will be published periodically. Final decisions on papers will be made by the Editorial Board.

The following format is recommended for papers:

Title: The title should be capitalized and be as brief as possible. It should be followed by the author's name(s) and address(es).

Abstract: Each paper should have an abstract, not exceeding about 200 words immediately before the beginning of the paper.

Introduction: This should contain clearly stated objectives, justification for the study and a brief review of literature.

Theoretical development: This should be included where appropriate.

Experimental Procedure: This should state how major measurements were done and degree of accuracy (if any). Sufficient information should be provided to permit repetition of the experimental work.

Results and Discussions: These should be pertinent to the work done and should clearly indicate the degree of reliability of the results.

Conclusions: These should succinctly summarize any important conclusions emerging from the work.

Acknowledgements: (if any)

Notations: Special symbols defined and used in the text should be indicated.

References:

Citing: references in the text should be by the last name and year. E.g. (Ahmed, 1987); Okonkwo et al. (1986); Thomas and Dada (1986).

Listing: This should be in alphabetical order. The recommended format for listing references is as follows: Name(s) and initials of authors, exact title of paper (in quote), the title of the periodical as in World list of Scientific Periodicals 4th Edition (1963-65), vol. (Number):initial and final page numbers, year. Only names actually cited in the text should be listed.

Serial: Okonkwo, E.P., Suru O.O. and Ahmed, T.A., "Properties of farm animal excreta". Ife Journal of Tech. 1(2):274-277, 1987.

Book: Schwarts, R.J., "the complete dictionary of abbreviations" T.Y. Cromwell Co., New York, 1955.

Heading and Sub-Heading: All headings and sub-headings should be numbered. All headings should be written in capital letters and should start at the left margin, while sub-headings should have only the first letter of major words capitalized.

Tables: A table should contain enough information to understand it without reference to the text. Tables are to be numbered in Arabic numerals in ascending numerical order as reference is made to them in the text (e.g. Table 2: Taste panel scores for yam flour). They should be placed at the end of the text and should contain no vertical lines. Captions must be placed at the top.

Figures: Illustrations, whether line drawings, graphs or photographs, should be given a figure number by Arabic numerals in ascending numerical order as reference is first made to them in the text (e.g. Fig. 3). Line drawings should be in Indian ink on tracing paper and only black and white photographs with good contrast are acceptable. Figure captions should be clear, precise and placed below the figure.

Equations: Equations should be distinctly typed or written with subscript or superscripts clearly indicated, preferably using Equation Editors. Avoid powers of "e" and use "exp". Equations should be centered on the line, numbered consecutively by Arabic numerals in parenthesis at the right margin. In the text, such equations should be cited as Equation (1) etc.

Units: S.I. Units should be used.

Page Charges: publication charges are N1500.00 ($15.00) per page.

Reprints: Fifteen reprints will be supplied to authors free of charge. Additional reprints may be ordered when the galley proofs are being returned.

Note: Submission of an article implies that the work has never been published, is not being considered for publication elsewhere, and that the authors are completely responsible for the statements made in their articles.